UPTAKE PATHWAYS OF METHYL MERCURIC CHLORIDE AND MERCURIC CHLORIDE BY RAINBOW TROUT (SALMO GAIRDNERI) WITH SPECIAL REFERENCE TO ULTRASTRUCTURAL CHANGES OF THE GILL

Thesis for the Degree of Ph. D.
MICHIGAN STATE UNIVERSITY
KENNETH R. OLSON
1972

This is to certify that the

thesis entitled

Uptake Pathways of Methyl Mercuric Chloride and Mercuric Chloride by Rainbow Trout (Salmo gairdneri) with Special Reference to Ultrastructural Changes of the Gill

presented by

Kenneth Robert Olson

has been accepted towards fulfillment
of the requirements for

Ph.D. degree in Physiology

Paul O. From

Major professor

Date 11/6/72

O-7639

ABSTRACT

UPTAKE PATHWAYS OF METHYL MERCURIC CHLORIDE AND MERCURIC CHLORIDE BY RAINBOW TROUT (SALMO GAIRDNERI) WITH SPECIAL REFERENCE TO ULTRASTRUCTURAL CHANGES OF THE GILL

By

Kenneth R. Olson

The environmental mercury problem has received considerable attention with respect to its effect as a human health hazard, however, little is known of the effects of mercury on aquatic animals. The purpose of this study was to determine the pathway of mercury uptake into rainbow trout and the effects of two mercurials, $HgCl_2$ and CH_3HgCl, on the tissues most closely associated with the uptake process.

Uptake of either $^{203}HgCl_2$ or $CH_3{}^{203}HgCl$ by trout was not affected by esophageal ligation thus uptake of these two mercurials appears to be by way of either the gills or skin. Low transcutaneous molecular fluxes reported by numerous investigators support the hypothesis of the gill as the primary pathway. In 24 hours both mercurials are found in tissues at concentrations exceeding those of the environment with gill, liver and kidney showing the

greatest accumulation. Uptake of methyl mercury is much greater than inorganic mercury uptake after 24 hours and relative tissue distributions show preference for either mercurial depending on the individual tissue.

Electron microprobe tissue analysis and radioautographic studies of gill tissue failed to show specific concentration of $HgCl_2$ at either the respiratory or ion exchange sites, however, large accumulations of mercury were found trapped in the mucus coating the gill surface and in the cartilaginous filamental support.

Transmission and scanning electron micrographs revealed ultrastructural changes following either methyl or inorganic mercury exposure. Loss of lamellar epithelial cell ridges, appearance of highly vacuolated epithelial cells and chloride cell degeneration was common after exposure to either mercurial. In addition, methyl mercury specifically produced red cell vacuolation and exposure to inorganic mercury resulted in appearance of a new lamellar epithelial cell type.

In vitro experiments using radioactive mercurials demonstrated high affinity of methyl mercury for red cells (up to 90% of the mercurial was bound to red cells in 40 minutes). Only 9% of inorganic mercury was taken up by red cells, however, this percentage was increased up to 65% if the cells were washed and suspended in Ringer solution

prior to incubation with mercury. In spite of the affinity of washed cells for mercury, concentrations as high as 100 ppm of either mercurial had no effect on the oxygen carrying capacity.

UPTAKE PATHWAYS OF METHYL MERCURIC CHLORIDE AND MERCURIC CHLORIDE BY RAINBOW TROUT (SALMO GAIRDNERI) WITH SPECIAL REFERENCE TO ULTRASTRUCTURAL CHANGES OF THE GILL

By

Kenneth R. Olson

A THESIS

Submitted to
Michigan State University
in partial fulfillment of the requirements
for the degree of

DOCTOR OF PHILOSOPHY

Department of Physiology

1972

Dedicated to my wife, Marilyn,

and daughter, Nicole,

for their understanding, tolerance and sacrifice

during the completion of this dissertation

and for the many words of encouragement and support

along the way.

Dedicated also to my parents,

Mildred and Robert Olson,

for their continual encouragement and concern

which made my entire education possible.

ACKNOWLEDGMENTS

The author wishes to express his sincere appreciation to Dr. P. O. Fromm for his guidance, suggestions and support in the preparation of this dissertation.

I am also grateful to Dr. J. R. Hoffert for his valuable suggestions on many laboratory procedures as well as help with the photographic preparation of the micrographs in this thesis.

Thanks is also expressed to Harold Bergman, Dan O'Connor, Dick Walker and other graduate students on this campus for their assistance, and to my wife, Marilyn, and Mrs. Esther Brenke for laboratory assistance and aid in preparation and typing of the rough draft of this thesis. Special recognition is also given to Mrs. C. Smith for her interest in environmental problems.

The author is also indebted to Drs. W. Willford and R. E. Reinert, Great Lakes Fishery Laboratory, Bureau of Sport Fisheries and Wildlife, for their discussion and generous supply of mercury exposed fish.

This research was supported by Environmental Protection Agency, Grant No. R-801034, and Public Health Service Training Grant No. HL-05873.

TABLE OF CONTENTS

LIST OF TABLES

LIST OF FIGURES

INTRODUCTION

Although known to be toxic to man since the first century AD, the status of mercury as an environmental contaminant was largely overlooked until the disastrous epidemics of Minamata and Niigata in the 1950's and early 1960's which left numerous people dead and many more crippled. Subsequent poisonings due in part to the use of mercurials as seed dressing and for medicinal purposes has promoted a revision in the heretofore promiscuous use of mercury compounds and their subsequent release into the environment. As somewhat of an afterthought came the realization that mercury contamination of the environment might also affect non-human organisms, and since much of the mercury is eventually carried in its water soluble form, the aquatic environment became one of the first subjects of investigation.

With respect to teleosts, the two major research foci became: 1) how much mercury is present in the tissues of fish from different geographical areas (with reference to polluted and unpolluted waters), and 2) what concentrations of the various forms of mercury are lethal to fish under controlled conditions for short time periods

(toxilogical bioassay procedures)? Relatively little emphasis has been placed on studies of the pathway of mercury uptake by fish and on the effects of sublethal mercury concentrations on the vital homeostatic mechanisms which operate in teleosts. The purpose of the present study was to compare and contrast two forms of mercury most commonly involved in water pollution (mercuric chloride and methyl mercuric chloride) with respect to: 1) pattern of uptake by teleosts, 2) interaction with tissues primarily involved in uptake, and 3) morphological and physiological changes which occur in tissues most closely involved with the uptake process.

Initially, study was directed toward mercury-induced physiological changes which could occur at one of the possible uptake sites, the gill. An isolated-perfused gill preparation was developed which, for up to 10 hours, demonstrated capabilities for active sodium transport (as evidenced by saturation kinetics and metabolic inhibition) and exhibited a characteristic membrane permeability shown by urea diffusion. It became evident that while mercury might have an effect on sodium transport and permeability, it could also affect any one of a number of other physiological processes carried out by the gill. Even if measurements of physiological parameters were limited to only the organs involved in mercury uptake, the magnitude

of the studies involved therein would be prohibitive. Thus, the most logical approach was to determine the primary pathway for mercury uptake and then investigate the action of mercury on the physiology and morphology of tissues involved in the uptake process. Therefore, this dissertation was limited mainly to a study of morphological changes in rainbow trout exposed to two mercurials. The physiological alterations could then be inferred from the morphological information and a "hit-or-miss" study of pathophysiology thereby avoided.

Very few anatomical studies of gill ultrastructure have been reported on rainbow trout which involved the use of the transmission electron microscope and, to the author's knowledge, no information on gills from any teleost has been obtained with either the scanning electron microscope or the electron microprobe. In depth studies of this nature on control fish are, of necessity, included in this thesis.

LITERATURE REVIEW

Mercury Uptake

The extensive literature dealing with the importance of mercury as a health hazard and its environmental disposition has been recently reviewed Löfroth (1969), Selikoff (1971), Friberg and Vostal (1972), and D'Itri (1972). Other information has appeared as a published discussion from a symposium on "Mercury in Man's Environment" and a geological survey, "Mercury in the Environment." These extensive reviews obviate the need to recapitulate the ecological notoriety of mercury compounds, hence, the present review will be limited to only those articles pertinent to a discussion of the action of mercury on fish with respect to pathways for uptake, and possible effects of mercury on the organ systems involved.

Primary Uptake Pathway

The movement of mercury into fish could be by one or more routes: the gills, skin and gastrointestinal (GI) tract. For reasons discussed below, the gills appear to

have the greatest potential for mercury transport irrespective of whether the uptake is passive or active.

(1) Gills.--In addition to their well known respiratory function, the gills also function as the major site for nitrogen excretion (Smith, 1929; Goldstein & Forster, 1961; Goldstein et al., 1964), ion regulation (Smith, 1930; Keys, 1931; Krogh, 1937) and probably blood pH regulation (see reviews by Maetz, 1971, and Motais and Garcia-Romeu, 1972). To attain optimal functional activity, adequate ventilation of both the internal and external surfaces of the gill epithelium is required. On the external surface relatively large volumes of water (31 to 571 ml/min for 210-770 g rainbow trout) continually perfuse the gill epithelium (Holeton & Randall, 1967; Stevens & Randall, 1967; Cameron & Davis, 1970; Davis & Cameron, 1970) and insures that considerable quantities of any water borne pollutant (e.g., mercurials) are exposed to this potential uptake pathway. In addition to a large water flow, the surface area (SA) of the gills is large in comparison to body surface area. Hughes (1966) reports that the total lamellar area for a 175 g brown trout (Salmo trutta) is around 600 cm^2 and Muir (1969) found similar surface area (SA)/unit weight (wt) values for other fish. The gill SA/wt ratio is even higher in some species of marine fish

such as the skipjack tuna (Muir & Hughes, 1969) in which the total surface area for a 100 g fish has been calculated to be 2,620 cm^2. Hughes (1966) found that "more active fish" have larger gill surface areas and conditions for gas exchange are better than in "less active forms." Rainbow trout are considered "active" thus the postulated increase in surface area would in this species further enhance the probability that the gills are sites for mercury uptake.

Exposure of fish to mercury compounds routinely results in very high (up to several thousand times that of the bathing media) mercury concentrations being found associated with gill tissues (Hannerz, 1968; Rucker & Amend, 1969; Backström, 1969). These very high concentrations, however, may not always indicate that mercury is present in gill tissue, i.e., the mercury compound might be adsorbed on the epithelial surface or merely trapped in the mucous coat. Mercury has been shown to enter the gill at a relatively high rate ($0.3\text{-}3.2 \times 10^{-5}$ mg $Hg(NO_3)_2$/hr in perfused eel gills with ambient Hg at 0.74 ppm) (Hibiya & Oguri, 1961). In these experiments the gills were perfused with Key's physiological saline (lack of plasma proteins and red blood cells may affect uptake rates) and whole body uptake was not determined under comparable conditions, so the data presented do not provide definitive proof that

the gill is the primary site for uptake of mercury in teleosts.

Three characteristics (e.g., large transepithelial molecular fluxes, surface area greater than remainder of body, and continual ventilation with environmental water) coupled with demonstrated uptake of divalent mercury provide the gill with many criteria which would enable it to be the major pathway for mercury uptake. There are, however, no conclusive studies reported in the literature to verify this postulate.

(2) Skin Absorption of Mercury.--Friberg & Vostal (1972) have reviewed the literature on skin absorption of mercurials in mammals and their conclusions can be summarized as follows: The skin can serve as a route of entry for both inorganic mercury (such as HgO, $HgCl_2$, and $HgNH_2Cl$) and organic mercury (methyl mercury, dicyandiamide or methyl mercury thiacetamide). Absorption rates for both forms of mercury are slow (maximum of 6% of the total mercury dose absorbed via the cutaneous route by guinea pigs after five hours exposure to either mercuric chloride or mercuric dicyandiamide). Other pathways for uptake during many of the above experiments cannot be excluded, that is, mercury applied topically could enter the body as a mercury vapor or through the digestive tract due to the experimental

animals licking the skin. Silberberg (1968 & 1972) demonstrated that within five minutes after cutaneous applications of mercuric chloride to humans, a gold-mercury reaction product could be detected intracellularly and extracellularly within the stratum corneum by means of electron microscopy. This reaction product was observed to spread deeper and become more concentrated with time (up to 48 hours). Characteristics of the histochemical procedures, however, prevented quantification of the mercury movement and the extent of skin participation.

High molecular weight organic mercurials have also been shown to penetrate the cornea (Ancill et al., 1968). Although descriptions of their experimental methods and results are very abbreviated, they found an increase in blood mercury after topical application of the mercurials on the corneas of rats. Relatively little is known of the movement of molecules across the teleostean skin and to this author's knowledge there are no papers dealing with the subject of mercury absorption by this organ. Even water, which permeates tissues more readily than ions, traverses the skin at a slow rate. Bentley (1962), using his own data and values from the literature, calculated that the time required to move 1 ml of water across 1 cm^2 of membrane (skin) at ΔP of 1 atmosphere was 91 days for

a lamprey, 30 days for a frog, and 5 years for the teleost Anguilla. The teleost skin is approximately 0.016 times as permeable to water as the frog skin. Evans (1969) and Motais et al. (1969), using ^{3}HOH, conclude that compared to the gill, the skin plays a minor role in diffusional water flow. With respect to ions, Knoll (1962) has demonstrated the inability of hexavalent chromium to penetrate the skin of rainbow trout.

In conclusion, while there is no direct evidence on the absorption of mercury compounds by the skin of teleosts, it is probable that although some mercury can be absorbed cutaneously, the efficiency of such absorptive processes must be low and thus relegate this pathway as one of minor importance.

(3) Uptake of Mercury by the Alimentary Tract.-- Uptake of mercury via the digestive system requires: 1) ingestion of mercury into the gut, and 2) absorption of mercury from the lumen of the gut into the blood stream. The latter criteria has been investigated in animals with respect to both inorganic and organic mercury compounds.

Mercury was administered orally as mercuric acetate to rats by Ellis and Fang (1967), who found that with increased doses (from 3 to 9 µg mercuric acetate per rat) the percent of the initial dose of mercury excreted in the

feces after 48 hours decreased from 87.3% to 77.4%. After 168 hours, 97.8% of the 3 µg/rat dose and 88.6% of the 9 µg/rat dose had been recovered in the feces. These results demonstrated that around 13 to 23% of Hg^{++} is either absorbed by the GI tract in 48 hours or retained in the lumen or lumenal boundaries and excreted over a longer time period. Appearance of mercury in the urine at 48 hours suggests the former is in part responsible. Intestinal uptake of Hg^{++} following oral doses of mercuric chloride or mercuric nitrate occurs in rats (Swensson et al., 1959) but low adsorption rates were reported. Alimentary tract absorption of $HgCl_2$ has also been inferred in the dairy cow (Potter et al., 1972) from the appearance of mercury in milk, urine and body organs. This absorption is also probably low in that 95% of the ingested dose appears in the feces; however, absorption and subsequent bilary excretion cannot be ruled out.

In the quail, intestinal absorption of Hg^{++} has also been observed using whole-body autoradiography following 1.0 mg/kg peroral administration (Backström, 1969). Only traces of mercury were found in the body tissues indicating low resorption and no quantitative data were given.

Studies on the quantitative absorption of mercuric salts in the GI tract of teleosts have been limited.

Backström (1969), again using autoradiography and presenting no quantitative data, reported that 10 days following per-oral administration of mercuric nitrate to salmon "large amounts" remained unabsorbed.

Inorganic mercury appears to be poorly absorbed from the digestive tract in all vertebrates studies; however, intestinal absorption cannot be ruled out as an important pathway for mercury uptake in trout.

Organic mercurials, especially methyl mercury, are rapidly absorbed from the digestive system. Friberg and Vostal (1972) have reviewed the recent findings on rats, cats, and monkeys and conclude that more than 90% of the ingested mercury is absorbed via this pathway. The absorption is the same irrespective of the form of methyl mercury, i.e., methyl mercuric chloride or protein bound methyl mercury. They also report that in humans, absorption of either form of methyl mercury is nearly complete.

Study of GI absorption of methyl mercury (as well as inorganic mercury) by fish is hindered by three problems: 1) mercury must be rapidly and completely ingested to prevent increased mercury concentrations in the ambient water and thus expose the mercury to other routes of entry, 2) routinely, when mercury is force-fed, all or part of the bolus is regurgitated (Miettinen, J. K., et al., 1969;

Miettinen, J. K., et al., 1970; Miettinen, V. et al., 1970; and Jarvenpaa et al., 1970), and 3) if mercury is fed to a "food chain" animal which is in turn fed to a fish, the mercury might not retain its original chemical characteristics and absorption rates would not typify the compound in question. In spite of these problems, the general consensus is that organic mercury, especially methyl mercury, is rapidly absorbed by the gut of teleosts. Low fecal excretion rates, down to 8% of the administered dose, accompanied by high tissue levels following forced feeding of methyl mercury or other Hg-organics, support this contention.

If the hypothesis can be accepted that methyl mercury (and to a lesser extent mercuric chloride) is absorbed by the GI tract, then an indication of the contribution of this pathway to total uptake can be ascertained from measurements of the amount of mercury "carrier" viz., environmental water, which reaches these tissues. Drinking rates of teleosts would thus reflect exposure of the GI mucosa to mercury solutions and thereby provide an index of contribution of this pathway to the total mercury uptake rate. Drinking rates in salt water fish have been reported to be from 40 to 200 ml salt water/kg/day for an eel or sculpin (Prosser, 1966); whereas, freshwater species such as rainbow

trout drink little if any water (Shendadeh and Gordon, 1969). Other evidence indicates, however, that freshwater adapted eels do in fact drink water with regularity. Maetz and Skadhauge (1968) using ^{131}I phenol red as a tracer calculated the drinking rate of an eel in fresh water to be 13.5 + 27.7 µl/hr/100g for 17 fish. Even at this rate only 3.24 ml of water would enter the stomach in a 24 hour period and this would hardly account for the high tissue to water mercury ratios (of up to 2,000:1 after 10 days exposure) as reported by Hannerz (1968).

The high absorptive capacity of the GI tract for mercury suggests this tissue could be of prime importance as a pathway for mercury uptake; however, the relatively low drinking rates found in freshwater teleosts would severly limit the quantity of mercury delivered to the absorptive site. Under stressful conditions such as mercury exposure, drinking rates might change and increase the importance of this uptake route.

Secondary Uptake Pathway

Subsequent to its entry into a fish, mercury is distributed to the various organs of the body as demonstrated by tissue accumulation of mercury after im, iv, or ip injection or oral administration. The most probable carrier

during this distribution process is the blood. Mercury can be transported in either the plasma or cells and its relative disposition appears to be more dependent on the chemical form of mercury (organic or inorganic) than on the species investigated.

Inorganic Mercury: Hg^{++}.--Distribution of the inorganic mercuric ion generally favors the plasma fraction although much variation has been reported. In humans, Swensson et al. (1959, p. 432) found the plasma mercury/whole blood mercury ratio for $Hg(NO_3)_2$ to be 0.80, whereas Lundgren et al. (1967) reported an equal distribution between blood and plasma fractions. Rahola et al. (1971) and Miettinen (in press, quoted by Friberg & Vostal, 1972) gave RBC/plasma ratios ranging from 0.4 to 1 in humans following oral ingestion of ^{203}Hg labeled proteinate. Swensson et al. (1959, p. 467) report that in rats "nearly all of the Hg^{++} appears in plasma," however, no data were presented. Ulfarvson (1962, quoted in Norseth & Clarkson, 1970) reported equal distribution of mercury in the same species. Somewhat different distribution has been reported for the cow by Potter et al. (1972). Calculations using their data indicate that 86% of the Hg^{++} (given orally as $HgCl_2$) is carried by the red blood cells.

Mercuric ions penetrate the red cell slowly (equilibrium achieved after two hours in the rabbit, Berlin & Gibson, 1963) if whole blood is used as the incubation medium. Penetration is extremely rapid (equilibrium under 5 min., Weed et al., 1962) if red cells are washed to remove plasma proteins and then suspended in Ringer solution. Thus plasma proteins appear to be involved in binding the mercury and establishing an equilibrium (mercury-plasma protein $\rightleftharpoons$ red cell (protein-mercury) with a characteristically slower uptake of Hg by red cells than would be seen if mercury was exposed to red cells in a nonprotein environment.

Relatively little information is available pertaining to inorganic mercury uptake by non-mammalian blood. Backström (1969) reported that in the quail the ratio of mercury between the cell and plasma fractions after injection of $Hg(NO_3)_2$ is about 0.8. He found this ratio to be fairly constant from 10 min to 10 days after injection which would imply a rapid attainment of equilibrium. He also reported that less than 1% of plasma ^{203}Hg activity remained in solution after protein precipitation with alcohol. To the author's knowledge there are no reports in the literature on the binding of inorganic mercury compounds by teleost blood.

Organic Mercury Compounds.--Transport of organic mercurials in blood is generally agreed to be effected by the cellular components irrespective of the species from which the blood was sampled or the organic mercurial in question. In rats, mercury administered as phenyl mercuric acetate, methyl mercuric hydroxide or cyano (methyl mercuri guanidine) is distributed almost exclusively in the red cell (Swensson et al., 1959, 1967). Also in rats, Norseth and Clarkson (1970) found a whole blood to plasma ratio of mercury of about 271 to 1 after iv injection of methyl mercuric chloride. This ratio remained fairly constant even if the mercury was injected ip and it remained steady over the experimental concentrations studied (1 to 10 mg Hg/kg). Methyl mercury is also tightly bound to the red cells and even after 10 days there was still 23% of the injected dose of mercury in the blood compared to 6 and 7% in the liver and kidney respectively. In the dog, rabbit and human, 75, 80, and 90% respectively of the methyl mercuric hydroxide is bound to the red cell (Swensson et al., 1959, p. 432). These authors report that in the rabbit, erythrocyte binding of mercury is weak, as demonstrated by a rapid loss of 80% of the mercury from the blood to the tissues without any accompanying change in percent mercury bound to the red cell.

Backström (1969) has described a similar red cell affinity for organic mercurials in quail blood. He found that the ratio of mercury between blood cells and plasma, 10 min., 1 hour, 1 day and 10 days post iv injection remained relatively constant for methyl mercury (12.7, 32.5, 28.2, and 28.7) and decreased for phenylmercury (16.5, 26.2, 1.6, and 0.5) and methoxyethyl mercury (5.3, 4.4, 1.1, and 0.3). All (99% or more) mercury in the plasma fraction was protein bound.

Rucker and Amend (1969) reported the distribution of ethylmercuric phosphate in rainbow trout to be mainly in the cellular fraction with only traces in the serum; however, no quantitative data were presented.

Again, lack of literature pertinent to binding studies of organic mercurials, especially methyl mercury, precludes definitive agreement on its disposition. From data obtained using higher vertebrates it may be inferred that when present, organic mercury should be mostly in the cellular fraction of fish blood and inorganic mercury (Hg^{++}) is either evenly distributed between cells and plasma or primarily in the plasma fractions. These extrapolations and assumptions may or may not be warranted.

Effects of Mercurials on Tissues

Biochemical Effects

The chemistry and biochemistry of the various inorganic and organic compounds has been reviewed extensively by Webb (1966) and is beyond the scope of this thesis. For general perspective, a brief summary of some biochemical properties of inorganic mercury (Hg^{++}) and monomethyl mercury (CH_3Hg^{+}) are listed below:

1. Specificity of both mercurials for sulfhydryl (SH) enzymes is great, and, more often than not, SH groups are in some way related to enzyme function which could be altered by mercurial interactions.

2. Hg^{++} mercurials co-react with two SH groups: CH_3Hg^{+} reacts with only one (see No. 8).

3. Simple amines, amino acids (especially SH amino groups), nucleotides and nucleic acids form complexes with Hg^{++}.

4. Hg halides are more soluble in water than organic mercurials and the reverse is true in organic solvents. Thus the organic mercurials can penetrate cell membranes more readily.

5. Inorganic mercurials are smaller than the organic molecules and as such are more likely to bind with SH groups within an enzyme and are less affected by steric hindrance.

6. The affinity of organic Hg for ligands is slightly greater than that of inorganic compounds; however, this difference is probably of minor importance.

7. The C-Hg bond is relatively weak, 15-19 kcal/mole, and it is quite possible that many effects attributed to organic mercurial compounds may be actually due to Hg^{++}.

8. Several inorganic Hg and organic Hg combinations with monothiols and dithiols are shown below. This variety of reactions enhances the probability of protein SH interaction and subsequent enzymatic or structural dysfunction.

	Organic mercurial combinations	Inorganic mercurial combinations
Monothiols	$R'-Hg^{+}$	Hg^{++}
$R-SH$	$R-SHg-R'$	$R-S-Hg^{+}$
		$R-S-Hg-S-R$
Dithiols		
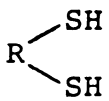	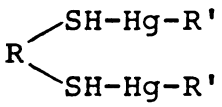	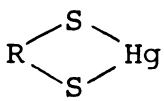
		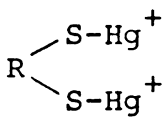
		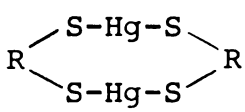
		$(-R-S-Hg-S-)_n$

9. Affinity of mercurials for SH groups is greater than for any other single ligand thus in a mixture with thiols and other complexing ligands the mercurial will be primarily associated with the thiol.

10. Reactions of either of the mercurials with -S-S- bonds of most protein molecules at physiological conditions generally do not occur.

11. Mercurial-protein combinations are stoichiometric and do not necessarily result in protein precipitation or denaturation.

12. Mercurial-SH protein bonds are usually not as strong as mercurial-thiol bonds and thus mercury can be freed from a protein by addition of a thiol.

13. Mercurials are capable of binding to non-SH sites on proteins possibly COO^- or CONH groups.

14. Enzyme inhibition by mercurials is generally through formation of enzyme-mercurial complexes and not through nonspecific denaturation and precipitation. Inhibition can be due to mercurial bond to a SH group on or near the active or catalytic site of the enzyme or due to conformational changes in secondary, tertiary or quaternary structure.

15. Low concentrations of mercurials may act to increase enzyme activity.

16. Mercurials at the concentrations given have been shown to inhibit one or more enzymes in the following biochemical pathways: Glycolysis (1 mM), TCA cycle (0.01 mM), ATPase, electron transport and oxidative phosphorylation (0.001 mM), lipid synthesis (0.1 mM), protein synthesis (5 mM), porphyrin synthesis (0.04 mM), bioluminescence, photosynthesis (0.005 mM), active glucose and ion transmembrane transport and diffusion,

erythrocyte hemolysis, generalized inhibitory effects on mitosis, growth and differentiation.

Physiological and Morphological Effects

Gills.--Histopathological changes in gill epithelium after exposure to mercurials has been noted by several investigators. Characteristically, the changes followed exposure to high doses of the mercurial and were observed using standard light microscopic techniques.

In general, both inorganic and organic mercurials produce marked hyperplasia and hypertrophy of gill epithelial cells with occasional separation of the epithelial layer from the supporting cells. Table 1 summarizes these observations.

Impairment by mercurials of physiological functions performed by the gill has received little attention. In the only reported study of this nature, Meyer (1952) described effects of mercuric ion on ion fluxes across goldfish gills. He reported that 10^{-5} M Hg^{++} (approximately 2 ppm) administered as $HgCl_2$ completely inhibited active sodium uptake by the gills and caused a 10-fold increase in branchial passive sodium loss. A 10-fold reduction of the mercury concentration (10^{-6} M Hg^{++}) depressed active sodium uptake by 25% from the control and

Table 1.--Effect of mercurials on gill structure.

Chemical form	Concentration	Fish studied	Hyperplasia	Hypertrophy	Epithelial separation	Source
Ethyl mercury phosphate	0.125 ppm 1 hr exposure per day	Rainbow trout		+	+	Amend et al., 1969
Methyl mercury	Average of 13.6-24.7 mg Hg/kg (oral ingestion)	Pike	General	Gill necrosis		Miettinen, 1970
Methyl mercury	∿ 10 mg Hg/kg (oral ingestion)	Rainbow trout	No gill damage			Miettinen, 1970
Ethyl mercury phosphate	125 ppm 1 hr exposure per day Total 4-11 exposures	Rainbow trout	+	+		Rucker and Amend, 1969
Hg^{++}	Not given	Carp		+		Schweiger, 1957

increased sodium loss by 43% over the control. No other studies on mercury induced pathophysiology of the gill have been reported.

Blood.--Physiological effects of mercurials on erythrocytes have been studied in detail; however, the primary objective of the research in this area has been the localization and identification of various sulfhydryl groups either associated with the red cell membrane or within the cell. Frequently differentiation of SH groups has been accomplished by the use of various high molecular weight organic mercurials which penetrate the cell membrane to different degrees depending on molecular weight and side chain characteristics. Inorganic mercury compounds have also been used, but there is no data on methyl mercury salts.

Inorganic mercury (around 10^{-5} M $HgCl_2$) produces increased potassium loss from rabbit erythrocytes (Joyce et al., 1954; Vincent and Blackburn, 1958; Weed et al., 1962). Concomitant with the K^+ loss Weed et al. (1962) has described inhibition of active glucose uptake by these cells.

Organic mercurials such as chlormerodrin (CM), parachloromercuribenzoate (PCMB), parachloromercuribenzenesulfonate (PCMBS) and parachloromercuriphenylsulfonic acid (PCMPS) affect ion fluxes and glucose absorption in

erythrocytes. In the human, CM, PCMB, and PCMBS inhibit active or facilitated transport of many sugars and amino acids into red cells (VanSteveninck et al., 1965; Martin, 1971) and produce potassium loss, sodium accumulation and hemolysis of the cells (Sutherland et al., 1967; Shapiro et al., 1970; Knauf, I and II, 1971). These authors indicate that sulfhydryl groups on the interior of the red cell membrane are active in the regulation of cation flux and that anion flux is governed by membrane protein amino groups near the exterior of the membrane. This would account for the lack of effect of mercurials on anion fluxes. PCMB has also been shown to readily dissociate the α and β chains of hemoglobin (Bucci, 1965) and this technique is now used routinely for such purposes. In spite of the actions of mercurials on red cell sulfhydryl groups, none of the organic mercurials studied decrease the oxygen carrying capacity of blood. In fact, PCMB, 2 chloromercuri-4-nitrophenol and 4 chloromercuri-2-nitro phenol have been shown to slighly increase the amount of oxygen carried by hemoglobin (Webb, 1966; Giardina et al., 1971).

Histological effects (other than hemolytic studies) of mercurials on erythrocytes has received surprisingly little attention. Kostenko and Iakouleva (1971) described a change in mouse erythrocyte shape after exposure to

mercuric ions. These authors reported increasing concentrations of Hg^{+} up to 10^{-5} M initially caused the cells to become crenated in shape, but without loss of volume. As the Hg^{++} concentration approached 10^{-5} M the cells became spherical and somewhat swollen. Very rapid hemolysis was observed at 10^{-4} M Hg^{++}.

Mercurials have variable effects on the red cell in vivo. Yamaguchi (1969) has shown that both hemoglobin concentration and red cell count decreased after administration of either one-third or one-fifty LD_{50} of ethyl mercuric phosphate. The author, however, failed to mention what the LD_{50} was. Erythrocytes from rainbow trout exposed to 0.125 ppm ethyl mercury phosphate (EMP) one hour daily for eleven days appeared normal even though the blood mercury concentration was near 23 ppm and gill tissues from the same fish exhibited extensive hypertrophy and hyperplasia (Rucker and Amend, 1969). The authors also reported that twelve weekly, one hour exposures to 0.125 ppm EMP produced gill hyperplasia with no concurrent red cell abnormalities. Miettinen, V. et al. (1970) observed that after ingestion of around 10 mg methyl mercury per Kg body weight, the spleen of rainbow trout became swollen and darker than normal. These authors postulated erythrocyte damage.

Summary

The environmental mercury problem is a well appreciated fact; however, the effects of sublethal concentrations of this all too common pollutant on aquatic animals, and especially teleosts, are virtually unknown. Much of the mercurial induced pathophysiology and pathomorphology can only be deduced via extrapolations from mammalian experiments which involved chemical forms of mercury not routinely encountered in polluted waters. Considering the obvious differences between mammals and fish and possible chemical dissimilarity between the small molecular weight mercurials commonly associated with pollution and larger organic mercurials utilized in the mammalian experiments, such inferences can only be tenuous at best. Universality of sulfhydryl groups associated with enzymes and preponderant interactions of mercury with sulfhydryl groups promulgate the need for adequate assessment of the physiological consequences of mercury on aquatic organisms.

MATERIALS AND METHODS

Experimental Animals

Rainbow trout (Salmo gairdneri) were obtained from the Department of Natural Resources, Fish Research Laboratory at Grayling, Michigan, and from the Great Lakes Fishery Laboratory, Bureau of Sport Fisheries and Wildlife at Ann Arbor, Michigan. They were transported to East Lansing, Michigan, in an insulated metal tank, the lining of which had previously been coated with nontoxic paint. Viability of the fish was insured en route by oxygenation of the water with mechanical aerator and the addition of ice to keep water temperature near the optimal 13° C. At Michigan State University the trout were maintained at 13 ± 1° C in 120 gallon fiberglass tanks under a 14 hour daily photoperiod. Water in the holding tanks was aerated and continually flushed with tap water from which iron and chlorine had been removed. Commercial trout pellets 3/16 inch) were fed to the fish biweekly.

Exposure Protocol

Trout (60-200 g) were exposed to various concentrations of either CH_3HgCl or $HgCl_2$ in 100 liter tanks. To

prevent build-up of toxic ammonia and to maintain the mercury concentrations, 80% of the water was removed daily and replaced with aged tap water containing the appropriate mercury concentrations. Exposure schedules applicable to the respective experiments were as follows:

Dose	Duration (days)	Experiment
		$HgCl_2$
0.25 ppm	24 hrs[1]	Microprobe, SEM, TEM, and Light Microscopy[2]
0.25 ppm	72 hrs[1]	SEM, TEM, and Light Microscopy
0.25 ppm	5 days[1]	Microprobe, SEM, TEM, and Light Microscopy
0.05 ppm	40 days	SEM, and Light Microscopy
275.0 ppt	24 hrs	Isotope Tissue Distribution Experiment and Radioautography
		CH_3HgCl
300.0 ppt	28 days[3]	SEM, TEM, and Light Microscopy
300.0 ppt	56 days[3,5]	SEM, TEM, and Light Microscopy
0.05 ppm[6]	24 hrs[4]	Microprobe, SEM, TEM, and Light Microscopy
0.05 ppm[6]	5 days[4]	Microprobe, SEM, TEM, and Light Microscopy
275.0 ppt[6]	24 hrs	Isotope Tissue Distribution Experiment and Radioautography

[1]Dose equivalent of Hg salt added 1 hr prior to tissue sampling for microprobe studies only.

[2]SEM = Scanning electron microscopy; TEM = Transmission electron microscopy.

[3]Fish exposed at Ann Arbor to methyl mercury through the courtesy of Drs. Robert E. Reinert and Wayne Willford.

[4]Dose equivalent of Hg salt added to tank 1 hr prior to tissue sampling.

[5]Exposed to mercury at 5° and 15°.

[6]ppm = parts per million (mg/Kg); ppt = parts per trillion (ng/Kg).

Radioisotope Methodology

Radioactive mercury, as either $^{203}HgCl_2$ or $CH_3{}^{203}HgCl$, was obtained from ICN Chemical and Radioisotope Division, Irvine, California. The specific activity for each compound was indicated with each shipment and assumed to be correct as direct mercury analysis in the laboratory was not available. Detection of the 0.279 Mev gamma radiation was achieved either with a two-inch thallium activated sodium iodide NaI(Tl) crystal Model DS 202(v) well detector and activity displayed on a Model 8725 Analyzer/Scaler, both from Nuclear-Chicago, Des Plaines, Illinois, or with a multichannel analyzer and automatic 100 tube sample changer also from Nuclear-Chicago. Use of the multichannel analyses and tube changer system was through the courtesy of Dr. Niles Kevern and Mr. James Seelye of the Department of Fisheries and Wildlife, Michigan State University. Constant counting geometry was not always possible during the various experiments. Correction for this was made by counting known amounts of the isotope under the various geometries encountered and determination of the respective counting efficiencies. During routine counting the window width was centered around the 0.279 Mev gamma peak. The region of interest was determined by multichannel analysis to give a high peak to background ratio.

The amount of mercury in a given experiment was determined by the equation:

$$mgHg = \left(\frac{\frac{cpm_o}{\% \text{ efficiency}}}{2.22 \times 10^9 \text{ dpm/mCi}} \right) \left(\frac{mgHg}{mCi} \right)$$

Where: cpm_o = counts per minute at t_o (time at which specific activity determinations were made at ICN)

% efficiency = calculated efficiency at constant geometry

mgHb/mCi = specific activity of the Hg at t_o

cpm_o is in turn calculated from the formula:

$$cpm_o = \frac{cpm_t}{e^{-\lambda t}}$$

Where: cpm_t = the counts at time of experiments

$\lambda = 0.693/46.6$

t = time between t_o and experiment (in days)

46.6 = $t_{1/2}$ for ^{203}Hg

Blood Studies

Blood samples were collected from the caudal vein by insertion of 1-1/2 inch 21 gauge needle into the ventral

side of the haemal arch approximately 0.5 cm distal to the anal fin. Two or three ml of blood were then slowly drawn into a heparinized syringe. Blood experiments were initiated within two hours after the blood sample was taken. All glassware used in conjunction with ^{203}Hg-blood studies was coated with silicone (Siliclad®, Clay Adams, Inc., New York, N.Y.) to prevent adsorption of ^{203}Hg onto the glass.

Hematocrit and Hemoglobin Determinations

Heparinized microhematocrit capillary tubes (Division American Hospital Supply Corp., Miami, Fla.) containing aliquots of blood used during each experiment were centrifuged for 3 min at 11,500 rpm on an IEC Model MB Microhematocrit centrifuge. Percent red cell volume was determined with an IEC Circular Microcapillary Tube Reader.

Hemoglobin concentrations were determined by the cyanmethemoglobin method (Oser, 1965). Twenty µl of blood were added to 5 ml of cyanmethemoglobin reagent (Hycel, Houston, Tex.) and compared spectrophotometrically (B & L Spectronic 20 Colorimeter, Rochester, N.Y.) to known hemoglobin concentration standards (cyanmethemoglobin certified standards, Hycel, Houston, Tex.). The unknown hemoglobin concentrations were then calculated from the formula:

$$\text{Hb concentration}_{\text{unknown}} = \frac{\text{O.D. unknown (Hb conc. of standard)}}{\text{O.D. standard}}$$

Mercury Uptake by Red Blood Cells (Uptake Rate)

The rate of mercury uptake by red blood cells was determined by incubating either whole blood or washed cells with $^{203}HgCl_2$ or $CH_3{}^{203}HgCl$ at 14° C for various time periods. Heparinized whole blood (2.2 ml) or 2.4 ml washed cells (0.40 ml cells washed 3 times in 3 volumes Ringer and resuspended in 2 ml Ringer or phosphate Ringer--see Appendix I for composition of Ringer solutions--was placed in a 25 ml stoppered Erlenmeyer flask. The mercury solution was added to the blood at time zero and the flask stirred at 16 rpm with a multipurpose rotator, model 150V (Scientific Industries, Inc., Springfield, Mass.). At timed intervals 0.20 ml of blood was removed and immediately placed in a 0.4 ml polyethylene microcentrifuge tube (A. H. Thomas, Phila., Pa.) and centrifuged in a Beckman Microfuge Model 152 (Fullerton, Calif.). The supernatant was drawn off and placed in a second microcentrifuge tube. The packed red cells were then resuspended in Ringer solution, centrifuged and this supernatant "wash" was placed in a third microcentrifuge tube. The concentration of mercury in the packed red cells, plasma (or Ringer) and

wash solution in the microcentrifuge tubes was determined by scintilation counting. The percent uptake of mercury into the cellular fraction was corrected for equal volumes of red cells and plasma and calculated according to the following formula:

$$\% \text{ incorp. into RBC} = \frac{\frac{1-Hct}{Hct}\,(\text{activity in red cell fraction})}{\frac{1-Hct}{Hct}\,(\text{activity in red cell fraction}) + (\text{activity in plasma fraction}) + (\text{activity in wash})} \times 100$$

The percent uptake vs. time was plotted. Component analysis of the equilibrium curve and flux rate determinations are given in Appendix 2.

If mercury is bound to the red cells it must exhibit certain binding characteristics (i.e., it must have an affinity for the red cell), there must be a quantity of binding sites which can be saturated and there must be certain chemicals which inhibit mercury binding to the red cell either through competition for the binding site on the hemoglobin or through binding of the mercury to the inhibitor, thus sequestering it (Hg) from the solvent.

Binding Characteristics

The binding characteristics of mercury as CH_3HgCl and $HgCl_2$ was determined on washed red cells suspended in

Ringer solution by incubating the cells with various concentrations of mercury for 90 minutes (equilibrium conditions were reached in this time period). Following incubation the suspended cells were centrifuged, washed, and the percent activity in the cellular fraction determined as described above. The radioactive mercury was diluted with non-radioactive mercury of the same molecular form to maintain the total amount of ^{203}Hg constant. The mercury concentrations used in the medium (Table 2) are calculated both in terms of ppm in the total cell-Ringer mixture and as ppm in the red cell volume only.

Table 2.--Ambient mercury concentrations.

Methyl mercury (CH_3HgCl)						
ppm total	0.0133	0.133	1.133	10.133	100.1	1000
ppm (mg Hg/l RBC)	0.0947	0.947	8.09	72.38	715.0	7144
Inorganic mercury $HgCl_2$						
ppm total	0.054	0.540	1.454	14.05	140.05	
ppm (mg Hg/l RBC)	0.387	3.87	10.39	100.4	1000.0	

Note: Mercury concentrations lower than those used were not possible due to lack of sufficient total ^{203}Hg necessary for reliable counts, and higher concentrations produced RBC hemolysis.

This facilitates comparison of environmental blood mercury analysis (ppm whole blood) and gives an idea of the mercury concentration "seen" by the red cell (this is usually most important with respect to mercury uptake by cells, Vincent and Blackburn, 1958).

The binding affinity of the two mercury compounds at various concentrations was tested by adding sulfhydryl agents to red cells previously equilibrated for 90 mins with mercury. Sulfhydryl agents selected were 1.37×10^{-5}M bovine albumin (Mann Res. Labs, N.Y., N.Y.), 1.37×10^{-4}M l-cysteine (Sigma Chem. Co., St. Louis, Mo.) and 1.37×10^{-4}M reduced glutathione (Sigma Chem. Co.). Red cells and sulfhydryl agents were incubated an additional 90 minutes after which the percent mercury in the cellular fraction was determined.

Oxygen-Carrying Capacity--
Effect of CH_3HgCl and $HgCl_2$

The oxygen carrying capacity of red blood cells exposed to various concentrations of organic and inorganic mercury was determined using the method of Klingenmaier et al. (1969) as modified by Hoffert (in press). This technique allows measurement of red cell oxygen content by determination of the increase in oxygen tension following

oxygen release by exposure to carbon monoxide. Change in oxygen tension is monitored with an oxygen electrode.

Apparatus for CO Saturation of Ringer Solution.--Approximately 400 ml phosphate buffered Ringer solution was placed in a pyrex gas washing bottle (tall form with frittered disc, Corning Glass Works, Corning, N.Y.) and deoxygenated by bubbling nitrogen through it for 8-10 hours. After deoxygenation 200 ml of this solution was flushed into a round bottom flask containing 100% CO (Matheson Gas Co., Joliet, Ill.). Saturation of the Ringer solution with CO was accomplished in 2 to 3 hours by flushing the system several times with fresh CO and mixing with a magnetic stirrer. Prior to each day's experiment 30-40 ml of the CO-saturated Ringer was drawn off into a 50 ml glass syringe and placed in the cold room to equilibrate to 15° C. The luer end of the syringe was fitted with a two-way stopcock and a 2.5 ml glass syringe minus the barrel which permitted rapid sampling of the CO-Ringer solution by introduction of a small volume into the 2.5 ml syringe without contamination of the entire Ringer solution with room air.

Blood Incubation.--Washed red cells (0.15 ml) were added to 1.0 ml of phosphate buffered Ringer containing

0.1 or 100 ppm Hg as $HgCl_2$ or CH_3HgCl and incubated either with room air or low PO_2 gas for 3 hours. Regulation of the low PO_2 environment was achieved by a constant flow of 6% oxygen, 94% nitrogen gas saturated with water over the cells. Mixing of the cells was accomplished by use of a shaker (L. Olson, Ph.D. Thesis, 1969).

Liberation of Oxygen from Red Cells.--At the end of the mercury incubation period a sample of known volume was taken, mixed with CO-Ringer for 1 min and the oxygen tension determined. Collection of the blood and CO-Ringer was by means of a 1 cc syringe fitted with a blunt 18 gauge needle which in turn was inserted into approximately 4.5 cm of intramedic polyethylene tubing, PE 190. After all air and liquid was eliminated from the syringe by a mercury (metallic) plug, blood was drawn into the PE tubing until the Hg-blood interface reached the needle. The PE tubing was then inserted into the 2.5 cc syringe and CO-Ringer drawn into the 1 cc syringe until the plunger volume was at 0.6 ml. The solution was then mixed. The exact volume of blood and CO-Ringer taken up was determined by filling the syringe to the appropriate mark with mercury and then weighing the syringe and calculating the volume of mercury contained. Correction was also made for the mercury plug.

Oxygen Tension Determinations and Calculations.-- Oxygen tension in the solution after release by the red cells was determined on a blood gas analyzer Radiometer BMS 3 Blood microsystem with PHM 71 Acid Base Analyzer equipped with P_{O_2} and P_{CO_2} modules (Radiometer, Copenhagen, Denmark). Blood incubations as well as P_{O_2} determinations were carried out in the cold room (15° C) during the $HgCl_2$ study. The blood gas analyzer was calibrated prior to each determination with air saturated water (20.95% O_2) and 0% oxygen solution (P_{O_2}-zero solution type 10-S4150, London Co.). The procedures used in calibration and sample determination were as described in the London Technical Manual with the exception that due to the low working temperature, response time was extremely long and therefore it became necessary to read the sample on the analog read-out at 4 minutes after introduction into the P_{O_2} electrode. Although this procedure was not ideal, reproducibility was good enough (± 2 mm Hg) to warrant its use. Blood incubation with CH_3HgCl was also at 15° C, but the radiometer was calibrated and maintained at 37° during the experiment.

The oxygen carrying capacity was calculated using the following formula (Klingenmaier et al., 1969):

$$C_{O_2} = \frac{100 \cdot \lambda}{U \cdot P_B} \cdot P_2V - P_1(V-U)$$

Where: C_{O_2} = oxygen content (ml/100 ml)

P_B = barometric pressure corrected for water vapor

P_1 = partial pressure of oxygen in the CO-Ringer

P_2 = partial pressure of oxygen in 1 cc diluting syringe

U = volume of PE tubing

V = total volume of diluting syringe at 0.6 cc mark minus Hg plug

λ = solubility of oxygen in Ringer at 15° C = 0.034

For comparisons within each experiment, the volume of oxygen is expressed in terms of ml O_2/g Hb. Since only the effects of mercury on O_2 carrying capacity were of interest, no attempt was made to correct for the higher Radiometer temperatures used in the methyl mercury experiment.

Gill Histology

Light Microscopy

The first and third pair of gill arches were excised from control fish and fish exposed to various concentrations of both CH_3HgCl and $HgCl_2$ (see exposure schedule) and fixed for 48 hours in Detrich's fixative (see Appendix I). Tissues were dehydrated in tetrahydrofuran (Fisher Sci. Co., Fairlawn, N.J.), vacuum embedded in Paraplast (A. H. Thomas,

Phila., Pa.) and sectioned at 8μ. One-half of the sections were stained with hematoxylin and eosin and the remainder with Alcin blue (ph 1.0 method) for identification of sulfated mucosubstances. Both procedures are described in the Manual of Histologic Staining Methods of the Armed Forces Institute of Pathology (Luna, 1968).

Transmission Electron Microscopy

Filaments from the second arch on the right side of the fish were excised and fixed at 4° C in glutaraldehyde (Fisher Sci. Co.) diluted to 4% or 6% with Sørensen buffer (see Appendix III). The second arch was chosen for all TEM and SEM work because this arch is normally exposed to the greatest volume of water during normal respiration (Paling, 1968). After fixation for 3-6 hours the tissues were rinsed twice (30 min each) in Sørensen buffer solution and post fixed in 1% osmium tetraoxide (OsO_4) for 3 hours. (As tissue stains for electron microscopy are of necessity electron dense, an attempt was made to use mercury as a supravital stain, thus some tissues were neither post fixed with OsO_4 nor stained after sectioning.) Following post fixation the tissues were dehydrated in graded concentrations of either ethanol or acetone and embedded in Spurr's low viscosity embedding media (Polyscience Inc., Warrington,

Pa.). Sections approximately 600A thick were cut with a Sorvall MT2-B "Porter-Blum" ultra-microtome (Ivan Sorvall, Inc., Norwalk, Conn.) mounted on 300 mesh copper grids and stained with uranyl acetate (UA) (Watson, 1958) followed by lead citrate (LC) (Reynolds, 1963). Thick sections (2-3μ) of the same area were cut and observed under phase contrast microscopy for orientation purposes.

Transmission Electron Microscopy was done on a Philips EM 300 Electron Microscope (Philips Electronic Instruments, Mt. Vernon, N.Y.). Accelerating voltage of 40-60 KV was used for all stained specimens and 20 or 40 KV accelerating voltage for unstained tissues. Photomicrographs were recorded on Kodak Electron Microscope film, ESTAR, thick base, 3-1/4 x 4 inches (Eastman Kodak Co., Rochester, N.Y.).

Scanning Electron Microscopy

The second gill arch on the left side was routinely used for all SEM studies. After removal from the fish the arch was fixed for 6 hours at 4° C in either 4% glutaraldehyde-Sørensen or 50% glutaraldehyde stock solution. Preliminary studies showed that when 4% glutaraldehyde was used most of the lamellar surface was coated with mucus (see Figure 9B). Fifty percent glutaraldehyde prevented

the mucus coat and produced no significant change in the appearance of the ultrastructure of the lamella and it was used exclusively in latter experiments. After fixation the gills were rinsed 6 times in Sørensen buffer (30 min each) and dehydrated by freeze-drying (Atmo-Vac Freeze Dryer, Refrigeration for Science, Inc., Island Park, N.Y.) or by the critical point drying method (DCP1 Critical Point Dryer, Denton Vacuum Inc.). See Appendix IV for both methods. As critical point dried tissues are generally superior to the freeze-dried specimens (Anderson, 1951, and Horridge & Tomm, 1969) in terms of ultrastructure preservation, this method was used whenever possible. Filaments from the dry gill arches were dissected free from each other and glued with Duco cement (E. I. du Pont de Nemours and Co., Wilmington, Del.) to a 12 mm glass cover slide, lamellar side up. The tissue and slide were then glued to aluminum stubs with an electron conducting cement and coated with carbon (approx. 100-200A thick) and gold palladium (100A) in a Ladd evaporator (Ladd Research Industries, Inc., Burlington, Vt.). They were then placed in an AMR Model 900 Scanning Electron Microscope (Advanced Metals Research, Burlington, Mass.) for observation. Photomicrographs were recorded on Polaroid Type N/P positive-negative film.

Electron-Microprobe

Sample Preparation.--The second pair of gill arches from fish exposed to pharmacological concentrations of either methyl mercuric chloride or mercuric chloride were removed within 15 sec after the fish was killed and quick frozen in isopentane (2 methyl butane, Eastman Kodak Co.) cooled to near -160° C with liquid nitrogen. Frozen tissues were then mounted on a brass stub and embedded with Ames O.C.T. compound at -30° C (Ames Company Division, Miles Labs., Inc., Elkhart, Ind.). Originally tissues were embedded in ice; however, sectioning was difficult due to crystal rearrangement and subsequent shattering. This was overcome by using the O.C.T. compound which sections easily at -30° C. Four or ten micron frozen sections were cut on a Model CTD-International Harris Cryostat (International Equip. Co., Needham Heights, Mass.) and fastened with Eastman 910 adhesive (Eastman Chemical Products, Kingsport, Tenn.) to either quartz slides or carbon discs. Standard glass slides could not be used as the high amounts of impurities they contain would produce excess background radiation in the microprobe. After the 910 adhesive had polymerized (1-3 hours) the tissues were freeze dried for 36 hours. Although all tissues were stored in a dessicator

until just prior to examination, care was taken to schedule the experiments such that no more than 12 hours elapsed between completion of freeze drying and initiation of the microprobe studies to prevent small molecular weight ion shifts due to tissue rehydration. Small crystals of $HgCl_2$ were glued to a corner of each slide in such a position that they were at least 5 mm from the tissues. These crystals were subsequently used to localize the L and M peaks in the microprobe.

Microprobe Analysis.--Dried tissues were carbon coated (about 100A thickness) with a varian model VE10 evaporator to reduce mercury evaporation and placed in an ARL Microprobe, Model EMX-SM (Applied Research Laboratories, Sunland, Calif.). Accelerating electron voltage ranged up to 30 KV with the elements in question and was generally in excess of 23 KV with the mercury analyses. Elemental analyses were accomplished either by a tissue scan (for characteristic x-ray emission) which was then compared to an image scan (secondary electron detection) of the tissues or by a single line scan with x-ray activity plotted on a x-y recorder as a function of distance across the tissue. The tissue scan and image scan micrographs were recorded on Polaroid 200 black and white film and the

line scan recorded on a Hewlett Packard x-y recorder. Low peak to background ratios and inherent difficulties with the L and M line spectra of mercury made the tissue scan procedure questionable for this element; however, line scan procedures proved adequate. Line scan and tissue scan procedures were also used for detection of other elements as both an aid in tissue orientation and a check on diffusional ion movements which might have occurred during sample preparation. The small (0.5μ) diameter of the primary electron beam permits fairly high resolution of ions with a given area especially with the line scan procedure. All ion analyses were qualitative in nature and only semi-quantitative due primarily to the existing state of the art (Rasmussen et al., 1968) and partially to the tremendous time requirements for quantitative analysis.

Pathway of Mercury Uptake

Esophageal Ligation

The pathway for mercury uptake was determined by comparing the relative amounts of ^{203}Hg in various tissues of normal rainbow trout to concentrations of the isotope in trout whose esophagus had been ligated or sham ligated. Uptake of both $^{203}HgCl_2$ and $CH_3{}^{203}HgCl$ was determined.

Ligation Procedure.--Prior to surgery the fish were anesthetized with tricainemethane sulfonate (MS 222) and placed ventral side up in a trough. Gill ventilation and anesthesia were maintained by a pulsatile flow of aerated-MS 222 treated water through a rubber tube which was placed in the oral cavity. An incision was made on the ventral side about 3-4 mm lateral and parallel to the midline. The anterior portion of the 30-40 mm incision approached the pericardial sac, but did not penetrate it. The anterior portion of the stomach was located and ligated with heavy thread after which the incision was closed with 9 mm wound clips (Auto Clips No. B-2355-100, Clay Adams Inc., N.Y., N.Y.). See Figure 1. Sham surgery was performed in a similar manner except that the anterior stomach was located but not ligated. All animals were allowed to recover for 6 days before exposure to the mercury solution. Autopsies of the ligated fish revealed that the ligatures were at the anterior end of the stomachs and had remained tight during the course of the experiment.

Fish from each group (control, sham, and ligated) were placed into 100 liters of aged tap water which contained either $^{203}HgCl_2$ or $^{203}HgCh_3Cl$. After 24 hours exposure the fish were randomly removed and blood samples taken as described earlier. They were then killed by cervical

Figure 1.--Position of incision (I) and ligature (L) for esophageal ligation experiments.

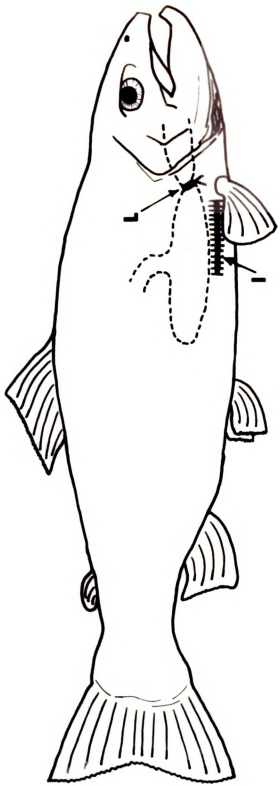
L
I

disl

hear

and

sub

bal

Rai

pr

ch

1

We

C

dislocation and tissue samples from the gills, liver, kidney, heart, skeletal muscle, stomach and intestine were removed and placed into pre-weighted 12 x 75 mm disposable culture tubes. The tubes were then covered and weighed on a Mettler balance to the nearest µg to obtain tissue wet weights. Radioactivity in the samples was then counted as described previously using a multichannel analyser-automatic sample changer system. The tissues and tube were then dried at 110° C for 48-72 hours and reweighed to obtain tissue dry weights. Analysis of these data was done on a Control Data Corporation 6500 computer.

In conjunction with the above experiment, several samples of gill and stomach tissue were prepared for radioautography.

Radioautography

Radioautographs were used to aid in the localization of the pathway of mercury uptake in trout. The 0.279 Mev gamma ray emitted by ^{203}Hg is of suitable energy to permit such studies. Tissues were removed from a trout which had been exposed to ^{203}Hg as noted above and quick frozen in ethanol cooled with dry ice. Frozen tissues were embedded on a brass stub with distilled water and 6µ sections cut with the Cryostat-Microtome at -30° C. The frozen sections were attached to albumin coated glass slides (Albumin

Fixative, Mayer Scientific Products, Allen Park, Mich.) by finger thawing and refreezing. The slides were then freeze dried for 24 hours. After drying they were dipped in 0.05% celloidin (Parlodion, Mallinckrodt, N.Y., N.Y.) dried and dipped in NBT-2 Nuclear Tracking emulsion (Eastman Kodak, Rochester, N.Y.). The slides were dried in a vertical position for two hours (horizontal drying often results in a very thick emulsion coat) and stored in a Con-Rad/Joftes exposure chamber (Controls for Radiation, Inc., Cambridge, Mass.) until sufficient time had elapsed and the emulsion could be developed. Developing was accomplished with D-19 developer as recommended by Eastman Kodak.

Numerous problems were encountered with this procedure. It became apparent that some radioactivity was lost in the radioautography procedure. This was indicated by the lack of correspondence between tissue activity (cpm/g tissue) and grain count especially with respect to gill tissues. The loss of activity could have resulted from any one of the numerous steps involved; however, no attempt was made to investigate which one(s) were critical. Instead an entirely different approach was tried.

Tissues were removed and quick frozen in isopentane cooled with liquid nitrogen after which they were embedded

on brass stubs with O.C.T. embedding media. Again 6μ sections were cut with the Cryostat-Microtome and were glued to glass slides with Eastman 910 adhesive followed by lyophilization for 24 hours. This procedure results in slight ion movement as shown by the electron microprobe studies. Dried sections were processed as described previously; thus, failure to localize mercury could only be due to (1) failure of mercury to bind at sites specific enough to be resolved by emulsion thickness and/or light microscope methods, (2) movement of mercury during coating with celloidin or the tracking emulsion, (3) gross emulsion film shifts during drying or staining or (4) sublimation of ^{203}Hg.

Species Study

To compare the normal ultrastructure of gills from various species of freshwater teleosts samples were taken from ten species ranging on the evolutionary scale from very "old," i.e., fresh-water dogfish (bowfin) and gar, to more "modern" species such as trout and perch. With the exception of the trout, all species studied were obtained through the courtesy of Dr. J. B. Hunn and the Fish Control Laboratory, Bureau of Sport Fisheries and Wildlife at La Crosse, Wisconsin. To minimize gill damage as a result

of transportation of live fish, representatives of each species were killed and gill tissues fixed for SEM and TEM studies prior to the return to East Lansing.

RESULTS AND DISCUSSION

The results and discussion sections for this thesis have been combined into one section in which data from each experiment is presented and discussed as a unit. Due to the large number of electron micrographs included herein, it is believed that separated "results" and "discussion" sections would lead to unnecessary redundancy and loss of continuity. A brief literature review of the teleost gill is presented in conjunction with trout anatomical studies for purposes of orientation and clarification.

Pathway of Mercury Uptake

Uptake of divalent mercuric ions as well as methyl mercuric ions occurs primarily by way of the gills as can be seen in Table 3. Ligation of the esophagous has no apparent effect on 24 hr accumulation of either form of mercury by any tissue with the exception of gill inorganic mercury levels. In this instance gills from the sham operated fish had significantly higher levels of mercury than either the control or ligated fish. The reason for this is unknown. Surgical trauma might result in an

TABLE 3.--Effect of esophageal ligation on twenty-four hour uptake of 275 ppt mercury as either $HgCl_2$ or CH_3HgCl.

	Tissue activity (ng Hg/g dry weight)					
	$HgCl_2$ Control	Sham	Ligated	CH_3HgCl Control	Sham	Ligated
Gill	28.08±1.381[a]	37.31±1.857	30.54±1.331	404.6 ±24.74	580.9 ±47.29	557.8 ±39.3
Liver	2.60±0.387	2.96±0.246	2.72±0.331	29.3 ± 2.794	40.4 ± 4.993	29.9 ± 4.184
Stomach	2.34±1.155	1.75±0.654	0.99±0.160	9.64± 1.055	10.81± 0.988	9.79± 2.112
Intestine	12.26±5.080	2.14±0.786	2.02±0.698	15.92± 2.591	16.77± 2.160	13.88± 3.477
Heart	2.60±0.206	3.42±0.357	3.30±0.916	30.65± 3.139	48.37± 6.737	41.18± 6.548
Kidney	4.64±0.570	5.43±0.447	4.28±0.332	92.07±13.563	118.12±11.316	92.92± 9.567
Muscle	0.16±0.021	0.18±0.039	0.18±0.015	2.39± 0.439	2.34± 0.274	1.96± 0.399
Blood	15.38±1.166	21.63±2.230	17.70±1.626	81.82± 9.073	141.34±13.542	131.05±20.530
No. of Observations	8	8	8	8	7	5

[a] One group is significantly different from the other two at the $P \leq 0.05$ level (one way ANOVA).

Mean±MSE

elevated respiratory frequency, however, this should be reflected also by the ligated fish. It is interesting to note that although not statistically significant, the concentration of either form of mercury is frequently higher in the sham operated fish than either controls or ligated groups. This difference could be coincidental or suggestive of possible traumatic effects of the ligation procedure which suppresses ventilation to some extent. In any event the uptake differences between the control, sham and ligated groups are sufficiently small to permit the conclusion that the gill is the primary pathway for uptake of either Hg^{+} or CH_3Hg^{+} in nonfeeding rainbow trout.

Surgical manipulations used during this experiment necessarily produce an open wound which can be closed with wound clips but which might reopen during the experiment and allow ^{203}Hg to enter the body cavity. As a check on the "leakiness" of the incision, $\frac{\text{dry weight}}{\text{wet weight}}$ ratios were calculated for all tissues to measure any water influx and are given in Table 4. Values were combined from fish exposed to inorganic and organic mercury, and one way ANOVA used for statistical comparisons

Only liver and kidney tissues appeared hydrated after surgical procedures; heart and muscle followed this trend but the differences were not significant even at the

Table 4.--Effects of surgical incision on tissue hydration.

	dry weight/wet weight x 100%		
	Control	Sham	Ligated
Gill	19.17±0.348[a]	18.97±0.261	19.22±0.606
Liver[c]	24.94±0.204	23.03±0.296	22.58±0.296
Stomach	28.84±1.540	30.65±2.837	27.95±4.005
Intestine	31.81±2.904	35.14±2.158	32.56±3.853
Heart	17.79±0.631	16.71±0.299	16.82±0.705
Kidney[b]	18.81±0.297	17.92±0.246	17.58±0.353
Muscle	23.66±1.195	22.71±1.385	20.14±0.446
Blood	13.26±0.572	14.13±0.742	13.41±0.642
Number of Observations	16	15	13

[a]Mean±MSE

[b]One mean is significantly different from the other two at the $P = 0.05$ level (one way ANOVA).

[c]One mean is significantly different from the other two at the $P \leq 0.01$ level (one way ANOVA).

P = 0.10 level. Blood, which should provide a good index of internal hydration, was not affected by the incision. Lack of hydration throughout the tissues studied suggests that water influx through the incision either must be slight or there is a preferential accumulation of water by liver and kidney tissues, while other tissues are not affected. The latter seems unlikely.

Differential uptake rates of the two mercurials illustrates one important difference between the organic and inorganic forms of these two compounds. Data for control fish from Table 3 are plotted in Figure 2 for comparison of tissue mercury values. Methyl mercury is taken up by all tissues at a much faster rate over the twenty-four hour experimental period. Large concentration differences observed between the two compounds in gill tissues are due to greater penetration by the methylated form. Mucus which continually coats the gill epithelium can act as an ion binding resin to trap mercury and prevent access into the tissue. Concentrations of both mercurials were identical for the experiment and if both compounds were trapped or precipitated by the mucus, inorganic mercury concentrations at the gill should be no less than one-half that of the organic form if one assumes that one SH binding site is occupied by each CH_3Hg^+ ion

Figure 2.--Mercury concentrations in tissues from trout exposed for 24 hours to either inorganic (Hg^{++}, stippled) or organic (CH_3Hg^{+}, open) mercury (275 ppt Hg for each). Means ± S.E. (n = 8).

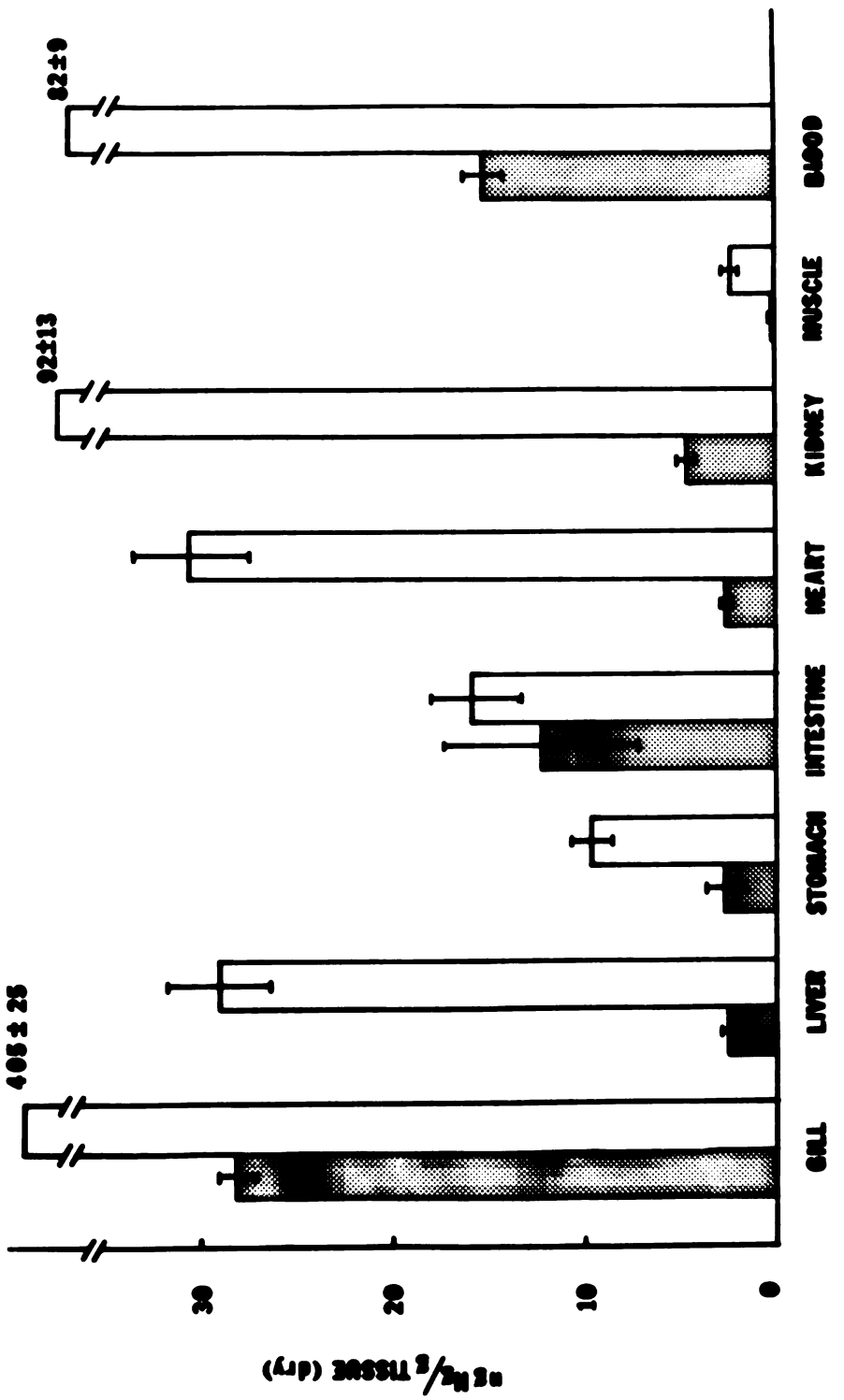
405 ± 25
92±13
82±9
CELL
LIVER
STOMACH
INTESTINE
HEART
KIDNEY
MUSCLE
BLOOD
0
10
20
30

and a maximum of 2 SH sites per Hg^{++}. Additional binding of the methylated form must either reflect entry into the gill tissues where additional sites are available or increased mucus secretion from methyl mercury exposure. Observations on the fish from this experiment and numerous other experiments have shown, however, that inorganic mercury is the more potent stimulator of mucus secretion. Thus gill tissue levels of methyl mercury must reflect an increased penetration and binding of this compound to gill tissue.

Comparison of the distribution of the two mercury compounds within one tissue demonstrates preferential accumulation of mercury based on its chemical form. The ratios of methyl mercury to inorganic mercury in the tissues are calculated to be:

	Gill	Liver	Stomach	Intestine	Heart	Kidney	Muscle	Blood
$\frac{\text{Hg as } CH_3HgCl}{\text{Hg as } HgCl_2}$	14.4	11.3	3.5	1.3	11.8	19.8	15.4	5.3

These ratios are partially attributable to increased uptake of methyl mercury by the gill, however, the tissues should all exhibit approximately the same ratios if there is no selectivity by the tissues for specific forms of mercury. The differences in these ratios show that tissues such as the kidney, muscle, gill, heart and liver preferentially accumulate the methylated form and blood, stomach and intestine do not. Low ratios for the last three tissues could be due to selective accumulation of the inorganic form which is masked by higher uptake rates of the organic compound. Halbhuber et al. (1970) have demonstrated, using radioautography, selective accumulation of $^{203}Hg^{++}$ by the Paneth cells in the intestine of the rat and guinea pig. They postulated a divalent heavy metal excretory function for these cells. Paneth cells in the trout gut might have a similar function and sequester divalent mercury but not methylated forms. Blood distribution reflects binding of the methylated form to red cells and inorganic form to plasma proteins (see section on blood in results and discussion).

Uptake ratios of $\frac{\text{phenylmercuric acetate}}{\text{mercuric acetate}}$ calculated from Ellis and Fang (1967) also show increased tissue accumulation of the organic mercurial compounds to the inorganic 24 hours after oral administration. Calculated

ratios were highest for blood (44) followed by liver (10), heart (6), kidney (2.5), and muscle (1.7). These ratios are not similar to those calculated for trout. Differences could be due to either differences between methyl and phenyl mercury with respect to tissue binding or to the pathway for uptake, i.e. intestinal vs. branchial routes.

Backström (1969) administered methyl and inorganic mercury iv into speckled trout. After 24 hours, distribution patterns of methyl mercury were identical to that in the present study with the exception of the gills. Low gill values reported by Backström are likely due to the mode of administration of the mercurial. Backström also reported highest inorganic mercury concentrations in the kidney; blood and gill values were approximately 50% lower. This discrepancy in distribution as compared to data presented in this thesis is also probably due to mode of administration of the mercurial. Hannerz (1968) reported 24 hour tissue mercury distributions in cod exposed to water borne mercurials which are similar with respect to relative distributions of the mercurial found in the present experiment. Hannerz postulates gill uptake as the principal source of mercury concentrations in the cod and pike and his postulate is confirmed by the ligation experiments reported above.

Pathway of Mercury through the Gill

Uptake of mercury by the gill could involve one or both of the two physiological and anatomical pathways found on the gill. Figure 3 is a sketch of a cross section through a gill arch. The arch is composed of a cartilaginous base (C) which supports paired filaments (F) and a gill raker (Gr). The filaments contain a center cartilage shaft, afferent and efferent arteries and supportive tissues. Projecting at right angles from either side of the filament are the secondary (respiratory) lamellae (L). In most teleosts a lamella is eccentrically shaped and water flows over its surface as indicated by the large arrows in Figure 3. A lamella consists of two layers of squamous epithelial cells sandwiched over pillar cells (Lowenstein, 1962). The pillar cells separate the layers of epithelium and thus impose a sinus network. Blood flows from the afferent filamental artery (Fa) around the pillar cells through the sinus and into the efferent filamental artery (Fv). Blood flow (small arrows, Figure 3) is counter to the water flow on the outside of the lamella. Respiratory exchange of CO_2 and O_2 can occur anywhere across the surface of the lamellar epithelium. The base of the lamellae (site of attachment to the filament) and the filamental spaces between lamellae contain cells responsible for active

Figure 3.--Cross section through a gill arch showing the relationship between the filaments (F), lamellae (L), and the pathway of water flow (large arrows) and blood flow (small arrows). Gill rakers (Gr); filament (F); lamella (L); afferent filamental artery (Fa); efferent filamental artery (Fv).

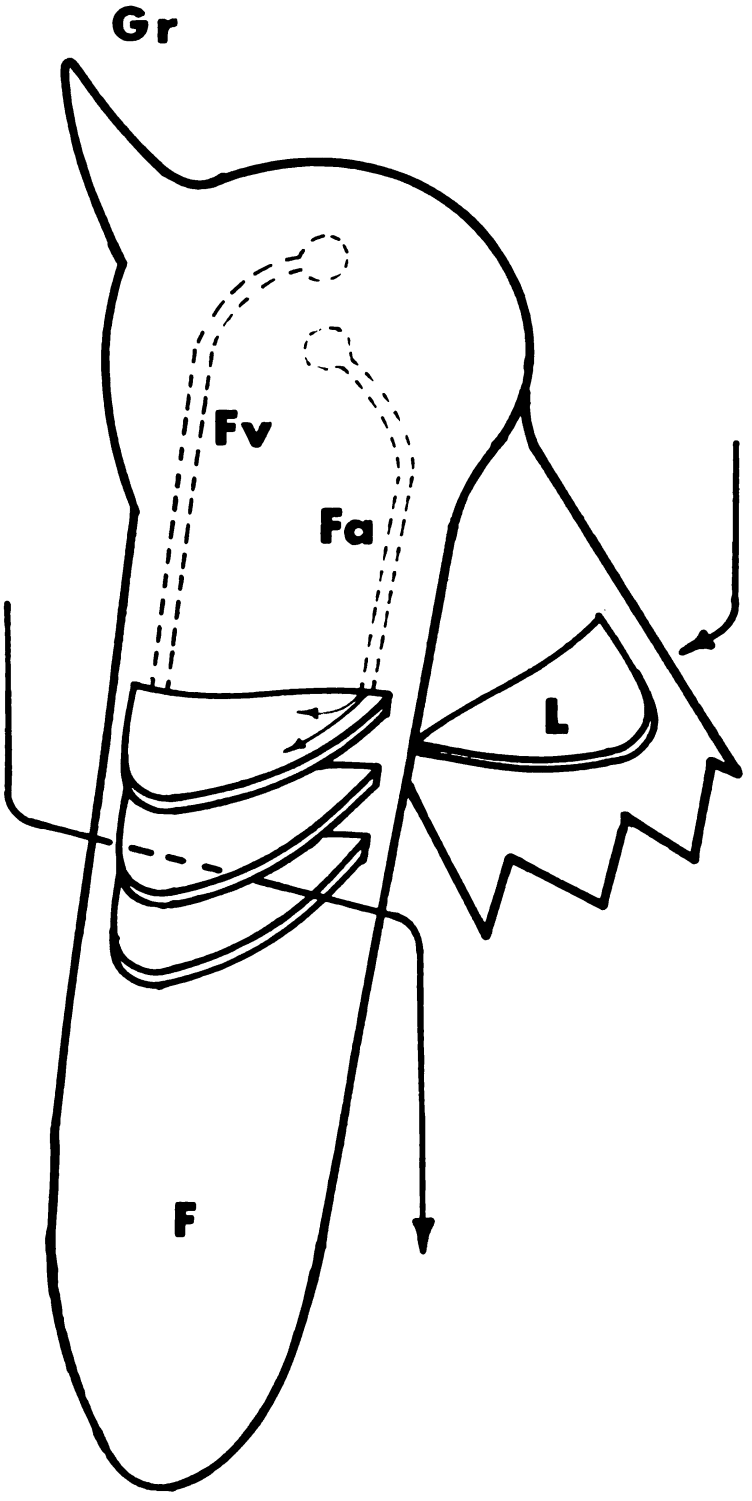
Gr
Fv
Fa
L
F

ion transport. These cells, named "chloride cells" by Keys and Willmer (1932), are thought to be involved in active transport of monovalent cations and anions. (For further description of the structure of the lamellae and chloride cells, see section on gill ultrastructure on page 81.)

Whether mercury enters the gill by diffusion through the respiratory lamellae or is transported by the chloride cells is unknown. Radioautographs of gills from fish exposed to either methyl or inorganic mercury exhibited a diffuse grain pattern which preluded identification of the uptake pathway. Lack of grain density around the chloride cell area showed that these cells were probably not specifically involved in uptake of either mercurial. Thinness of the lamellae in cross section and close apposition of adjacent lamellae (small interlamellar distance) prevented discrimination of preferential mercury binding sites or uptake pathways on the lamella. Dense grain patterns due to $^{203}Hg^{++}$ were found around the filamental cartilage. Presumably the mercury is associated with the chondroitin sulfate found in the ground substance of cartilage (Leeson and Leeson, 1970).

Microprobe analyses of tissues exposed to mercuric chloride for 24 hours revealed substantial amounts of

mercury in the interlamellar space (see Figures 4c and 5). Figure 4c shows the secondary electron output (SEM image) from a cross section through several lamella and the filament. The horizontal line depicts the beam tracing which corresponds to the line scan in Figure 5. As the beam moved from left to right in Figure 4c it traversed the filamental sinus (Richards, 1968), entered the filamental tissue and passed through the basal area of the lamellae on the filament where the chloride cells are located (see arrow). The beam then crossed three lamellae (white areas) and the associated interlamellar spaces. The line scan (Figure 5) shows the relative distribution of the natural elements Na, K, Ca and Cl and their relationship to mercury. The abscissa is divided by segments which correspond to the large squares in Figure 4c (10 squares full scale). The ordinate corresponds to the relative intensity of X radiation emitted by each element. Quantitative comparisons of elements are prevented by the use of different sensitivities for each element and displacement of the base line for graphic display. The left edge of Figure 5, between the ordinate and the first division, corresponds to a blood vessel or sinus space which is off the field of view in Figure 4c. Tissue blood space is indicated in Figure 5 by the tracings for sodium and

Figure 4.--Electron microprobe: Tissue scan. Figure a, SEM cross section of filament. Figures b, d, and e, elemental scans for potassium (K), calcium (Ca), and phosphorus (P). Figure c, SEM of longitudinal section of filament (400x). Figure f, areas scanned by microprobe shown as dark squares (40x). Arrows in a and e correspond to probable location of filamental sinus. Arrow in c points to chloride cell region and arrow in f to filamental cartilage. Black and white lines in a and c depict beam path for line scan.

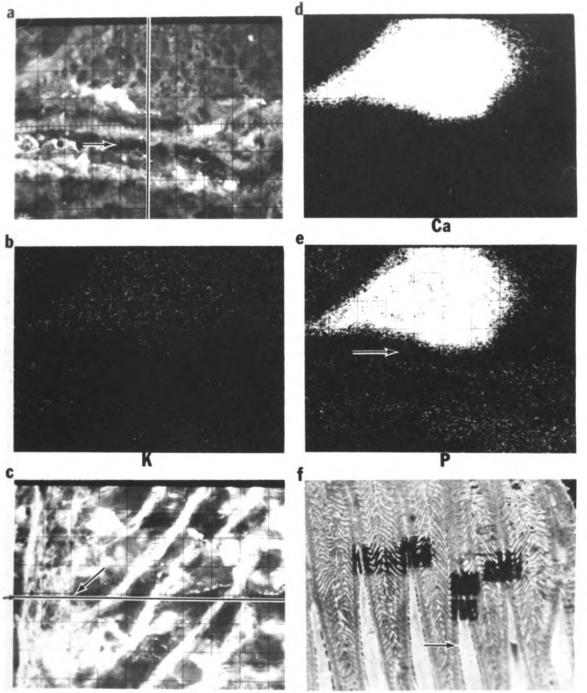
a
d
Ca
b
e
K
P
c
f

Figure 5.--Line scan of lamellar cross section (from Figure 4c). Sodium (Na); potassium (K); mercury (Hg); calcium (Ca); chlorine (Cl). Beam path for scan can be seen in Figure 4c as black and white line. Abscissa divisions correspond to grid divisions along beam path in 4c.

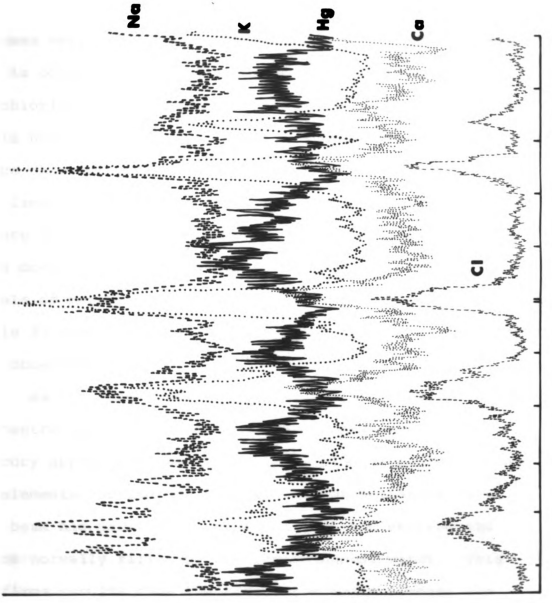
Na
K
Hg
Ca
Cl

chloride. It was found later that sodium is a very poor choice for plasma marker because in the vascular space it becomes very volatile when subjected to an electron beam and is often lost from the tissue. Why large quantities of chloride are not found in this space is unknown. Some could have been lost by diffusion although this is unlikely since chloride peaks correspond well to the location of the lamellae. The strong mercury peak at the left in Figure 5 suggests that the paucity of other ions in this area does not reflect tissue separation. Relatively high levels of mercury in the blood following exposure (see Table 3) would produce a mercury peak similar to that which was observed.

As the beam entered the area of the chloride cells, concentrations of all ions except mercury increased. Mercury appeared to be inversely related to concentrations of elements and did not increase in concentration until the beam had passed through the tissue and entered the space normally filled by the environmental water. This confirms results from the radioautographic studies and supports the concept that inorganic mercury is not selectively taken up by chloride cells nor concentrated by them in twenty-four hours. Other line scans of chloride cell areas on both horizontal and vertical axes substantiate

this finding. Figure 4f is a light micrograph of longitudinal sections of six filaments (40x). The black squares are areas examined by the microprobe during a routine experiment. Arrow points to the filamental cartilage which has been sectioned obliquely.

Interlamellar areas contained definite mercury peaks and there was an inverse relationship between mercury concentrations and concentrations of Na, K, Ca and Cl--all lamellar markers (Figure 5). The mercury peaks are due in large part to the mercury which was added one hour prior to sampling and demonstrated the effectiveness of mucus in this area to trap ions. Presumably mercury is contained in the interlamellar mucus from which it can either enter the gill or be sloughed off with the mucus. McKone et al. (unpublished data) found 79.3% of the gill mercury could be removed from the gill by an 80% ethanol wash following exposure of goldfish to 0.25 ppm $HgCl_2$ for three hours. They concluded that this fraction represented mercury trapped by the mucus coating the gill. The above author did not examine gill tissues after the ethanol wash to verify that only mucus was removed. Gills are very fragile and it is quite possible that some epithelium was also removed in the process.

Figure 4a is an SEM image of a filament cut in cross section. Figures 4b, 4d and 4e are tissue scans for several elements, two of which give good identification of the cartilage (elements are identified in the bottom center of each figure). The filamental sinus can be seen just below and parallel to the bottom edge of the cartilage (see arrows in Figures 4a and 4e). The beam path for the line scan can be seen in Figure 4a and the corresponding element analysis in Figure 6. Again mercury concentrations are highest in the cartilage and correspond to calcium levels. Figure 7 shows a tissue scan of a longitudinal section through a filament. The cartilage is indicated by an arrow and lamellae can be seen leaving the filament in the center of the SEM micrograph. Elemental scans are as indicated in Figures 7b-7d. Clarity of the lamella in the elemental scans demonstrates the low degree of ion diffusion during tissue preparation. Inorganic mercury binding to lamellae exhibited no preferential accumulation in either microprobe or radioautographic studies. Thus it appears that mercury can enter anywhere through general lamellar surface and active uptake is probably of little consequence in mercury influx. Once in the filament, inorganic mercury is accumulated by the cartilage. Other gill cells contain less mercury than the chondrocytes and chondroblasts

Figure 6.--Line scan of filamental cross section (see Figure 4a black and white line). Sodium (Na); mercury (Hg); calcium (Ca). Abscissa divisions correspond to grid divisions along beam path in 4a.

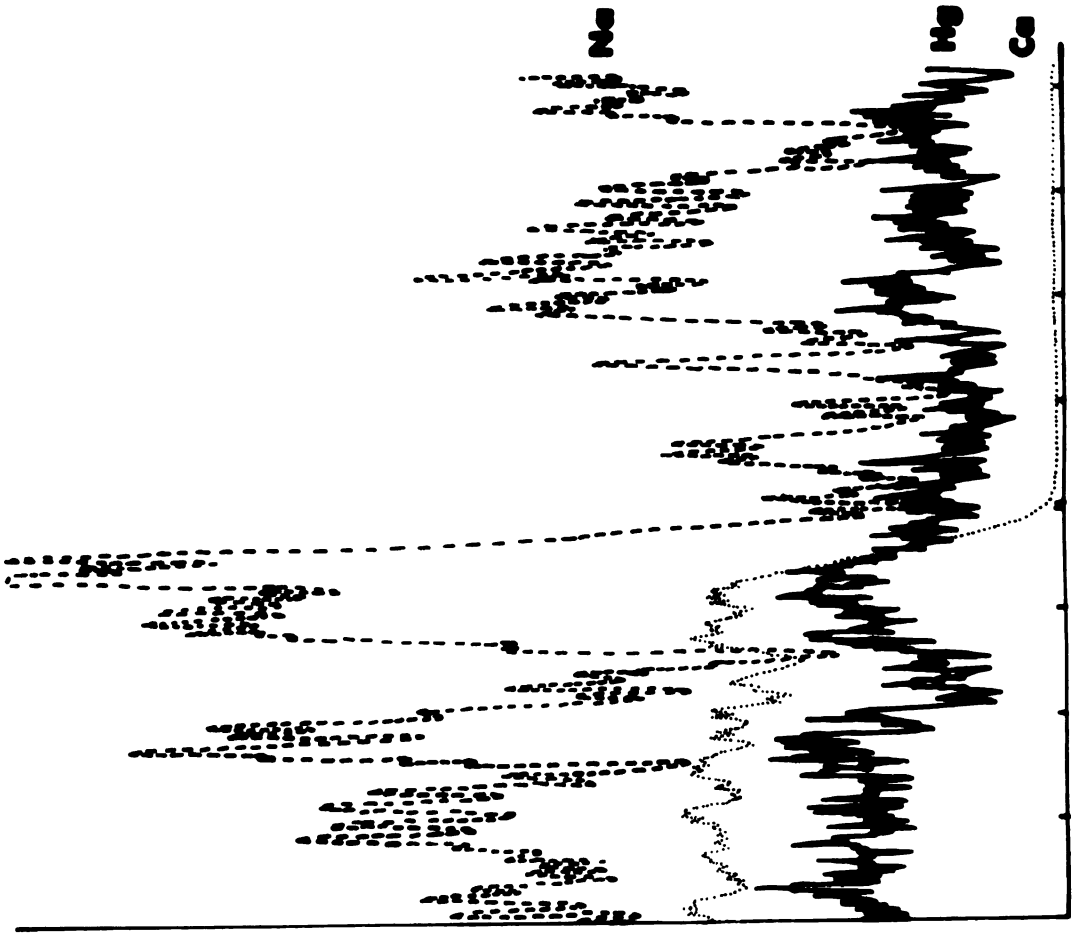
N
H
Ca

Figure 7.--Tissue scan of lamellar cross section. Figure a, SEM image (400x). Figures b-d, elemental scans for potassium (K), chlorine (Cl), and sulfur (S), respectively.

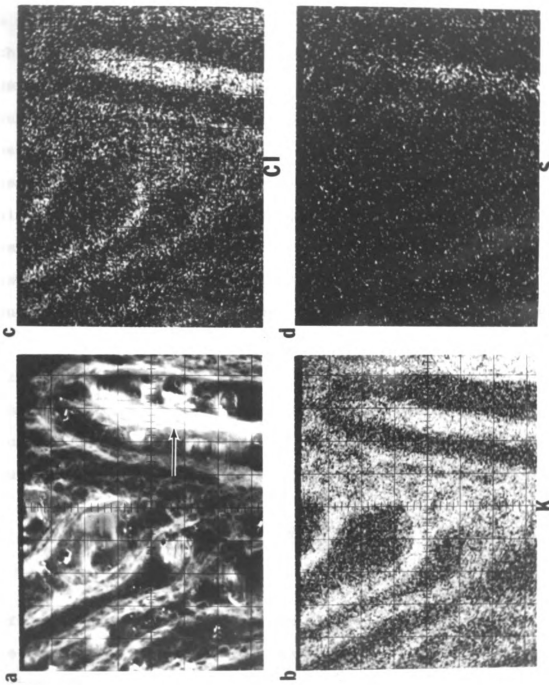
a
b
c
d
K
Cl
S

and show no preferential uptake of mercury with respect to a given cell type, i.e. epithelial cells, pillar cells or chloride cells. It was not possible to detect the presence of mercury in gills from trout exposed to methyl mercury using the microprobe. Since gills from trout exposed to $CH_3{}^{203}HgCl$ contain more label than $^{203}HgCl_2$ exposed tissues, it would seem that the microprobe analysis should also demonstrate more mercury after methyl mercury exposure. Complete lack of mercury after methyl mercury exposure could only be due to loss of this element during tissue preparation. Since methyl mercury crystals will sublime at room temperature, mercury could be lost during freeze drying, carbon evaporation or in the vacuum column of the microprobe. All of these processes require a high vacuum (around 5 microns pressure). The pathway for methyl mercury uptake through the gill thus remains obscure.

Mercurial Induced Structural Changes of the Gill--Light Microscopy

Gross structural changes of lamellar epithelium as described by Schweiger (1957), Amend et al. (1969), Rucker and Amend (1969) and Miettinen et al. (1970) were not observed in the present study. Following exposure to methyl mercury H and E stained sections of gill filaments showed cellular hypertrophy in the region of

chloride cells. Inorganic mercury produced slight separation of the lamellar epithelium from the pillar cells. Sections selectively stained for sulfated muco-substances revealed heavily stained areas on the lamellar epithelium, and filamental epithelium of all fish exposed to inorganic mercury. Exposure to methyl mercury did not produce any definite increase in the stain density when compared to control fish. Thus the inorganic form of mercury appears to act as a local irritant on the gill, producing increased mucus secretion; whereas methyl mercury does not have this effect.

Effects of Mercury on Gill Ultrastructure

Ultrastructure of the Normal Trout Gill

Before the mercurial induced morphological changes of the gill can be discussed it is necessary to consider the normal gill ultrastructure. Of primary interest are the secondary lamellae and chloride cells and, for clarity, these two tissues will be discussed separately.

Gross spatial and functional relationships between the lamellae and chloride cells have been previously discussed in this section (see "Pathway of Mercury through the Gill" and Figure 3). Figure 8 is a scanning electron

Figure 8.--Scanning electron micrograph of a pair of filaments. Gillraker (Gr); connective tissue (Ct); lamella (L). 24x.

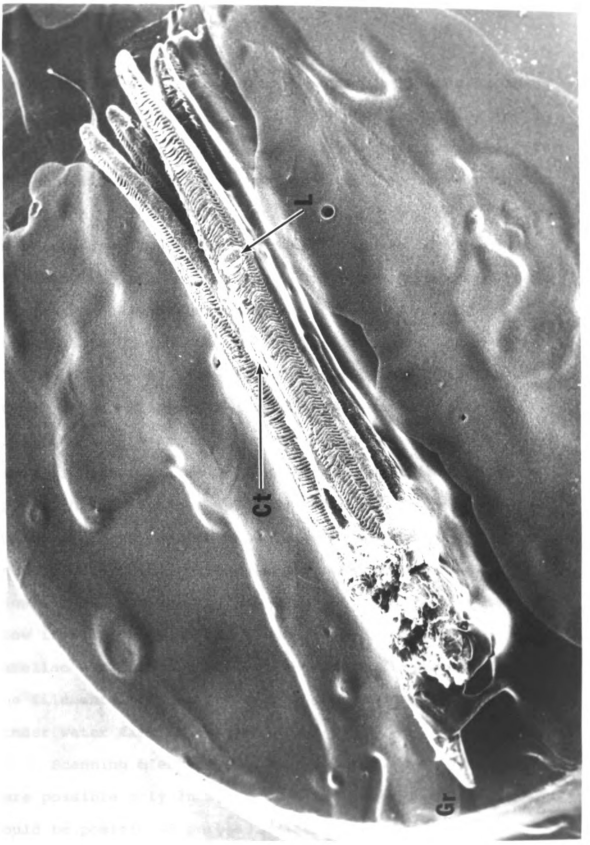
1
Ct
Gr

micrograph of a cross section through a gill arch exposing two filaments (as in Figure 3). The edge of the 12 mm diameter glass slide can be seen at the left. A gill raker (Gr) extends from the cartilaginous arch support in the lower left. Parallel filaments project from the cartilaginous arch support to the upper right corner of the figure with the lamellae extending upward, perpendicular to the filament. Filaments from rainbow trout are connected to each other by tissue on the inner edge of the filament (Ct) which extends from one-half to two-thirds of the length of the filament and prevents separation of the filamental pairs as well as separation of adjacent filaments along the entire arch. Presence of this tissue appears highly species specific (some species such as the bullhead has no connection between filaments) and it may greatly affect the resistance characteristics of water flow across lamellae in this area. Direction of water flow is from the outside of the filament across the lamellae and into the space between two filaments, thus the filamental connection as previously described could hinder water flow in this area.

Scanning electron microscopic studies of lamellae were possible only in areas when the lamellar surface could be positioned perpendicular to the electron

detectors. The parallel and closely appositioned nature of most lamellae hindered observation and it became necessary to find areas on the filament where the lamellar surfaces were exposed much like the pages of an open book (L, Figure 8). Figure 9A is a higher SEM magnification of an open lamellar area on a filament and illustrates several important features of the filament. The eccentric shape of the lamella is clearly shown and water would flow from bottom to top across the lamellae in the figure. Numerous goblet cells (G) are located on the filament; mucus secreting cells are also found on the lamella but they are structually different from goblet cells.

Fixation of tissues in 4% glutaraldehyde for SEM studies resulted in a coat of mucus over the filament and lamellae as in Figure 9B. Careful examination with the SEM of mucus coated lamellae revealed scattered openings through which the lamellar surface could be observed after 50% glutaraldehyde fixation. The mucus coat in Figure 9B suggests the importance of this secretion <u>in vivo</u> in providing a protective coating which acts as a buffer from gross physical and/or chemical trauma as well as serving as a precipitator of particulate matter.

Figure 9A.--Scanning electron micrograph of a gill filament; 50% glutaraldehyde fixation. Goblet cells (G). 450x.

Figure 9B.--Scanning electron micrograph of filament fixed in 4% glutaraldehyde. Mucus covers the filament and lamellae in this figure: compare to 9A which is free from mucus. 160x.

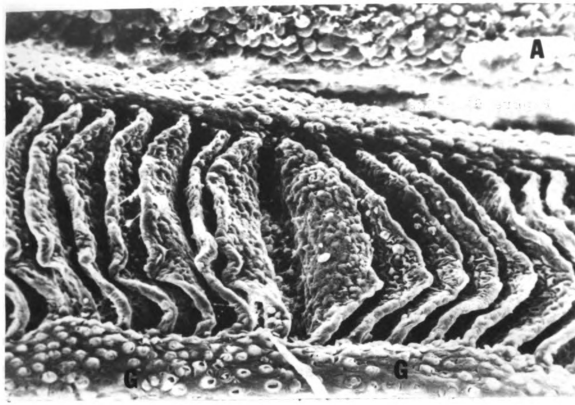
A
G
G

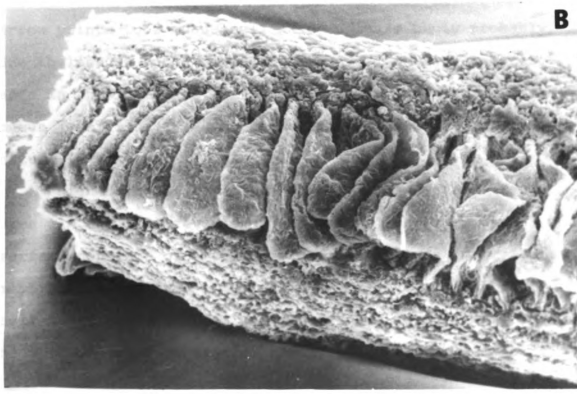
B

Figure 10 illustrates the structural features of the lamellar surface. Epithelial cells are outlined by raised cell junctions and are partially covered by scattered deposits of mucus (M); direction of water flow is indicated by the large black arrow. In this figure the lamella is shaped like a right triangle; the edges adjacent to the right angle correspond to the free edges of the lamella; junction of the lamella with the filament is obscured but would correspond to the hypotenuse of the triangle. "In-foldings" on the lamellar surface are probably due to shrinkage and rows of bumps (parallel to the lamellar-filamental junction) are due to either pillar cells or red cells underneath the epithelium. The small white and black arrow points to a mucus cell which appears empty probably due to loss of mucus during fixation. The white spheres, seen in the lower left of the figure, do not appear to be mucus (see Figure 13A for higher magnification). Their nature is unknown.

Higher magnification of the lamellar surface (Figures 11A and 11B) reveals epithelial cells whose outer surface consists of a random ridge like network of cellular membrane extensions. Double ridged characteristics of the cell junctions are shown in both figures (arrows) and can be seen in cross section in Figure 15A. Epithelial cells

Figure 10.--Scanning electron micrograph of the lamellar surface. Black arrow shows direction of water flow; black and white arrow shows a mucus cell opening. Scattered patches of mucus (M) coat the lamellar surface. The white spheres are not mucus; their function is unknown. 1100x.

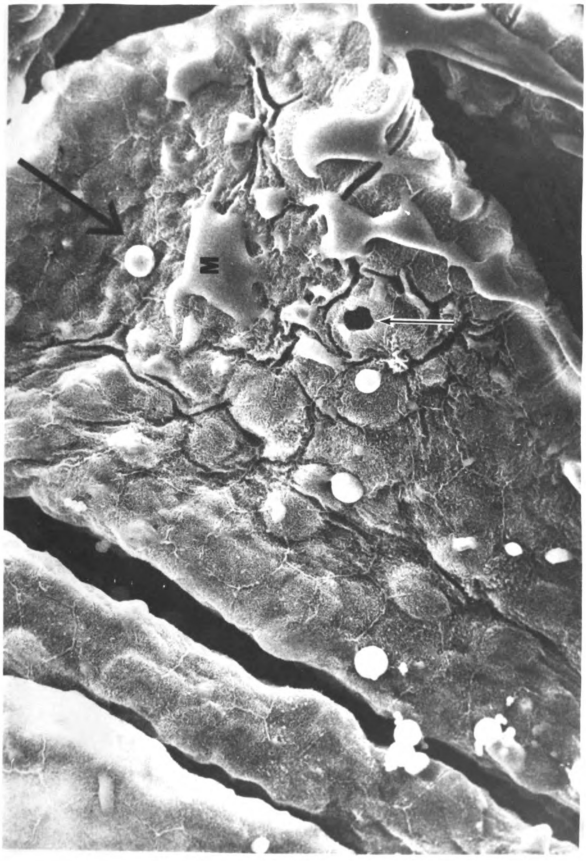

Figures 11A and 11B.--Scanning electron micrograph of lamellar surface showing short (A) and long (B) ridges. Raised epithelial cell junctions (black arrows) can be seen in both figures. Note scattered mucus deposits and also nonmucus structures (white spheres) on the epithelial cells. 50% glutaraldehyde fixation. Both figures 2900x.

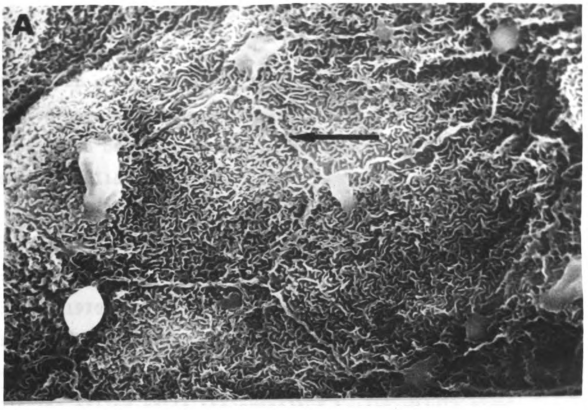
A

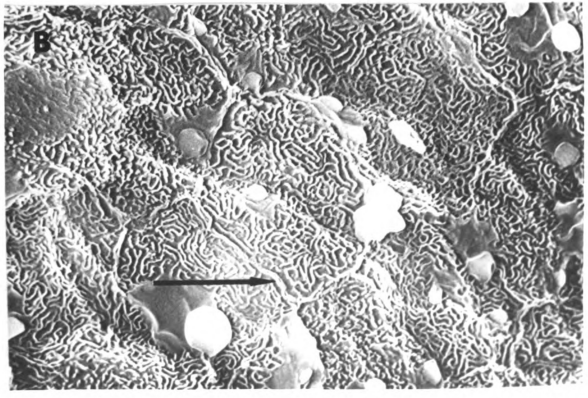
B

with short ridges (Figure 11A) generally seemed to be located near the filament; whereas, the long ridges appeared on cells which were found nearer the periphery of the lamella.

A cross section through a lamella (Figure 12) shows the relationship between the epithelial cells (Ep) and the underlying pillar cell (P) as described by Hughes and Wright (1970). (Nuclei for these cells stain dark.) Pillar cells separate the two layers of epithelial cells and flanges from these cells form a vascular space (V). Adjacent pillar cells are connected by interdigitating cell junctions of the flanges (black arrows). (See Appendix V for details of pillar cell body.) Within the vascular space on the right, a normal red blood cell (RC) is shown. Red cells characteristically have an amorphous cytoplasm with a darker staining nucleus, however, the plane of this section did not cut the nuclear structure (see Figure 14A for other red cells). The basement membrane or basal lamina (Bl) forms a continuous layer over all pillar cells and separates them from the epithelial layer. A small sinus space is present between the basement membrane and epithelial cells. Small vacuolated cells or cell fragments (C) are often found in this sinus space, in the vascular space or in the process of moving from one compartment to the other (mc). These

Figure 12.--Transmission electron micrograph of a cross section through the lamella. Epithelial cell (Ep); pillar cell (P); vascular space (V); red blood cell (RC); basal lamina (Bl); small vacuolated cell (c); migrating small vacuolated cell (mc). Junctions of pillar cell flanges (black arrows) are shown. Dark objects in pillar cell and epithelial cell are the cell nuclei. 4% glutaraldehyde fixation; 1% OsO_4 postfixed; lead citrate (LC) and uranyl acetate (UA) stained. 14,500x.

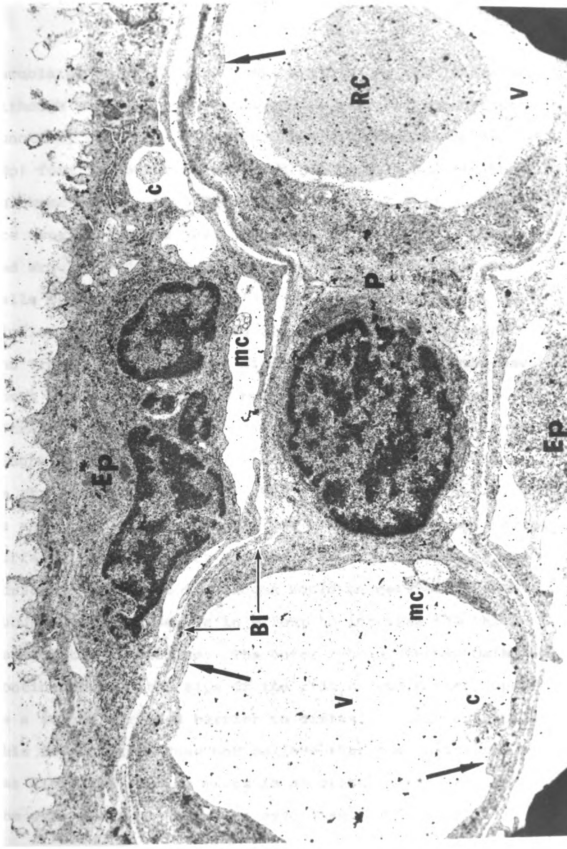
Ep
c
mc
P
RC
V
Bl
V
mc
c
Ep

vacuolated cells have not been reported in the literature. Although their vacuolated nature suggests a phagocytotic function, this remains speculative. Epithelial cells (Ep) form the outer boundary of the lamella and are the thickest barrier to diffusion. Epithelial cell nuclei are usually located just above pillar cell nuclei (Hughes and Wright, 1970). The outermost area of the epithelial cells is composed of finger-like protoplasmic extensions similar to intestinal microvilli. Tangential sections and Transmission electron micrographs from this area have shown these extensions to be ridge like in the guppy (Straus, 1963) and in several species of marine teleosts (Hughes and Wright, 1970); the function of these ridges as stated by Hughes and Wright (1970) is solely to serve as an anchor for the mucus film which coats the epithelial surface. These authors believe that any increase of the surface area due to the ridges would be negated by the mucus coat which serves in effect to increase the thickness of the epithelium. The outer edge of mucus, being continuous with the tips of the ridges, would then appear as a smooth surfaced barrier to diffusion. The author of this dissertation does not believe that the resistance to gas diffusion through mucus is as great as that through the cell plasma membrane or cytoplasm. The osmotic

gradient maintained across the outer epithelial surface (270 mOsm inside--10 mOsm outside) suggests a relatively impermeable membrane at least with respect to water and ion fluxes. If the plasma membrane is less permeable to diffusion than the mucus, it would act as the limiting barrier and any increase in its surface area would certainly increase the effective surface area for diffusion. Calculations based on dimensions of ridge height and width (from TEM studies) and on their length (from SEM) have shown that these ridges can increase the lamellar surface area an average of 2.47 times (N = 7). Thus the contribution of these ridges to total surface area could be very large.

Figures 13A and 13B are scanning electron micrographs of lamellar surfaces showing both raised (Figure 13A) and depressed (Figure 13B) cell junctions (black arrows) and possible pores (Figure 13B, black and white arrows). Sanger (personal communication) reports similar cell junctions and pores in the cell surface near the cell junction in preparations of the turkey sinus. Existence of pores in the epithelial cell surface of trout has not been verified using the transmission electron microscope. Small "holes" also were found in the center of epithelial cells (Figure 13A, black and white arrows) but again they were not observed using the TEM.

Figures 13A and 13B.--Scanning electron micrographs of the lamellar surface showing the microridges of the epithelial cells. Black arrows depict raised cell junctions (A) and depressed junctions (B). Holes appear on the cell surface (black and white arrows A and B). The large white sphere in the upper left corner in A does not appear to be mucus; its function is unknown. 50% glutaraldehyde fix. 7,300x (A) and 14,500x (B).

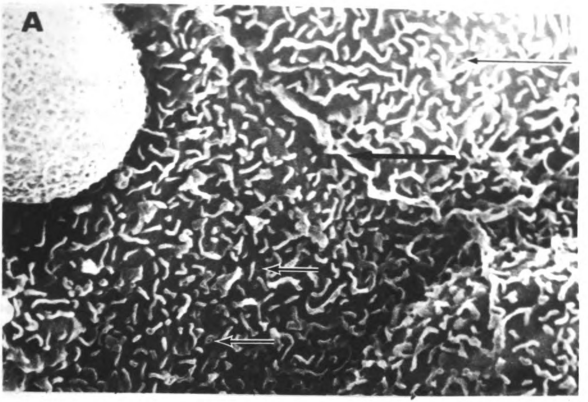
A

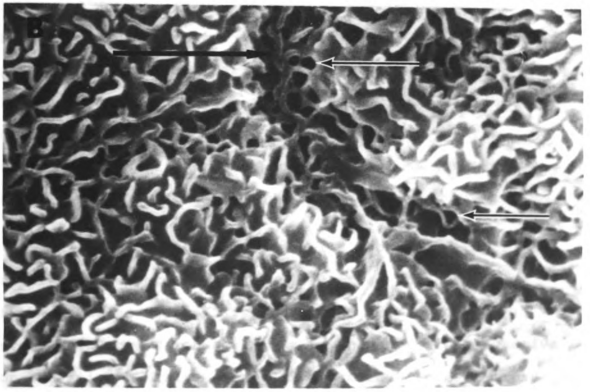

Normal red cells and the diffusional distance from them to the environmental water (W) are shown in Figure 14A. Note the amorphous nature of the erythrocyte cytoplasm and the nucleus in the red cell on the left.

Figure 14B shows the outer membrane of the epithelial cell ridges (arrow). Cell cytoplasm in the ridge area is agranular and absence of vacuoles suggests little if any specialized cellular function.

One type of epithelial cell junction is illustrated in Figure 15B. This raised junction (note the two lobes above the junction) consists of a tight junction (tj) and loose junction (lj) and is similar to that reported by Hughes and Wright (1970) for several species of marine teleosts and the septate junction found in molluscan gill epithelium (Gilula and Satir, 1971). Interdigitation of the loose junction is very pronounced. Figure 15A shows the second type of junction. There is lack of paired ridges above the tight junction and the loose junction in this figure is an abutment junction.

Chloride Cells.--Chloride cells located on the filamental surface between the lamellae or on the basal area of the lamellae are believed to be the primary cells involved in active ion uptake by fresh water fish or active ion excretion by salt water fish. Numerous investigators

Figure 14A.--Transmission electron micrograph of a cross section through a lamella. Red cells (RC) are characterized by amorphous cytoplasm. Environmental water space (w) and barriers to gas exchange are shown. 4% glutaraldehyde fix; 1% OsO_4 postfix. LC and UA stain. 12,500x.

Figure 14B.--Transmission electron micrograph of cross section through epithelial cell ridges. Arrow points to plasma membrane. 4% glutaraldehyde fix; 1% OsO_4 postfix; LC and UA stain. 56,000x.

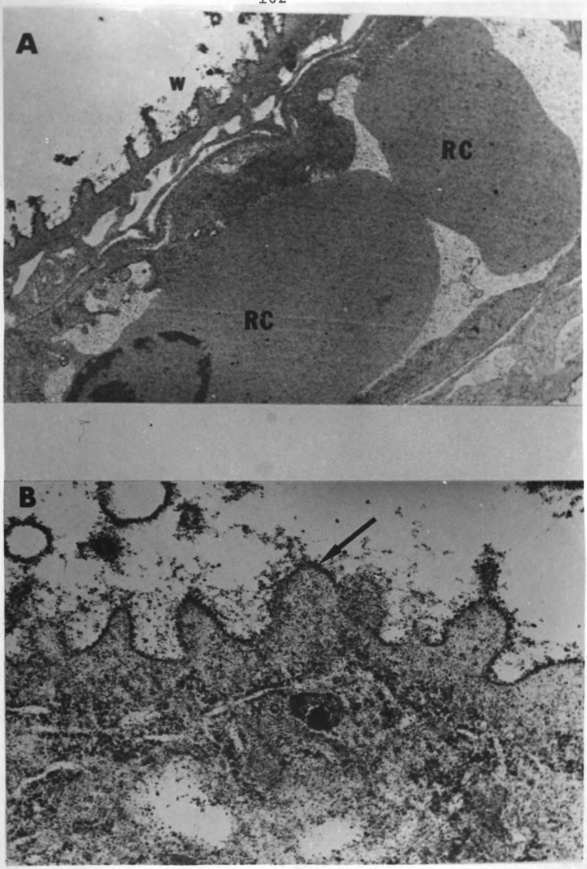
A
W
RC
RC
B

Figures 15A and 15B.--Transmission electron micrograph of lamellar epithelial cell junctions. Tight junction (tj); loose junction (lj). Depressed and abutment junction (A) 72,000x; and raised and interdigitating cell junction (B) 58,000x. Both 4% glutaraldehyde fix; 1% OsO_4 postfix; LC and UA stain.

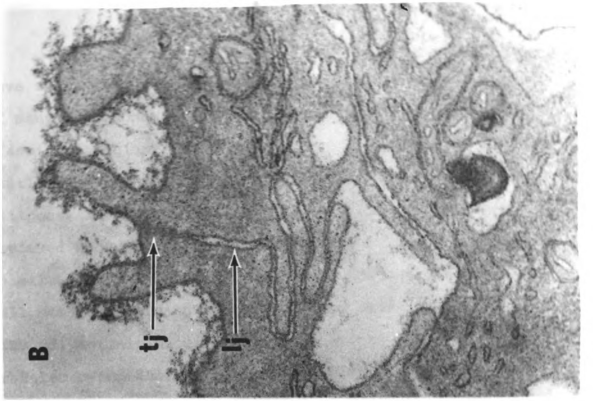
B
tj
tj

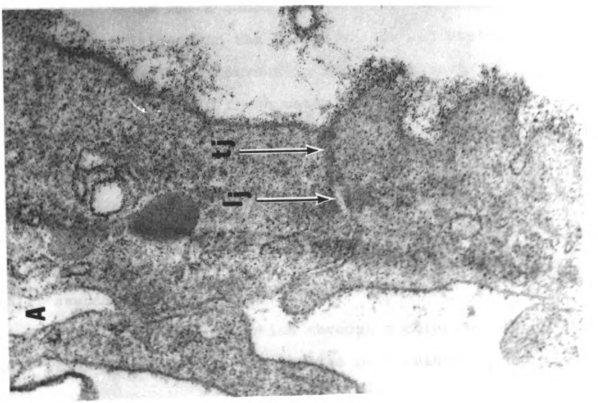
A
tj
tj

have shown these cells are characterized by the presence of many mitochondria and a dense network of smooth endoplasmic reticulum (SER) which has been shown to be continuous with the inner plasma membrane (Ritch and Philpott, 1969). Conte (see Hoar and Randall, 1969) has reviewed much of the recent literature on these cells. In salt water fish there is an involution of the outer cell membrane forming an apical crypt which is filled with polyanionic mucus. Below the apical crypt is a granular cytoplasmic region which is devoid of mitochondria and SER.

Chloride cells in fresh water fish also contain many mitochondria and a dense SER network. An apical crypt is well defined in the guppy (Straus and Doyle, 1961; Straus, 1963) but absent in the stickelback (Bierther, 1970) and in fresh water salmon (Threadgold and Houston, 1964). The apical surface of the salmon and stickelback chloride cells consists of many microvilli which are covered by a mucus haze. Adaptation of the fresh water salmon or stickelback to salt water results in formation of the apical crypt and loss of most microvilli associated with the Cl cell.

Figure 16 shows a section through a chloride cell (Cl) which is located on the lamella of a rainbow trout

Figure 16.--Transmission electron micrograph of a normal chloride cell on a lamella. Chloride cell (Cl); epithelial cell (Ep); degenerating chloride cell (D); red cell (RC). Dark lines are caused by knife marks on the section. 4% glutaraldehyde fix; 1% OsO_4 postfix; LC and UA stain. 12,000x.

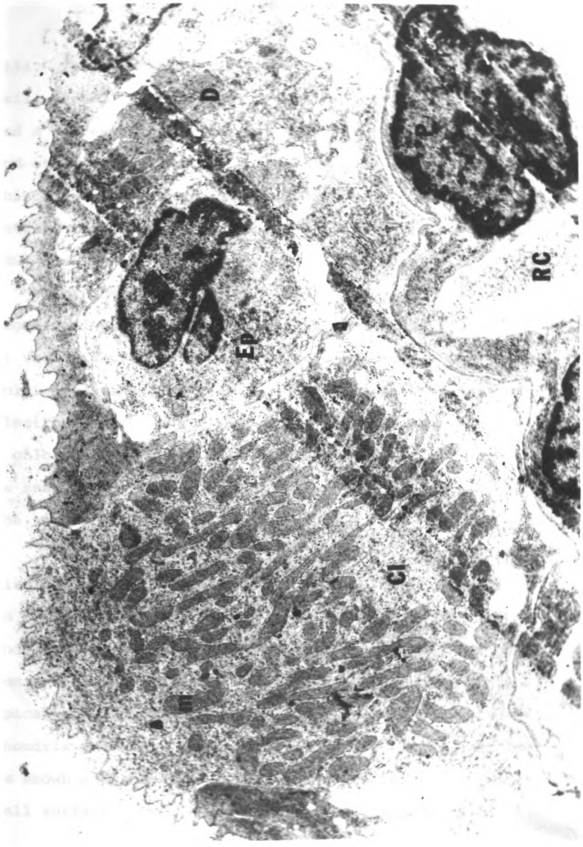
D
Ep
RC
Cl

gill. There are numerous mitochondria (m) within this cell, protoplasmic extensions of the apical cell surface and a depressed cell junction (abutment type) between it and other epithelial cells. Chloride cells identical to this were also seen in great abundance on the filament between the lamellae. Pillar cells and a red blood cell (RC) are in the bottom right of the micrograph.

Threadgold and Houston (1964) have identified degenerating chloride cells by the following criteria: 1) vacuolization of mitochondria, 2) vacuolization of the golgi apparatus, 3) cytoplasmic degeneration--decreased electron density and 4) inclusion bodies within the cell. A chloride cell which fulfills many of these criteria can be seen at the right of Figure 16. The dark lines across the tissue are due to knife marks.

The apical portion of a chloride cell and the junction between this cell and an epithelial cell are shown in Figure 17B. The numerous mitochondria (M) and smooth endoplasmic reticular network (tubular network) are predominant in the chloride cell. The sparsely granulated apical portion of this cell, however, lacks both the mitochondria and SER. A desmosome (d) of the tight junction is shown and this junction is depressed below the epithelial cell surface. Haze, present over the chloride cell

Figure 17A.--Transmission electron micrograph of a mucus cell on the lamellar surface. Mucin droplets (m); opening of mucus cell to the external environment (o); 4% glutaraldehyde fix, unstained. 9,000x.

Figure 17B.--Transmission electron micrograph of the apical portion of a chloride cell. Note dense, smooth endoplasmic reticulum network and granules in the cytoplasm. Haze covering the microvilli probably acts as an ion exchange resin. Mitochondria (m); desmosome (d). 4% glutaraldehyde fix, 1% OsO_4 postfix, LC and UA stain. 36,000x.

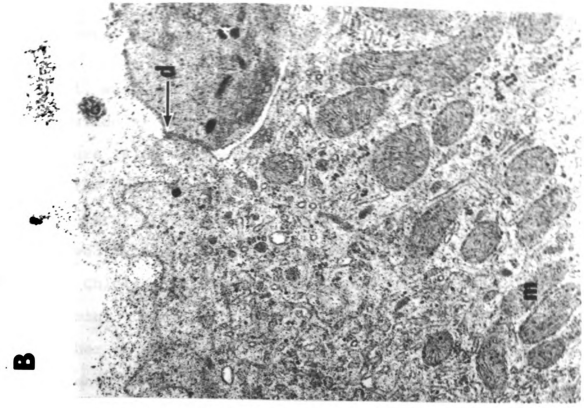
B
n
m

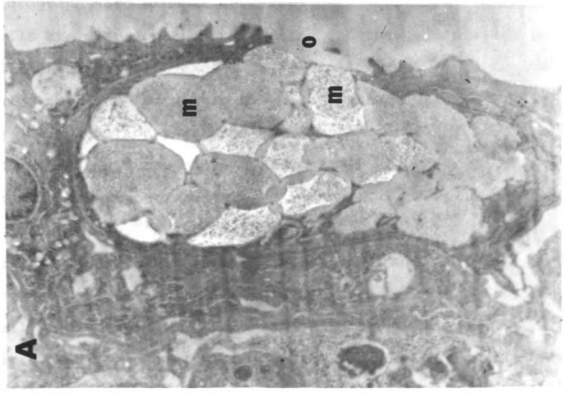
A
m
m
o

microvilli, was specific for these cells and aided in their identification at low magnification.

Figure 18 shows the relative distribution of chloride cells on the interlamellar filamental surface as seen by scanning electron microscopy. Lamellae (parallel rows, L) were removed by microdissection to expose the filamental surface. Chloride cells with depressed cell junction (arrows point to several) are quite numerous in this area.

Higher magnification of the chloride cells (Cl) on the filament (Figure 19) reveals the microvillar nature of the protoplasmic extensions of the cell surface. Six mature and several immature (I) chloride cells in this micrograph also exhibit depressed cell junctions. Chloride cells are also located on lamellae and they are similar to filamental Cl cells except that lamellar cells tend to bulge out from the general lamellar surface (Figure 20B).

In addition to exhibiting the characteristics described by Threadgold and Houston (1964), chloride cells from rainbow trout also showed a loss of microvilli on the apical surface. A degenerating (dcl) and a normal chloride cell (ncl) are shown in Figure 20A and Figure 21 (A and B) shows cross sections through several degenerating Cl cells. Cell vacuolation, mitochondrial disintegration and loss of microvilli are all distinct features of the degenerating cells.

Figure 18.--Scanning electron micrograph of the filamental surface. Lamellae have been removed (L) by microdissection to expose this area. Arrows point to only a few of the many chloride cells which are distinguished in this micrograph by depressed cell junctions. 50% glutaraldehyde fix. 700x.

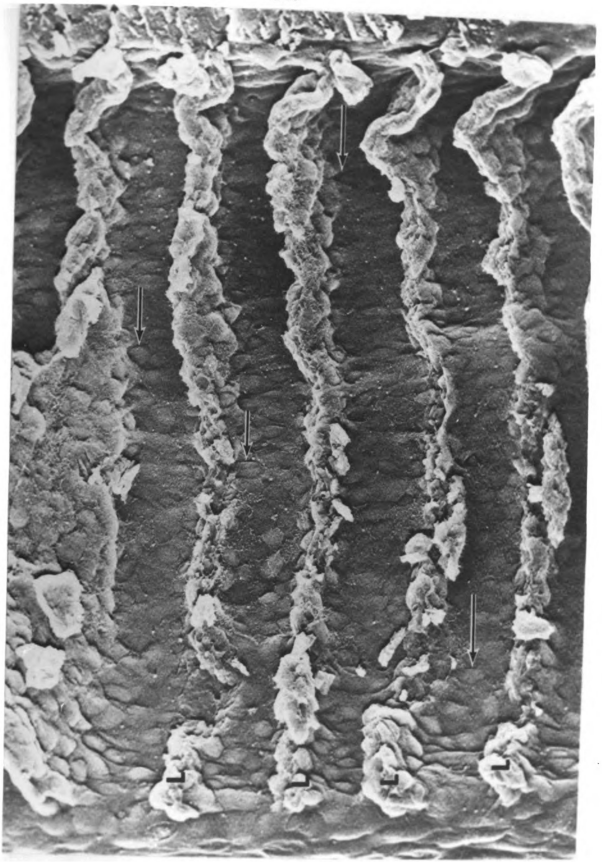

Figure 19.--Scanning electron micrograph of several chloride cells (Cl) on the filament. Arrows point to two chloride cells which demonstrate depressed cell junctions and the apical microvilli. Other chloride cells are also seen in this micrograph including a small immature cell (I). 50% glutaraldehyde fix. 7,000x.

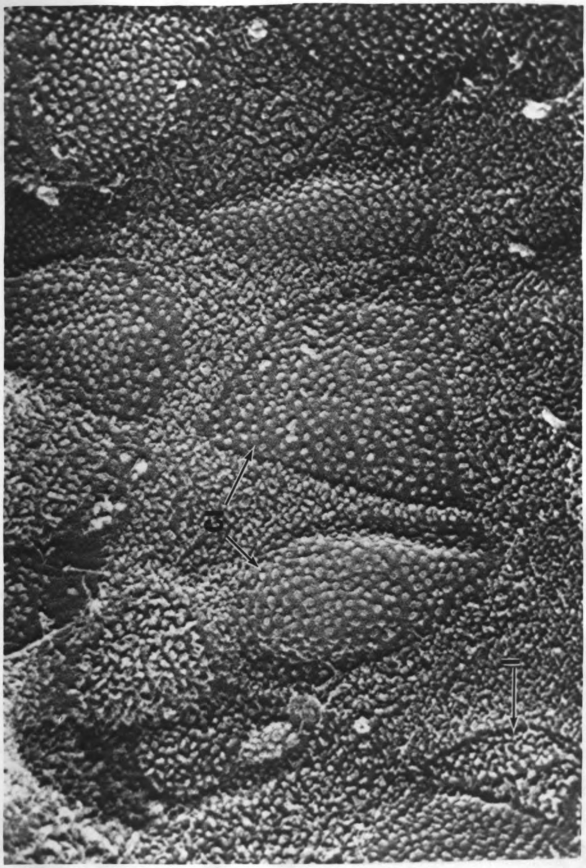

Figure 20A.--Scanning electron micrograph of chloride cells on filament. Normal chloride cell (ncl); degenerating chloride cell (dcl). Note loss of microvilli during chloride cell degeneration. 50% glutaraldehyde fix. 9,000x.

Figure 20B.--Scanning electron micrograph of chloride cells on a lamella. Chloride cell (Cl). 50% glutaraldehyde fix. 2,900x.

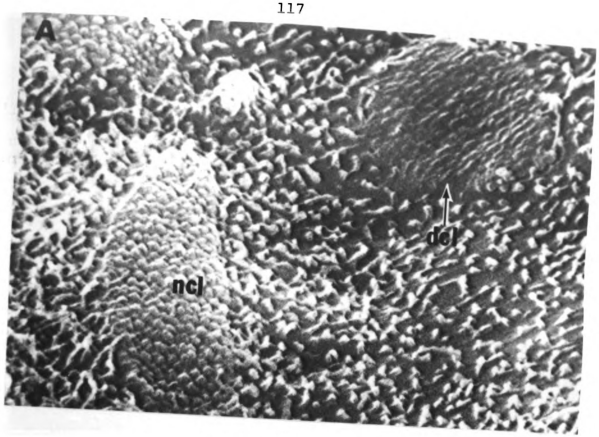
A
ncl
ncl

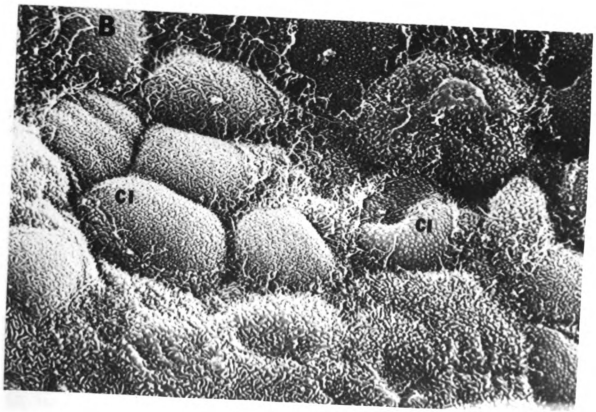
B
cl
cl

Figures 21A and 21B.--Transmission electron micrographs of degenerating chloride cells. Note loss of mitochondrial membranes, increased cellular vacuolation and loss of apical microvilli. 4% glutaraldehyde fix, 1% OsO_4 postfix, LC and UA stain. Both 19,000x.

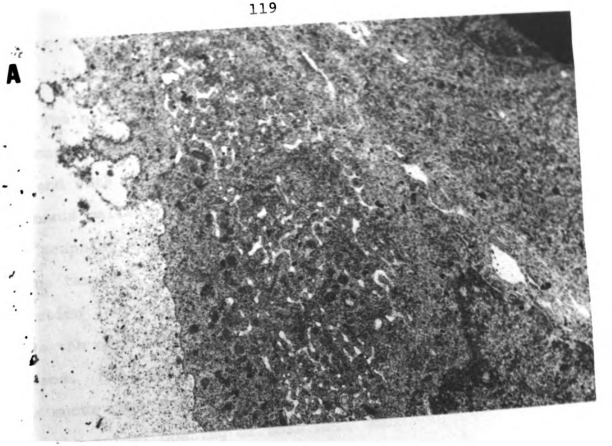
A

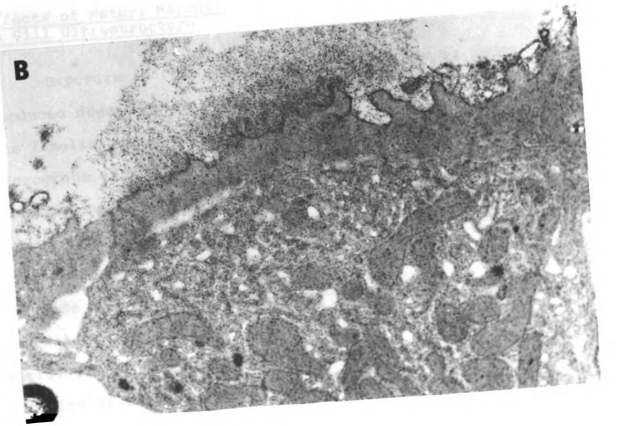
B

The other major cell type found in the epithelium is mucus cells. On the filament the mucus cells are goblet-like and with the SEM appear as in Figure 22A (G). Lamellar mucus cells are not of the goblet type. Figure 22B is a scanning electron micrograph of two such mucus cells on the lamellar surface in different stages of mucin secretion (arrows) and Figure 10 (black and white arrow) shows the opening of another mucus cell on the lamellar surface. Figure 17A is a transmission electron micrograph of a mucus cell containing droplets of mucin (m). Note also the apical opening of this cell (o).

Effects of Methyl Mercury on Gill Ultrastructure

Exposure to 0.05 ppm Hg (as CH_3HgCl) for 24 hours produced degenerative changes in the chloride cells and the lamellar surface. Figure 23 is a scanning electron micrograph of the filamental area between lamellae. Lamellae were removed by microdissection and the black arrows show numerous red blood cells in the lamellae at the point of section. Both normal and degenerating chloride cells (Cl, black and white arrows) are found on the filament as indicated by the presence or absence of microvilli of these cells. Figure 24B is a higher magnification of two degenerating chloride cells (Cl) on the

Figures 22A and 22B.--Scanning electron micrograph of mucus cells (G) on the filament in 22A and on the lamella (arrows) in 22B. Note different stages of mucus secretion by lamellar mucus cells (arrows, 22B). Both 50% glutaraldehyde fix. Both 2,900x.

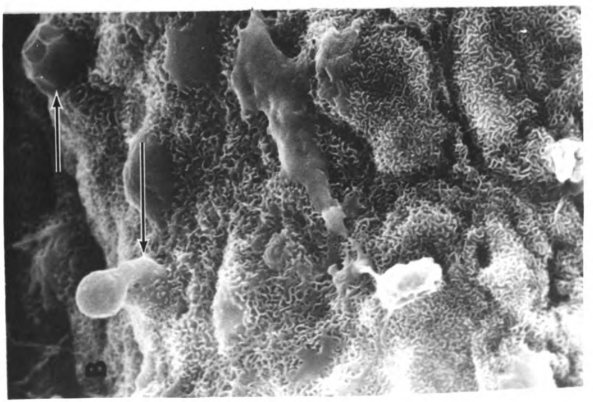
B

Figure 23.--Scanning electron micrograph of filament between lamellae. Trout exposed to 0.05 ppm Hg as (CH_3HgCl) for 24 hours. Many chloride cells (Cl, black and white arrows) have lost apical microvilli and appear to be degenerating. Chloride cell at left appears to be more normal. Black arrows indicate erythrocytes trapped in the lamellar sinuses during fixation. 50% glutaraldehyde fix. 2,100x.

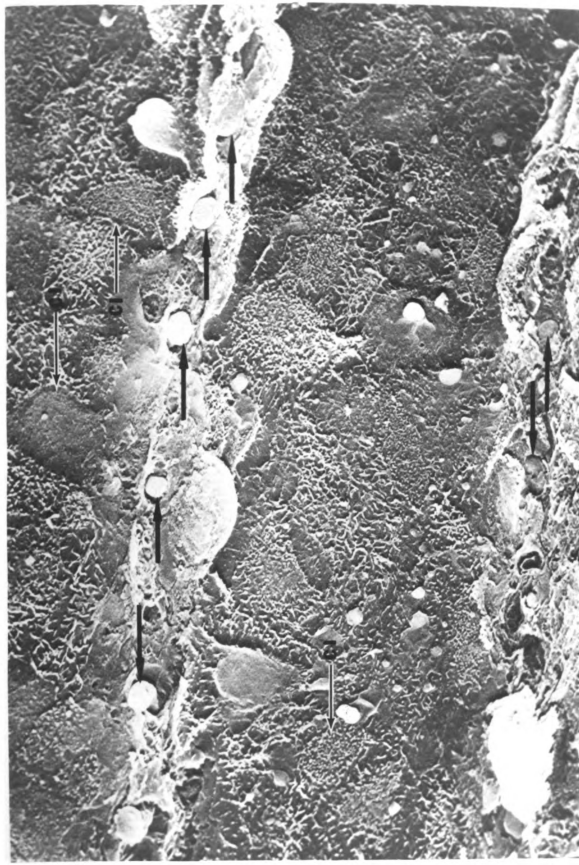

Figures 24A and 24B.--Scanning electron micrograph of trout exposed to 0.05 ppm Hg as (CH_3HgCl) for 24 hours.
A. Lamellar surface shows some loss of microridge structure; however, epithelial cell junctions appear normal. 50% glutaraldehyde fix. 2,900x.
B. Chloride cells on filament show loss of microvilli and appear to be degenerating. Black arrows point to erythrocytes trapped in the lamella. 50% glutaraldehyde fix. 2,900x.

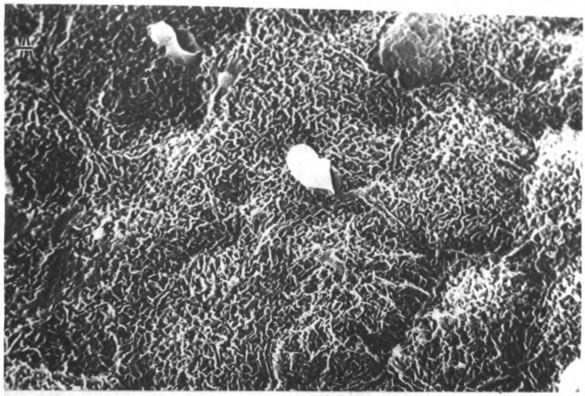

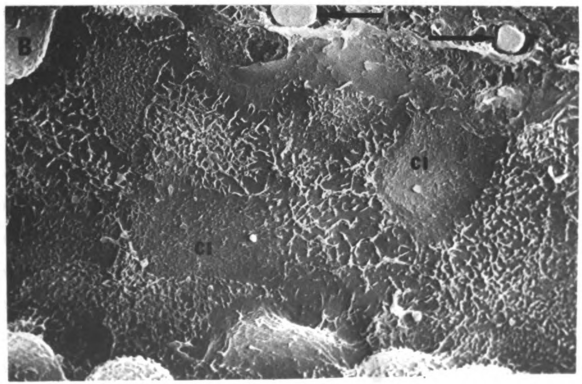
B
Cl
Cl

filament and loss of microvilli is obvious. Ridges on the lamellar epithelium (Figure 24A) appear to have lost some of their ordered nature at this mercury exposure.

Prolonged exposure (5 days) to the same mercury concentration (0.05 ppm) augmented the degeneration of chloride cells (Figures 25 and 26B) and lamellae (Figure 26A). Very few chloride cells on the filament in Figure 25 appear normal; most have lost all of their microvilli (arrows). Figure 26B shows a normal chloride cell immediately below the mucus (M) and a degenerating chloride cell to the left of the patch of mucus. Loss of ridge-like topography of the lamellar epithelial cells is also evident (Figure 26A) even though other epithelial areas were not abnormal. Cellular junctions (Figure 26A, arrows) appeared normal and indicated optimal beam and detector angles of the SEM.

No definite structural changes of the lamella were observed in cross sections after exposure to 0.05 ppm methyl mercury for either one or five days. Figure 27 shows a lamella from a fish exposed 5 days to 0.05 ppm. In this section even the ridges appeared normal. The white and black arrow points to a highly membranous structure in the vascular space and the black arrow to a heavily stained object in the sinus space. Both of these

Figure 25.--Scanning electron micrograph of the filament between the lamellae (L). Trout exposed to 0.05 ppm Hg as (CH_3HgCl) for 5 days. Black and white arrows indicate several degenerating chloride cells. 50% glutaraldehyde fix. 2,100x.

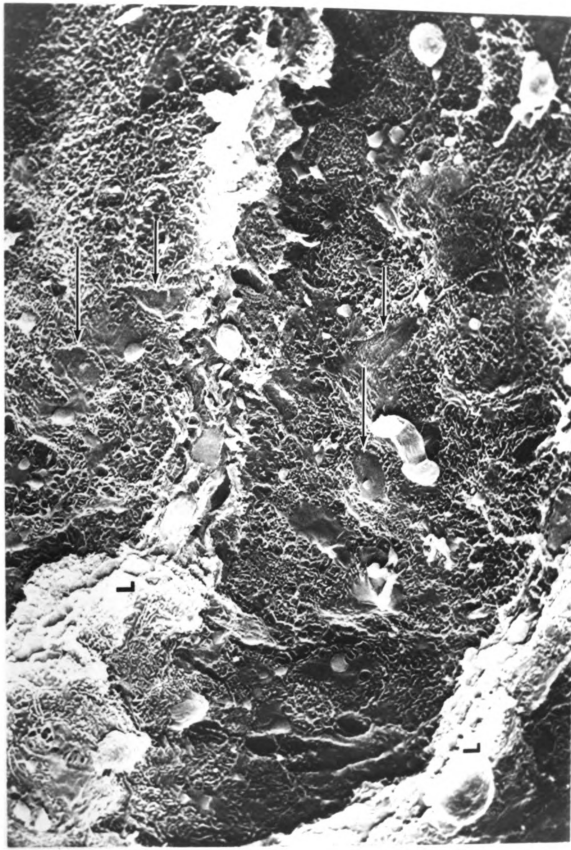

Figures 26A and 26B.--Scanning electron micrograph of trout exposed to 0.05 ppm Hg as (CH_3HgCl) for 5 days.
A. Lamellar surface shows degeneration of microridges; arrows indicate epithelial cell junctions. 50% glutaraldehyde fix. 2,900x.
B. Chloride cells on the filament. The chloride cell below the mucus patch (M) appears normal. The chloride cell to the left shows loss of microvilli, indicative of degeneration. 50% glutaraldehyde fix. 7,300x.

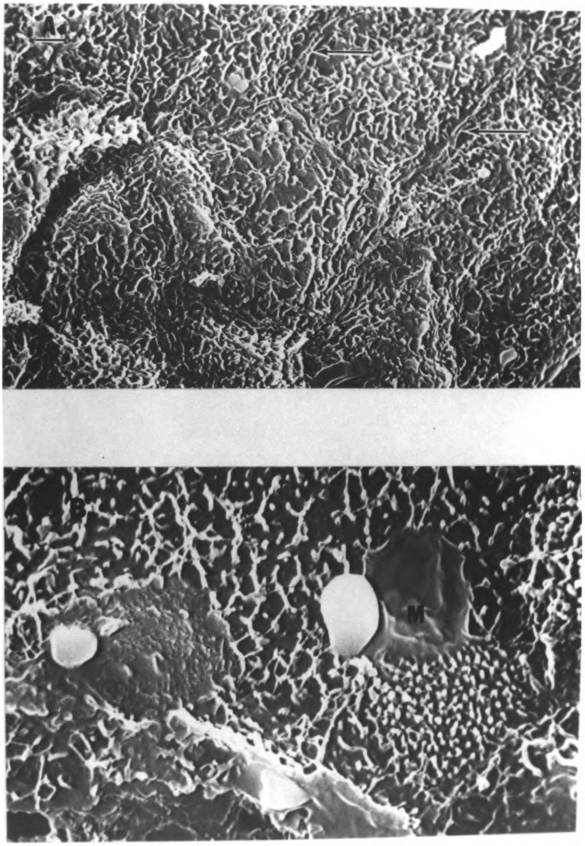

Figure 27.--Transmission electron micrograph of a cross section through the lamella from a trout exposed to 0.05 ppm Hg as (CH_3HgCl) for 5 days. The lamella appears normal although the erythrocyte in the center is slightly vacuolated and the erythrocyte in the right of the micrograph contains numerous mitochondria, indicative of a reticulocyte. Black arrow points to an unidentified electrondense object and the black and white arrow points to a highly membranous structure commonly found in the vasculature or sinus area of lamellae from either control or mercury exposed fish. Pillar cells (P), epithelial cells (Ep). 4% glutaraldehyde fix, 1% OsO_4 postfix, LC and UA stain. 12,500x.

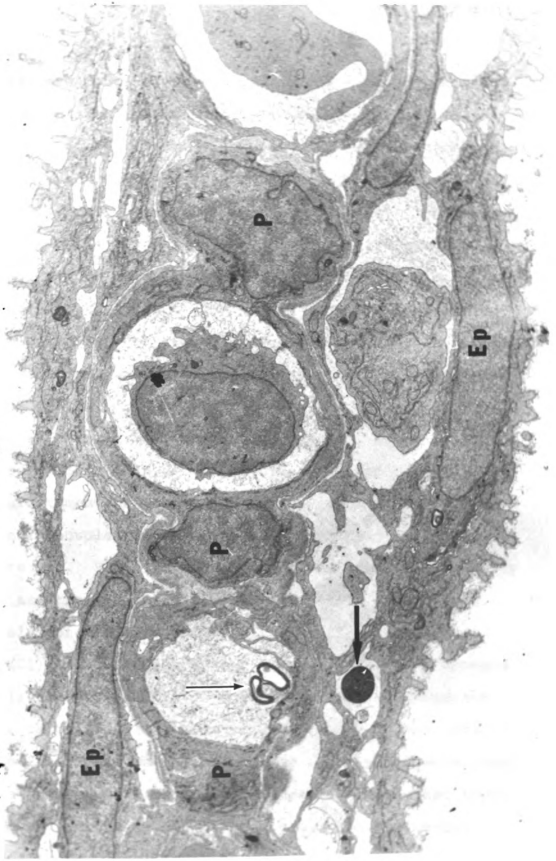
P
P
P
Ep
Ep

objects were found scattered throughout lamellae of all fish studied; their function is unknown. The red cell in the center of the figure (unlabeled) appears abnormal in that the outer membrane has become somewhat irregular and the cell cytoplasm has distinct vacuoles. The "ghost" red cell at the right of this figure contains numerous mitochondria which is indicative of a reticulocyte. Increased erythrocyte degeneration, assuming vacuolation is commensurate with degeneration, would logically increase circulating reticulocytes due to erythropoietic responses of the fish.

Low ambient mercury levels (300 ppt, Hg as CH_3HgCl) produce similar changes of the gills and red cells if exposure times are increased. Four week exposure produced red cell vacuolation and slight loss of ridge integrity (Figure 28). Vacuolation of two red cells (RC) is clearly shown and the vascular space (V) is filled with debris, possibly contents from ruptured red cells. A chloride cell (Cl) is located above the vascular space and appears normal; however, ridges on the epithelial cell adjacent to the chloride cell appear reduced in height and density. Figure 29A shows two vacuolated red cells which were found in the afferent filamental artery and indicate that these cells are present in circulating blood and not merely trapped in the lamellar sinus.

Figure 28.--Transmission electron micrograph of a cross section through a lamella from a trout exposed to 300 ppt Hg as (CH_3HgCl) for 4 weeks. Note the vacuolation of the erythrocytes (RC) and debris in the vascular space (V). The chloride cell (Cl) in this figure appears normal. 4% glutaraldehyde fix, 1% OsO_4 postfix, LC and UA stain. 5,700x.

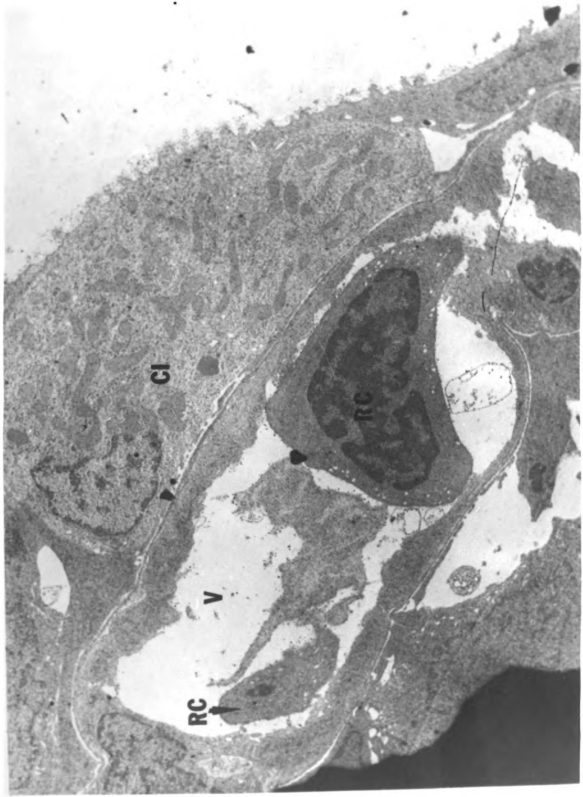
CI
RC
V
RC

Figure 29A.--Transmission electron micrograph of vacuolated red cells found in the afferent filamental artery. Trout was exposed to 300 ppt Hg as (CH_3HgCl) for 4 weeks. 4% glutaraldehyde fix, OsO_4 postfix, LC and UA stain. 27,000x.

Figure 29B.--Transmission electron micrograph of a lamellar cross section from trout exposed to 300 ppt Hg as (CH_3HgCl) for 4 weeks. A leukocyte (L) has moved into the sinus space between two degenerating chloride cells. 4% glutaraldehyde fix, OsO_4 postfix, LC and UA stain. 10,000x.

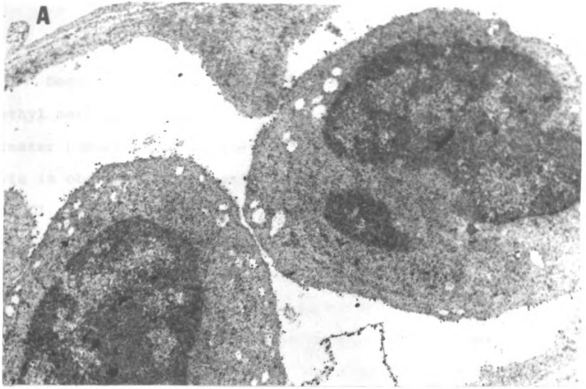
A

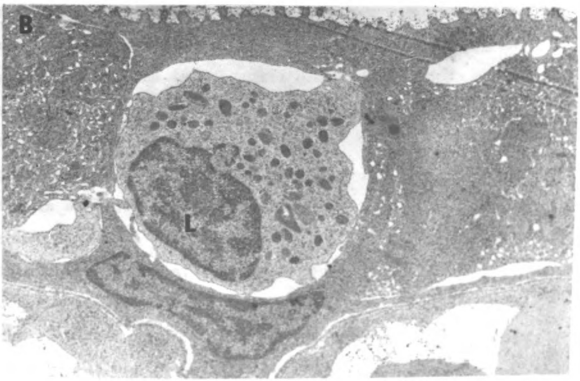
B
L

Degenerating chloride cells in fish exposed to methyl mercury (300 ppt, 4 wks) are also present in greater numbers than in control specimens. Often a leukocyte is observed in the sinus space adjacent to degenerating Cl cells (leukocyte (L) is between two chloride cells in Figure 29B) and is probably involved in phagocytosis of either chloride cells or "old" epithelial cells.

After an eight week exposure to 300 ppt methyl mercury at 5° C, a new cell type appears on the lamellar surface and is characterized by low electron density, relatively large cell volume, large spherical nucleus and reduction of surface ridges. Figure 30 is a micrograph of a section through two lamellae; two low density cells are present and have less cellular content than adjacent cells, one has the large spherical nucleus (N) (compare to pillar cell nucleus, P). Three highly vacuolated chloride cells (cl) are also shown. Erythrocytes (rc) appear normal in this micrograph; however, other sections of this same gill did contain vacuolated erythrocytes. Figure 31A shows large membranous vacuoles (va) in the low electron dense cells. Presence of many mitochondria and much SER suggest a secretory function for these cells. Loss of ridges from the surface of both epithelial cell types and an absence of intracellular structures in part of these low density cells were also noticed (Figure 31B).

Figure 30.--Transmission electron micrograph of cross sections through several lamellae of trout exposed to 300 ppt Hg as (CH_3HgCl) for 8 weeks at 5° C. Three degenerating chloride cells (Cl) can be seen to the left of the micrograph. Normal red cells (rc) and pillar cells (P) are also shown. Large epithelial cells are found on the lamellae which contain round nuclei (N), reduced microridges and are of decreased electron density. 4% glutaraldehyde fix, 1% OsO_4 postfix, LC and UA stain. 7,800x.

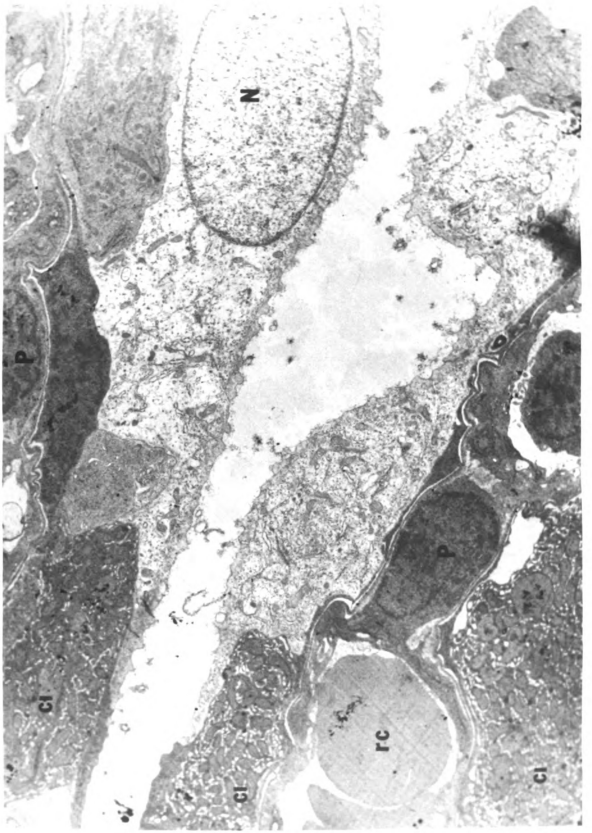
N
P
P
P
Cl
Cl
Cl
rc

Figures 31A and 31B.--Transmission electron micrograph of epithelial cells of low electron density on lamellae of trout exposed to 300 ppt Hg as (CH_3HgCl) for 8 weeks at 5° C. Nucleus (N); vacuoles (va); unidentified highly membranous structure (X). 4% glutaraldehyde fix, 1% OsO_4 postfix, LC and UA stain. Figure A: 18,000x; Figure B: 15,000x.

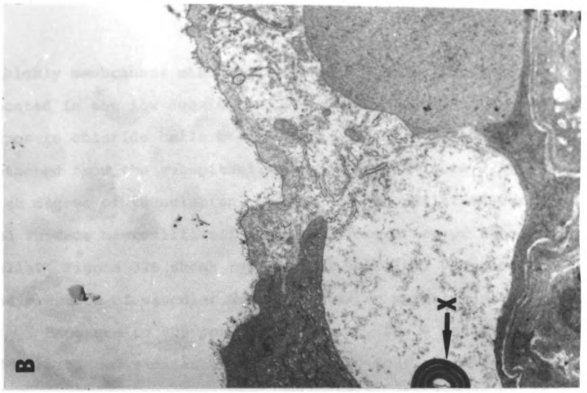
B
x

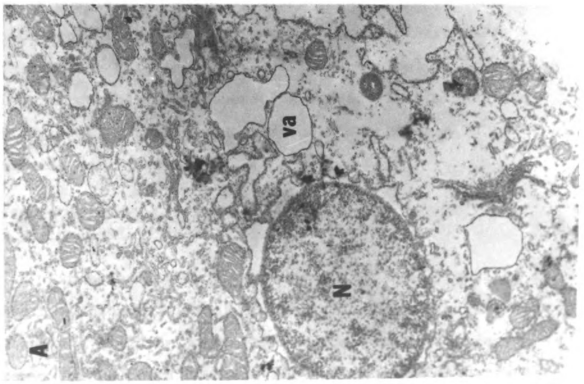
A
va
N

A highly membranous structure (X) with unknown function is located in the low density cell of Figure 31B. At this exposure chloride cells become highly vacuolated and were detached from the subepithelial structures (Figure 32A). High degree of vacuolation, loss of mitochondrial integrity and surface microvilli all suggest degeneration of these cells. Figure 32B shows typical red cell (RC) vacuolation and presence of vascular debris following mercury exposure.

Exposure to 300 ppt methyl mercury for 8 weeks at 15° C produced similar abnormalities of most chloride cells shown in Figure 33. The chloride cell in the far right of this figure appears to be separated from the epithelium and is completely devoid of microvilli. Loss of lamellar epithelial ridges was consistently found (Figure 34A). The chloride cell in Figure 34B shows typical cell vacuolation, mitochondrial degeneration (m) and loss of surface microvilli. A small vacuolated cell can be seen in the chloride cell (arrow).

Effects of Inorganic Mercury on Gill Ultrastructure

Exposure of fish to 0.25 ppm Hg as $HgCl_2$ resulted in distinct abnormalities of epithelial cells. Figure 35 is a scanning electron micrograph of the lamellar surface from a fish exposed to $HgCl_2$ for 5 days which illustrates

Figure 32A.--Transmission electron micrograph of a degenerating chloride cell on the lamella. Trout exposed to 300 ppt Hg as (CH_3HgCl) for 8 weeks at 5° C. Note extreme vacuolation of this cell. 4% glutaraldehyde fix, 1% OsO_4 postfix, LC and UA stain. 12,500x.

Figure 32B.--Transmission electron micrograph of a highly vacuolated red cell (RC) in the lamellar blood sinus. Trout exposed to 300 ppt Hg as (CH_3HgCl) for 8 weeks at 5° C. 4% glutaraldehyde fix, 1% OsO_4 postfix, LC and UA stain. 27,000x.

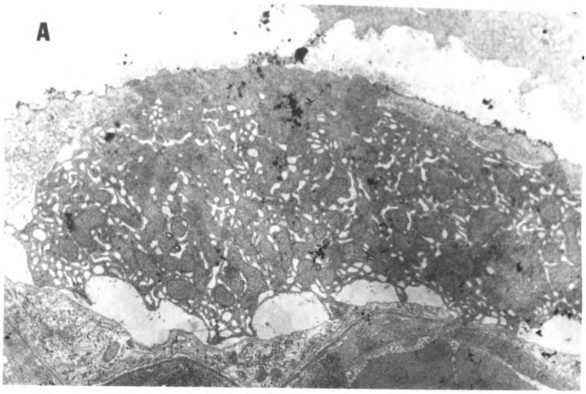
A

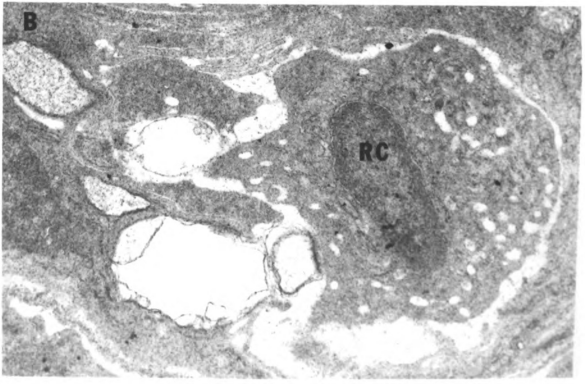
B
RC

Figure 33.--Scanning electron micrograph of degenerating chloride cells (black and white arrows) on the filament. Trout exposed to 300 ppt Hg as (CH_3HgCl) for 8 wweks at 15° C. 50% glutaraldehyde fix. 4,300x.

Figure 34A.--Transmission electron micrograph of an epithelial cell devoid of ridges. Trout exposed to 300 ppt Hg as (CH_3HgCl) for 8 weeks at 15° C. 4% glutaraldehyde fix, 1% OsO_4 postfix, LC and UA stain. 45,000x.

Figure 34B.--Transmission electron micrograph of a degenerating chloride cell and amorphous mitochondria (M). Note small vacuolated cell on cytoplasmic fragment (black and white arrow). Trout exposed to 300 ppt Hg as (CH_3HgCl) for 8 weeks at 15° C. Epithelial cell (Ep). 4% glutaraldehyde fix, 1% OsO_4 postfix, LC and UA stain. 16,000x.

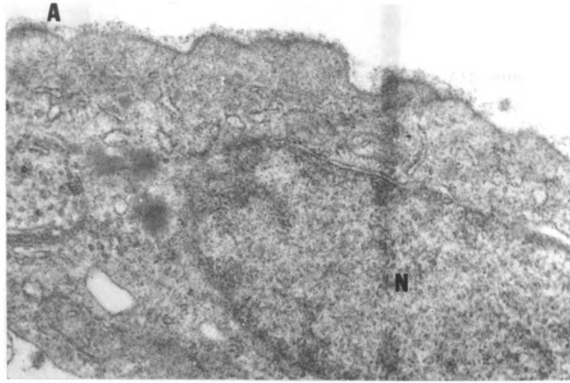
A
N

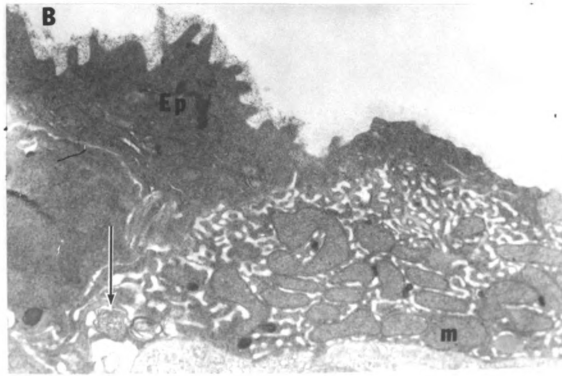
B
Ep
m

Figure 35.--Scanning electron micrograph of the lamella surface from a trout exposed to 0.25 ppm Hg as ($HgCl_2$) for 5 days. Black and white arrows point to degenerated chloride cells. Smooth epithelial cells can also be seen on the lamella. 50% glutaraldehyde fixation. 2,700x.

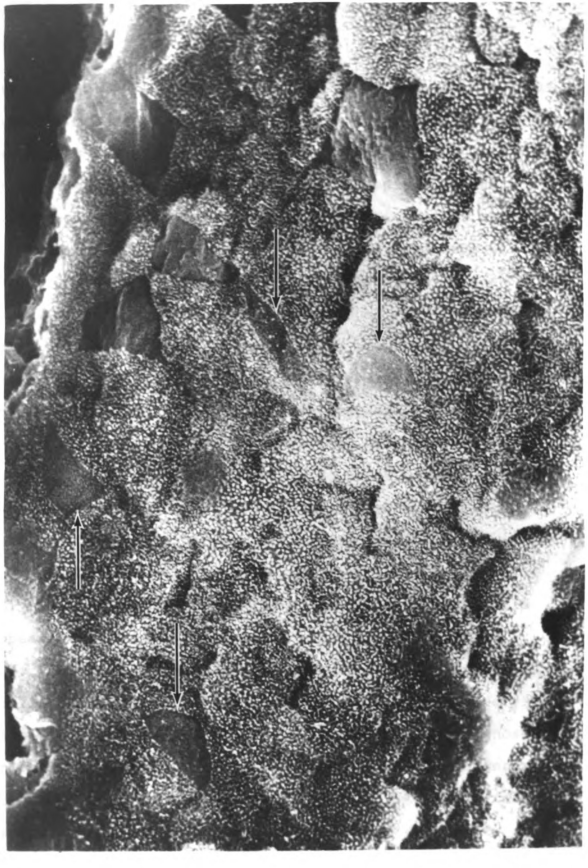

the propensity of smooth, i.e. non-ridged, epithelial cells (arrows). These cells, as seen in higher magnification in Figures 36A and 36B, appear to separate normal epithelial cell junctions (arrow, Figure 36A) and replace normal ridged cells on the lamellar surface. (Figure 36B shows difference between a chloride cell (arrow) and several smooth cells.) Cross sections of the lamellae (Figure 37) reveal large epithelial cells with smooth, i.e. non-ridged, outer cell membranes (S); these cells are not electron dense. They have a relatively large nucleus, a large cell body with numerous mitochondria, cytoplasmic vacuoles; thus, with the exception of the ridged epithelium, they are similar to epithelial cells from trout exposed to methyl mercury. No red cell abnormalities were observed in gills from inorganic mercury exposed fish. Figures 38A and 38B show the cell junction of smooth epithelial cells (S) with normal epithelial cells (Ep). The smooth cells appear to push the normal cells apart (black arrows).

Chloride cells from fish exposed to $HgCl_2$ have many small vacuoles at the apical edge of the cell (Figure 39). This is in contrast to methyl mercury exposed fish whose chloride cells initially become vacuolate from the inner border of the cell. This difference may reflect different penetration rates of the two mercurials or different

Figures 36A and 36B.--Scanning electron micrographs of lamellae with smooth epithelial cells. Trout exposed to 0.25 ppm Hg as ($HgCl_2$) for 5 days. Arrow in 36A points to separation of normal epithelial cell junctions and the overlap of these cells on the smooth cell. 50% glutaraldehyde fix. 5,700x.
Arrow in 36B points to a degenerating chloride cell. 50% glutaraldehyde fix. 4,700x.


A

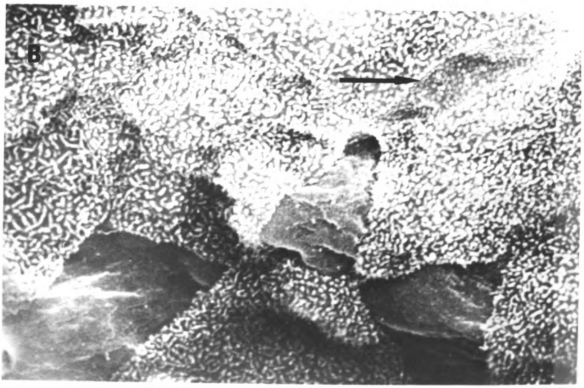
B

Figure 37.--Transmission electron micrograph of a lamellar cross section showing smooth epithelial cell (S). Trout exposed to 0.25 ppm Hg as ($HgCl_2$) for 5 days. Pillar cell (P); red blood cell (RC). 4% glutaraldehyde fix, 1% OsO_4 postfix, LC and UA stain. 14,500x.


RC
S
P

Figures 38A and 38B.--Transmission electron micrograph of the cell junctions (arrows) between a smooth epithelial cell (S) and a "normal" epithelial cell (Ep). Trout exposed to 0.25 ppm Hg as ($HgCl_2$) for 5 days. 5% glutaraldehyde fix, 1% OsO_4 postfix, LC and UA stain (both 38A and 38B). Figure 38A: 38,000x; Figure 38B: 57,500x.

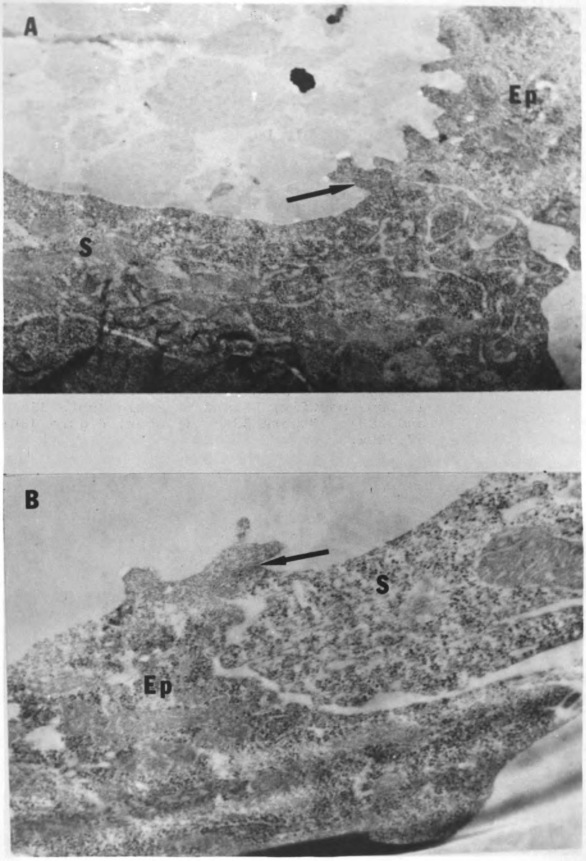
A
Ep
S
B
S
Ep

Figure 39.--Transmission electron micrograph of degenerating chloride cells (Cl) on the base of a lamella. Note electron density of large and small vacuoles within these cells. Trout exposed to 0.25 ppm Hg as ($HgCl_2$) for 5 days. 4% glutaraldehyde fix, 1% OsO_4 postfix, LC and UA stain. 18,500x.


CT

biochemical interactions. Large vessicles found in the chloride cells from inorganic mercury exposed fish were not found in those exposed to methyl mercury and may reflect differential biochemical action of the two mercurials.

Long term exposure (4 weeks) to a lower concentration (0.05 ppm, Hg as $HgCl_2$) produced similar smooth epithelial cells as shown in Figure 40 (arrows) and Figure 41B. Areas of the lamella from these fish also exhibited some changes in the epithelial cell ridges (Figure 41A); especially noticeable were a decrease in ridge height and fusion of numerous ridges into a "mat-like" appearance.

Loss of chloride cell ridges and aberrant forms of mitochondria in these cells has been shown to occur following a 30 minute exposure of the marine teleost Gadus callarias to 10^{-8} M rotenone (Öberg, 1967). Inhibition of electron transport by rotenone (White et al., 1968) and mercury (Webb, 1966) could explain the similarities between some of the chloride cell abnormalities in the present study and those found by Öberg.

Lindahl and Schwanborn (1971) using a rotary-flow technique measured the ability of the roach Leuciscus rutilus L. to maintain their position in flowing water

Figure 40.--Scanning electron micrograph of the lamellar surface from a trout exposed to 0.05 ppm Hg as ($HgCl_2$) for 4 weeks. Arrows point to smooth cells on the lamellar epithelium. 50% glutaraldehyde fix. 2,100x.

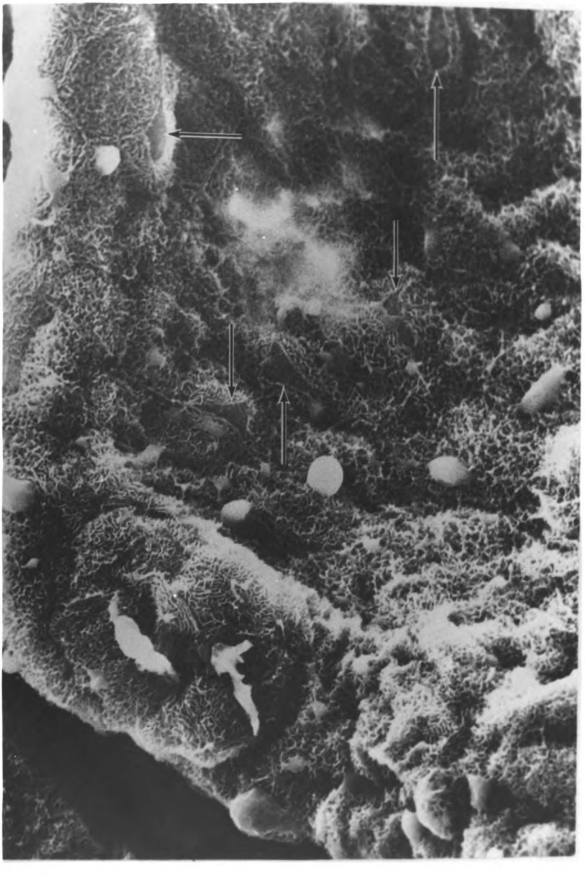

Figures 41A and 41B.--Scanning electron micrograph of the lamellar surface from trout exposed to 0.05 ppm Hg as ($HgCl_2$) for 4 weeks. Note loss of microridge structure (Figure 41A) and appearance of smooth epithelial cells (Figure 41B). 50% glutaraldehyde fix. Figure 41A: 2,900x; Figure 41B: 7,300x.

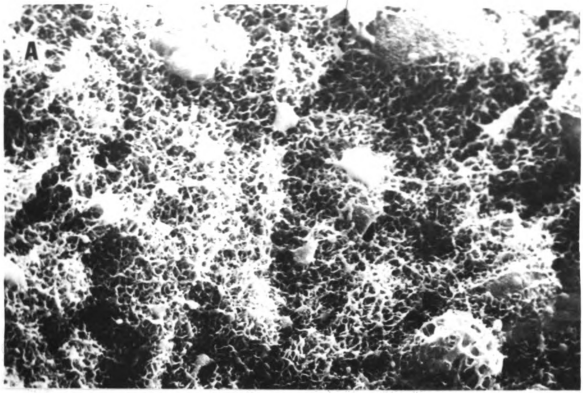
A

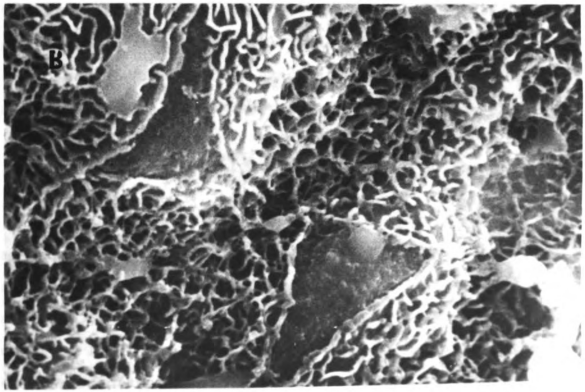
B

("fitness") and correlated this ability with the exposure history of the fish to environmental mercury. Fish were taken from two Swedish lakes, one with known high levels of ambient mercury (muscles of pike in the lake contained more than 1 ppm Hg) and another with relatively "pure water." They found that fish from the "pure water" lake could withstand a significantly greater water flow than the mercury exposed fish and there was a highly significant negative correlation between maximal rate of flow withstood and muscle mercury concentration. In view of the mercury induced changes of trout gill ultrastructure found in the present experiment, impairment of respiratory efficiency in gas exchange or osmoregulatory capability by mercurial action on the gill could indeed contribute to the loss of "fitness" of mercury exposed roach as suggested by Lindahl and Schwanborn.

Uptake and Distribution of Mercury in the Blood

Methyl mercury induced erythrocyte vacuolation and lack thereof following inorganic mercury exposure as noted in the transmission electron micrographs raised several questions on the role of blood as the secondary uptake pathway. In blood, are the two mercurials carried by the cellular or plasma fraction? Do red cells bind either

mercurial stoichiometrically? What are the physiological consequences of mercury in blood? The following experiments were designed to answer some of these questions.

Uptake Rates and Percent Incorporation of Mercury into Red Cells

The percent uptake into the erythrocyte of both mercurials as a function of time is plotted in Figure 42. With the exception of methyl mercury incubated with whole blood, all incubations attain equilibrium in less than 10 minutes. Methyl mercury did not reach equilibrium when incubated with whole blood until after 30-40 minutes. Component analysis (see Appendix II) of this reaction revealed a two component uptake system, the first component having a half time of under 1 minute, the second about 11 minutes. This can be explained by initial binding of a small percent of mercury to plasma proteins or thiols, the remainder being taken up by the red cells as a function of the free or non-plasma bound mercury. After the red cells have removed most of the unbound mercury from the plasma a new equilibrium (slow component) is established which is dependent on the dissociation of bound mercury from "plasma sites" prior to red cell uptake. This postulate is further supported by uptake of methyl mercury into

Figure 42.--Percent uptake of methyl mercury or divalent mercury by red blood cells as a function of time.

▲= CH_3HgCl incubated in whole blood (15);

◆= $HgCl_2$ in whole blood (6);

△= CH_3HgCl incubated with washed cells suspended in Abbott Ringer (4);

◇= $HgCl_2$ incubated with washed cells suspended in Abbott Ringer (4);

○= $HgCl_2$ incubated with washed cells suspended in Phosphate Buffered Ringer (4).

Exposure concentrations approximately 0.0133 total ppm CH_3HgCl and 0.054 ppm total $HgCl_2$. Number of observations (N). Standard errors are not shown on the graph as they were smaller than the diameter of the data points.

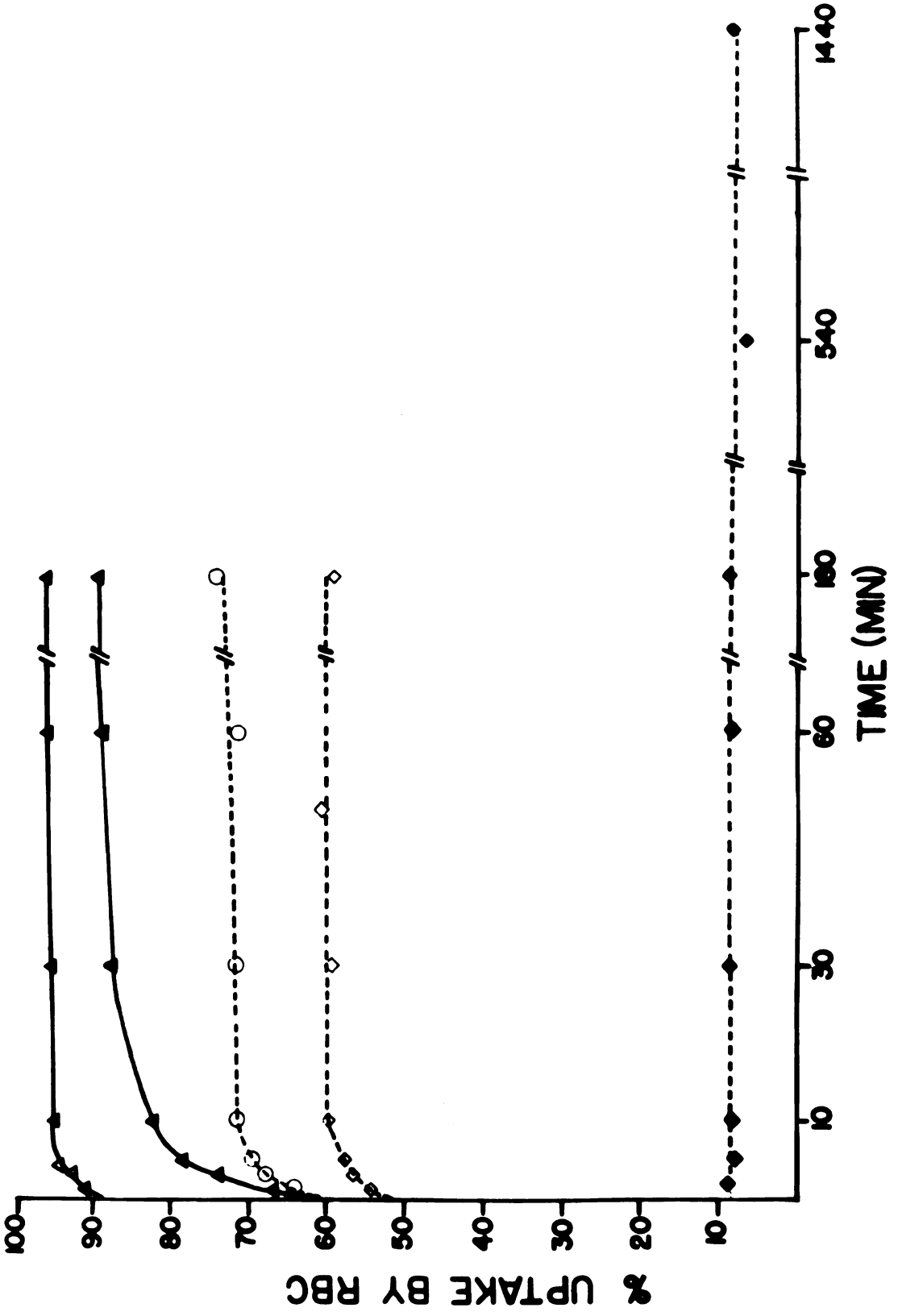
% UPTAKE BY RBC
100
90
80
70
60
50
40
30
20
10
10
30
60
180
540
1440
TIME (MIN)

cells suspended in Ringer solution. In this instance the uptake rate is so fast that one component can be determined. Increased CH_3Hg^+ binding at equilibrium by washed cells in Ringer solution compared to cells in plasma (95% compared to 90%) is probably indicative of some irreversible mercury binding to plasma protein. Failure of the washed cells to bind 100% of the mercury could be due to slight hemolysis coupled with some mercury binding by the incubating media and glassware.

Inorganic mercury incubated with whole blood binds almost exclusively to the plasma fraction; less than 9% was taken up by red cells after 1440 minutes. Such a distribution could explain why in vivo, methyl mercury produced ultrastructural abnormalities in erythrocytes and inorganic mercury did not.

Washed red cells suspended in Ringer solution take up 9 to 10 times more inorganic mercury than cells do in plasma. Removal of plasma proteins undoubtedly is the critical factor. There is also a significant difference between percent red cell uptake which is dependent on the suspending media; cells suspended in Abbott Ringer take up less Hg^{++} than cells suspended in phosphate buffered Ringer solution. Since the only difference between Abbott and phosphate buffered Ringer (PBR) is the presence

of magnesium and buffering capacity of the PBR, either the magnesium or pH (perhaps both) must enhance equilibrium binding by red cells. Weed et al. (1962) compared the effects of buffered to unbuffered solutions of saline on Hg^{++} uptake by human red cells and found no effect even if the pH of the unbuffered solution was decreased to 6.8. Thus magnesium or some other unaccounted for parameter must be the important factor(s).

Less than 100% of the available methyl or inorganic mercury was taken up by red cells. LeFevre (1947) found that the effect of mercury on the uptake of sugar by mammalian red cells was reduced if the cells were allowed to stand for some time before addition of mercury. He postulated that there was secretion of a mercury chelator by the cells which after a period of time reached sufficient levels to bind enough mercury to effectively reduce the free mercury available for cellular uptake. Weed et al. (1962) found similar results with respect to inorganic mercury uptake, i.e., the longer the cells were incubated without mercury, the less mercury would be taken up by them after this ion was added. In the present experiments percent mercury uptake before and at equilibrium was calculated for cells to which mercury was added within 1 minute after final suspension or whole blood sampling

and for cells which had been allowed to stand in Ringer solution or whole blood for 45 minutes prior to addition of mercury. Uptake of either methyl or inorganic mercury was in all instances independent of the length of the incubation period which preceded addition of mercury to the cell suspension. Thus, secretion of a chelator by trout red cells is not a factor in the failure of these cells (especially washed cells) to bind all mercury present.

In an attempt to determine the total number of binding sites in the red cell, washed cells were incubated for 90 min with increasing concentrations of mercury. Weed et al. (1962) have shown that the percent of inorganic mercury bound to the red cell decreases as ambient mercury increases, which is indicative of saturation of specific binding sites on or within the red cell. Figure 43 shows the results of his experiment in which increased levels of ambient mercury produced a characteristic saturation curve (Figure 43, open circles) and percent mercury bound decreased from 97 to 39 percent. These data do not correlate with methyl (open triangles) or inorganic (solid triangles) mercury binding from the present study as the present mercury bound remained constant for all levels of ambient mercury examined. Ambient mercury levels higher

Figure 43.--Concentration of mercury in the red blood cell fraction as a function of ambient mercury levels.

▲ = inorganic mercury, washed trout erythrocytes (4)

Δ = organic mercury, washed trout erythrocytes (4)

o = data from Weed et al. (1962), washed human erythrocytes (2)

Number of observations (N). Standard errors are smaller than diameter of data points.

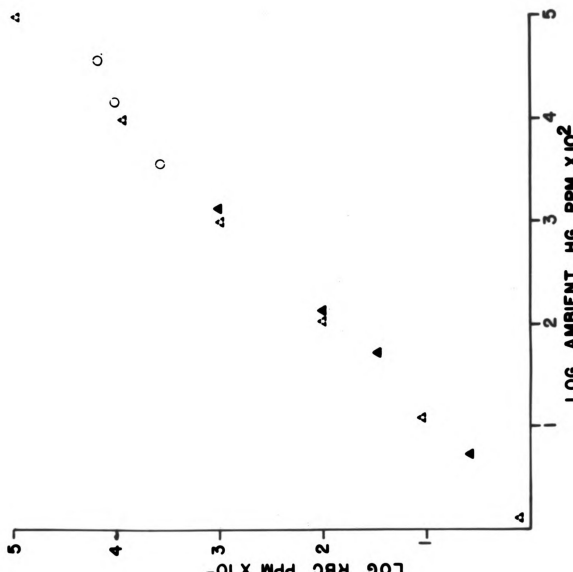
LOG RBC PPM X 10^2
LOG AMBIENT HG PPM X 10^2
1
2
3
4
5

than those plotted produced excessive red cell hemolysis in the trout blood experiments; Weed reported essentially no hemolysis for human erythrocytes irrespective of ambient mercury concentration.

It appears that saturation of trout erythrocytes with mercurials either must involve some group (SH, amino, acidic sugars, mucopoly saccharides, or other) which is responsible for cell membrane integrity and is not saturated at the time of hemolysis or mercury levels below total saturation sufficiently disrupt ionic balance and produce osmotic hemolysis.

Consistent RBC unbound/bound ratios for either mercurial at all ambient mercury concentrations studied is unexplainable in terms of a specific binding site theory since at low mercury concentrations a greater percentage of the available mercury should bind with the cell. Why 5% of the methyl mercury and approximately 25% of the inorganic mercury fail to bind to the red cell irrespective of a one hundred thousand fold increase of ambient methyl mercury or a three thousand fold increase of ambient inorganic mercury concentration is unknown.

Sulfhydryl containing compounds such as albumin, cysteine and reduced glutathione failed to remove either inorganic or organic mercury previously bound to red cells

Table 5.--Effects of sulfhydryl agents on mercury binding to red cells.

Inorganic mercury					
Hg concentration ppm total	0.054	0.54	1.454	14.054	140.054
ppm (mgHg/l red cells)	0.387	3.87	10.39	100.39	1000.4
Control % Incorporation into RBC ± S.E.	66.99±3.17	57.06±1.35	74.99±1.94	77.31±0.78	hemolysis
Effect of SH groups					
% Incorporation + Albumin (1.37×10^{-5}M)	66.85±3.76	59.59±2.22	79.88±1.73	77.38±1.23	-------
% Incorporation + Cysteine (1.37×10^{-4}M)	68.78±2.60	64.09±1.78	81.67±1.76	77.97±1.36	-------
% Incorporation + Reduced GSH' (1.37×10^{-4}M)	61.30±3.07	47.32±2.42	78.66±1.61	74.56±2.58	-------
Number of observations	6	4	6	6	

Table 5.--Continued.

	Methyl mercury				
Hg concentration ppm total	0.1326	1000.0			
ppm (mgHg/l red cells)	0.947	7143.8			
Control % Incorporation into RBC ± S.E.	95.15±0.21	96.88±0.68			
Effect of SH groups					
% Incorporation + Albumin (1.37×10^{-5}M)	95.98±0.10	97.44±0.21			
% Incorporation + Cysteine (1.37×10^{-4}M)	96.63±0.19	96.63±0.22			
% Incorporation + Reduced GSH' (1.37×10^{-4}M)	95.84±0.19	96.19±0.11			
Number of observations	4	4			

Means ± S.E.; GSH = glutathione

(see Table 5). In both experiments levels of sulfhydryl groups exceeded mercury concentrations at the low ambient mercury levels, yet all SH contributors failed to remove any mercury from the cells, which suggests strong mercury-red cell binding.

Effect of Mercurials on Oxygen Carrying Capacity of Red Cells

Methyl and inorganic mercury in concentrations up to 100 ppm (total Hg conc.) had no significant effect on the total amount of oxygen carried by red cells (Table 6).

Table 6.--Effects of CH_3HgCl and $HgCl_2$ on oxygen carrying capacity of washed red cells. Mean±SE (N).

Ambient mercury concentration (ppm)	Methyl mercury (ml O_2/g Hb)	Inorganic mercury (ml O_2/g Hb)
0	1.42 ± 0.114 (4)	0.50 ± 0.054 (4)
1	1.45 ± 0.119 (4)	0.62 ± 0.040 (4)
100	1.48 ± 0.163 (4)	0.63 ± 0.026 (4)

In spite of these results, effects of mercury on oxygen transport to the tissues cannot be ruled out. Incubation times of one to two hours, although adequate for saturation

of mercury binding sites, might not be sufficient to show mercurial effects on oxygen carrying capacity resulting from alteration of ionic balances or sugar transport. Mercury might also affect the oxygen dissociation curve which is of great physiological importance and would not be detectable in studies of oxygen carrying capacity. Long term exposure to mercurials could alter the number of circulating erythrocytes or their hemoglobin content. Mercurials such as para-hydroxymercuribenzoate and para-hydroxymercuriphenylsulphorate have, for example, been shown to block the uptake of transferrin bound iron by reticulocytes in humans (Fielding et al., 1969; Edwards and Fielding, 1971).

Mercury in sublethal concentrations has been shown to enter teleosts via the gill and have definite consequences on the ultrastructure of this organ. Many questions remain unanswered as to the physiological correlation with morphological alterations and the precise pathway and chemical form of mercury entering the gill and vasculature. Additional studies are certainly needed on the effects of environmental levels of mercurials on the various organ systems of aquatic animals. If man is going to establish meaningful criteria for water quality, he must set standards which will not only be safe for him but which will also insure the safety of all his natural resources.

CONCLUSIONS

1. The gill is the major pathway for uptake of mercury as either Hg^{++} of CH_3Hg^{+}) in nonfeeding rainbow trout.

2. Uptake rates of methyl mercury are higher than for inorganic mercury at 24 hours. The difference is due to increased permeation of gill tissue by the methylated form.

3. Accumulations of methyl mercury by tissues is highest for gill followed in decreasing order by kidney, blood, heart, liver, intestine, stomach and muscle. Inorganic mercury is concentrated primarily in the gill followed by blood, intestine, kidney, stomach, liver, heart and muscle.

4. Inorganic mercury is trapped by the mucus coat covering the gills. Uptake into the gill tissue appears to involve the general lamellar and filamental surface.

5. Inorganic mercury is not concentrated in and therefore probably not actively transported by the chloride cells.

6. Inorganic mercury has a greater stimulatory action on mucus secretion by the gills than methyl mercury.

7. Methyl mercury induced hyperplasia of cells on the filament between the lamella and inorganic mercury induced separation of the lamellae epithelial cells. Gross necrosis of the gills was not observed.

8. Protoplasmic extensions of the lamellar epithelial surface form a random network of ridges which increase surface area 2.45 times.

9. Chloride cells, characterized by many mitochondria, dense SER and presence of apical microvilli are in a state of constant turn over. Degenerating chloride cells are typified by cellular vacuolation, amorphous mitochondria, reduction and vacuolation of SER and loss of apical ridges.

10. Ultrastructural changes of gill tissue from trout exposed up to 8 wks to methyl mercury include loss of epithelial cell ridges, appearance of large highly vacuolated epithelial cells of low electron density and enhanced chloride cell degeneration.

11. Inorganic mercury exposure (up to 4 wks) produced ultrastructural changes in trout gill characterized

by appearance of large epithelial cells whose outer membrane was smooth, i.e., non-ridged, and chloride cell degeneration accompanied by atypical vacuolation.

12. Ultrastructural abnormalities were found in erythrocytes after fish were exposed to methyl mercury but not after inorganic mercury exposure. Methyl mercury exposed fish also exhibited greater numbers of reticulocytes (as evidenced by numerous mitochondria in the red cell) in the gill vasculature.

13. In whole blood, 89% of the methyl mercury is found in red cells compared to 8% for inorganic mercury. Washed red cells exposed to mercury in Ringer solution take up 95% of the methyl mercury and 55% of the inorganic mercury from the bath. Equilibrium in all instances is achieved in under 10 minutes except for methyl mercury in whole blood which achieves equilibrium in 40 minutes.

14. Rainbow trout erythrocytes do not secrete a compound capable of chelating either mercurial.

15. Percent of either mercurial bound to red cells was independent of ambient mercury concentration. Saturation of erythrocyte associated SH groups was prevented by red cell hemolysis.

16. Mercury bound to red cells could not be dissociated from them even after addition of thiols to the plasma.

17. Inorganic and organic mercury have no effect on oxygen carrying capacity of red cells.

REFERENCES

REFERENCES

Amend, D. F., W. T. Yasutake and R. Morgan. 1969. Some factors influencing susceptibility of rainbow trout to the acute toxicity of an ethyl mercury phosphate formulation (Timsan). Trans. Amer. Fish. Soc. 3:419-425.

Ancill, R. J., E. R. Richens and D. A. Norton. 1970. The reactions of organic mercurials on the cornea. Trans. Opthalmol. Soc. U.K. 89:863-866.

Anderson, T. F. 1951. Techniques for the preservation of three-dimensional structure in preparing specimens for the electron microscope. Trans. N.Y. Acad. Sci. 13:130-134.

Backström, J. 1969. Distribution studies of mercuric pesticides in quail and some fresh-water fishes. Acta Pharm. et. Toxicol. 27:5-103.

Bentley, P. J. 1962. Permeability of the skin of the cyclostome Lampetra fluviatilis to water and electrolytes. Comp. Biochem. Physiol. 6:95-97.

Berlin, M., and S. Gibson. 1963. Renal uptake, retention and excretion of mercury. I. A study in the rabbits during infusion of mercuric chloride. Arch. Environ. Health 6:617-622.

Bierther, M. 1970. Die chloridzellen des stichlings. Z. Zellforsch. 107:421-446.

Bucci, E., and C. Fronticelli. 1965. A new method for the preparation of α and β subunits of human hemoglobin. J. Biol. Chem. 240:551-552.

Cameron, J. N., and J. C. Davis. 1970. Gas exchange in rainbow trout (Salmo gairdneri) with varying blood oxygen capacity. J. Fish. Res. Bd. Canada 27:1069-1085.

Davis, J. C., and J. N. Cameron. 1971. Water flow and gas exchange at the gills of rainbow trout (Salmo gairdneri). J. Exp. Biol. 54:1-18.

D'Itri, F. M. 1972. Mercury in the aquatic ecosystem. Institute of Water Research. Michigan State University Technical Report #23. 101p.

Edwards, S. A., and J. Fielding. 1971. Studies of the effect of sulphydryl and other inhibitors on reticulocyte uptake of doubly-labelled transferrin. Br. J. Haematol. 20:405-416.

Ellis, R. W., and S. C. Fang. 1967. Elimination, tissue accumulation, and cellular incorporation of mercury in rats receiving an oral dose of ^{203}Hg-labeled phenylmercuric acetate and mercuric acetate. Toxicol. Appl. Pharm. 11:104-113.

Evans, D. H. 1969. Studies on the permeability to water of selected marine, freshwater and euryhaline teleosts. J. Exp. Biol. 50:689-703.

Fielding, J., S. A. Edwards and R. Ryall. 1969. Effect of sulphydryl inhibition on the uptake of transferrin-bound iron by reticulocytes. J. Clin. Path. 22: 677-679.

Friberg, L., and J. Vostal. 1972. (Eds.) Mercury in the Environment: an Epidemiologican and Toxicological Appraisal. Chemical Rubber Co. Cleveland, Ohio. 215p.

Giardina, B., I. Binotti, G. Amiconi, E. Antonini, M. Brunori and C. H. McMurry. 1971. Functional properties of human hemoglobin and isolated hemoglobin chains treated with organic mercurials. Eur. J. Biochem. 22:327-330.

Gilula, N. B., and P. Satir. 1971. Septate and gap junctions in molluscan gill epithelium. J. Cell. Biol. 51:869-872.

Goldstein, L., and R. P. Forster. 1961. Source of ammonia excreted by the gills of the marine teleost Myoxocephalus scorpius. Am. J. Physiol. 200:1116-1118.

Goldstein, L., R. P. Forster and G. M. Fanelli, Jr. 1964. Gill blood flow and ammonia excretion in the marine teleost Myoxocephalus scorpius. Comp. Biochem. Physiol. 12:489-499.

Halbhuber, von K. J., H. J. Stibenz, U. Halbhuber and G. Geyer. 1970. Autoradiographische untersuchungen uber die verteilung einiger metallisotope im darm von laboratoriumstieren. Ein beitrag zur ausscheidungsfunken der panethschen kornerzellen. Acta Histochem. 35:307-319.

Hannerz, L. 1968. Experimental investigations on the accumulation of mercury in water organisms. Rep. Inst. Freshwater Res. Sweden 48:120-176.

Hibiya, T., and M. Oguri. 1961. Gill absorption and tissue distribution of some radionuclides (Cr-51, Hg-203, Zn-65 and Ag-110m. 110) in fish. Bull. Japan. Soc. Sci. Fish. 27:996-1000.

Hoar, W. S., and D. J. Randall. 1969. (Eds.) Fish Physiology. Vol. I: Excretion, Ionic Regulation and Metabolism. Academic Press, New York. 465p.

Holeton, G. F., and D. J. Randall. 1967. The effect of hypoxia upon the partial pressure of gasses in the blood and water afferent and efferent to the gills of rainbow trout. J. Exp. Biol. 46:317-327.

Horridge, G. A., and S. L. Tamm. 1969. Critical point drying for scanning electron microscope study of cillary motion. Science 163:817-818.

Hughes, G. M. 1966. The dimensions of fish gills in relation to their function. J. Exp. Biol. 45:177-195.

Hughes, G. M., and E. R. Weibel. 1972. Similarity of supporting tissue in fish gills and the mammalian reticuloendothelium. J. Ultras. Res. 39:106-114.

Hughes, G. M., and D. E. Wright. 1970. A comparative study of the ultrastructure of the water-blood pathway in the secondary lamellae of teleost and elasmobranch fishes--Bethnic forms. Z. Zellforsch. 104: 478-493.

Järvenpää, T., M. Tillander and J. K. Miettinen. 1970. Methyl mercury: Half-time of elimination in flounder, pike and eel. Suomen Kemistilehti B 43:439-442.

Joyce, C. R. B., H. Moore and M. Weatherall. 1954. The effects of lead, mercury and gold on the potassium turnover of rabbit blood cells. Brit. J. Pharmacol. 9:463-470.

Keys, A. 1931. The heart-gill preparation of the eel and its perfusion for the study of a natural membrane in situ. Z. Vergl. Physiol. 15:352-363.

Keys, A., and E. N. Willmer. 1932. "Chloride secreting cells" in the gills of fishes with special reference to the common eel. J. Physiol. 76:368-378.

Klingenmaier, C. H., M. G. Behar and T. C. Smith. 1969. Blood oxygen content measured by oxygen tension after release by carbon monoxide. J. Appl. Physiol. 26: 653-655.

Knauf, P. A., and A. Rothstein. 1971. Chemical modification of membranes. I. Effects of sulfhydryl and amino reactive reagents on anion and cation permeability of the human red blood cell. J. Gen. Physiol. 58:190-210.

Knauf, P. A., and A. Rothstein. 1971. Chemical modification of membranes. II. Permeation paths for sulfhydryl agents. J. Gen. Physiol. 58:211-223.

Knoll, J. 1962. Sodium and chromate ion movement across isolated frog and fish skins with the effect of magnetic fields upon such movement. Ph.D. Thesis. Michigan State University, East Lansing, Michigan.

Kostenko, V. G., and V. I. Iaksuleva. 1971. Morphological and functional characteristics of changes in mouse erythrocytes in vitro in the presence of bivalent mercury and cadmium ions. Tsitologiia 13:1475-1482.

Krogh, A. 1937. Osmotic regulation in freshwater fishes by active absorption of chloride ions. Z. Vergl. Physiol. 24:656-666.

Leeson, T. S., and C. R. Leeson. 1970. (Eds.) Histology. W. B. Saunders Co., Philadelphia. 525p.

LeFevre, P. G. 1947. Evidence of active transfer of certain nonelectrolytes across the human red cell membrane. J. Gen. Physiol. 31:505.

Lindahl, P. E., and E. Schwanbom. 1971. Rotatory-flow technique as a means of detecting sublethal poisoning in fish populations. OIKOS 22:354-357.

Löfroth, G. 1969. Methylmercury. Ecological Research Committee Bulletin #4. Swedish Natural Science Research Council, Stockholm, Sweden. 38p.

Lowenstein, O. 1962. (Ed.) Advances in Comparative Physiology and Biochemistry. Vol. I. Academic Press, New York. 392p.

Luna, L. G. 1968. (Ed.) Manual of Histological Staining Methods of the Armed Forces Institute of Pathology. McGraw-Hill Book Co., New York. 258p.

Lundgren, K. D., A. Swensson and U. Ulfuarson. 1967. Studies in humans on the distribution of mercury in the blood and the excretion in urine after exposure to different mercury compounds. Scand. J. Clin. Lab. Invest. 20:164-170.

Maetz, J. 1971. Fish gills: mechanisms of salt transfer in freshwater and sea water. Phil. Trans. Roy. Soc. Lond. B 262:209-249.

Maetz, J., and E. Skadhauge. 1968. Drinking rates and gill ionic turnover in relation to external salinities in the eel. Nature 217:371-373.

Martin, K. 1971. Some properties of an SH group essential for choline transport in human erythrocytes. J. Physiol. (Lond.) 213:647-664.

McKone, C. E., R. G. Young, C. A. Bache and D. J. Lisk. Rapid uptake of mercuric ion by goldfish. (unpublished data).

Mercury in Man's Environment. 1971. Proceedings of the Symposium. The Royal Society of Canada. Ottawa, Ontario. 201p.

Mercury in the Environment. 1970. Geological Survey Professional Paper 713. U.S. Government Printing Office, Washington, D.C.

Meyer, D. K. 1952. Effects of mercuric ion on sodium movement through the gills of goldfish. Fed. Proc. 11:107-108.

Miettinen, J. K., M. Tillander, K. Rissanen, V. Miettinen and Y. Ohmomo. 1969. Distribution and excretion rate of phenyl and methyl mercury nitrate in fish, mussels, molluscs and crayfish. Reprinted from Proceedings of the 9th Japan conference on radio-isotopes. Atomic Energy Society of Japan.

Miettinen, J. K., M. Heyraud and S. Keckes. 1970. Mercury as a hydrospheric pollutant. II. Biological half-time of methyl mercury in four Mediterranean species: a fish, a crab, and two molluscs. FAO Technical conference on marine pollution and its effects on living resources and fishing. Rome, Italy.

Miettinen, V., E. Blankenstein, K. Rissanen, M. Tillander, J. K. Miettinen and M. Valtonen. 1970. Preliminary study on the distribution and effects of two chemical forms of methyl mercury in pike and rainbow trout. FAO technical conference on marine pollution and its effects on living resources and fishing. Rome, Italy.

Motais, R., J. Isaia, J. C. Rankin and J. Maetz. 1969. Adaptive changes of the water permeability of the teleostean gill epithelium in relation to external salinity. J. Exp. Biol. 51:529-546.

Motais, R., and F. Garcia-Romeu. 1972. Transport mechanisms in the teleostean gill and amphibian skin. Ann. Rev. Physiol. 34:141-176.

Muir, B. S. 1969. Gill dimensions as a function of fish size. Fish. Res. Bd. Canada 26:165-170.

Muir, B. S., and G. M. Hughes. 1969. Gill dimensions for three species of tunny. J. Exp. Biol. 51:271-285.

Norseth, T., and T. W. Clarkson. 1970. Studies on the biotransformation of ^{203}Hg-labeled methyl mercury chloride in rats. Arch. Environ. Health 21:717-727.

Öberg, K. C. 1967. The reversibility of the respiratory inhibition in gills and the ultrastructural changes in chloride cells from the rotenone-poisoned marine teleost, Gadus callarias L. Exp. Cell Res. 45: 590-602.

Olson, L. E. 1969. Glucose metabolism and maintenance of transparency in ocular tissue of rainbow trout. Ph.D. Thesis. Michigan State University, East Lansing, Michigan.

Osmer, B. L. 1965. (Ed.) Hawk's Physiological Chemistry. 14th ed. McGraw-Hill Book Co., New York. 1472p.

Paling, J. E. 1968. A method of estimating the relative volumes of water flowing over the different gills of a freshwater fish. J. Exp. Biol. 48:533-544.

Potter, G. D., D. R. McIntyre and G. M. Vottuone. 1972. Metabolism of ^{203}Hg administered as $HgCl_2$ in the dairy cow and calf. Health Physics 22:103-106.

Prosser, C. L., and F. A. Brown. 1966. Comparative Animal Physiology. W. B. Saunders Co., Philadelphia. 688p.

Rahola, T., T. Hattula, A. Korolainen and J. K. Miettinen. 1971. The biological half-time of inorganic mercury (Hg^{2+}) in man. Scand. J. clin. Lab. Invest., Abstr., 27 (Suppl. 116), 77.

Rasmussen, H. P., V. E. Shull and H. T. Dryer. 1968. Determination of element localization in plant tissue with the microprobe. Developments in Applied Spectroscopy 16:29-42.

Reynolds, E. S. 1963. The use of lead citrate of high pH as an electron opaque stain in electron microscopy. J. Cell Biol. 17:208-212.

Richards, B. D. 1968. Sodium uptake by isolated perfused gills of rainbow trout Salmo gairdneri with special reference to patterns of gill blood flow. Ph.D. Thesis. Michigan State University, East Lansing, Michigan.

Ritch, R., and C. W. Philpott. 1969. Repeating particles associated with an electrolyte-transport membrane. Exp. Cell Res. 55:17-24.

Rucker, R. R., and D. F. Amend. 1969. Absorption and retention of organic mercurials by rainbow trout and chinook and sockeye salmon. The Prog. Fish-Cult. 31:197-201.

Schweiger, G. 1957. Die toxikologische einwirkung von schwermetallsalzen auf fische und fischnahrtiere. Archiv. fur Fishereiwissenschaft 8:54-77.

Selikoff, I. J. 1971. Hazards of mercury. Environ. Res. 4: 1-69.

Shapiro, B., G. Kollmann and D. Martin. 1970. The diversity of sulfhydryl groups in the human erythrocyte membrane. J. Cell Physiol. 75:281-292.

Shehadeh, Z. H., and M. S. Gordon. 1969. The role of the intestine in salinity adaptation of the rainbow trout Salmo gairdneri. Comp. Biochem. Physiol. 30: 397-418.

Silberberg, I. 1968. Percutaneous absorption of mercury in man: I. A study by electronmicroscopy of the passage of topically applied mercury salts through stratum corneum of subjects not sensitive to mercury. J. Invest. Derm. 50: 323-331.

Silberberg, I. 1972. Ultrastructural identification of mercury in epidermis. Arch. Environ. Health. 24: 129-144.

Smith, H. W. 1929. The excretion of ammonia and urea by the gills of fish. J. Biol. Chem. 81:727-742.

Smith, H. W. 1930. The absorption and excretion of water and salts by marine teleosts. Amer. J. Physiol. 93:480-505.

Stevens, E. D., and D. J. Randall. 1967. Changes of gas concentrations in blood and water during moderate swimming activity in rainbow trout. J. Exp. Biol. 46:329-337.

Straus, L. P. 1963. A study of the fine structure of the so-called chloride cell in the gill of the guppy Lebistes reticulatus P. Physiol. Zool. 36:183-198.

Straus, L. P., and W. L. Doyle. 1961. Fine structure of the so-called chloride cells of the gills of the guppy. Am. Zoologist 1:392.

Sutherland, R. M., A. Rothstein and R. I. Weed. 1967. Erythrocyte membrane sulfhydryl groups and cation permeability. J. Cell Physiol. 64:185-195.

Swensson, A., K. D. Lundgren and O. Lindstrom. 1959. Distribution and excretion of mercury compounds after single injection. A.M.A. Arch. Ind. Health 20:432-443.

Swensson, A., K. D. Lundgren and O. Lindstrom. 1959. Retention of various mercury compounds after subacute administration. A.M.A. Arch. Ind. Health 20:467-472.

Threadgold, L. T., and A. H. Houston. 1964. An electron-microscopic study of the "chloride cell" of Salmo salar L. Exp. Cell Res. 34:1-23.

VanSteveninck, J., R. I. Weed and A. Rothstein. 1965. Localization of erythrocyte membrane sulfhydryl groups essential for glucose transport. J. Gen. Physiol. 48:617-632.

Vincent, P. C., and C. R. B. Blackburn. 1958. The effects of heavy metal ions on the human erythrocyte. I. Comparisons of the action of several heavy metals. Austral. J. Exp. Biol. 36:471-478.

Watson, M. L. 1958. Staining of tissue sections for electronmicroscopy with heavy metal. J. Biophys. Biochem. Cytol. 4:475.

Webb, J. L. 1966. Enzyme and Metabolic Inhibitors. Vol. 2. Academic Press, New York. 1237p.

Weed, R. I., J. Eber and A. Rothstein. 1962. Interaction of mercury with human erythrocytes. J. Gen. Physiol. 45:395-410.

White, A., P. Handler and L. Smith. 1968. Principles of Biochemistry. 4th ed. McGraw-Hill Book Co., New York. 1187p.

Yamaguchi, S. 1969. Toxicological studies on organo-mercuric pesticides. Nippon Hoigaku Zasshi (The Japanese Journal of Legal Medicine). 23:123-138. Translated by Fish. Res. Bd. Canada series #1477, 1970.

APPENDICES

APPENDIX I

SOLUTIONS

Dietrichs Fixative:

Glacial acetic acid	5 ml
40% formalin	25 ml
95% ethanol	75 ml
tap water	150 ml

Phosphate Buffered Ringer (PBR):

NaCl	8.00 g/Liter
KCl	0.20 g/Liter
Na_2HPO_4 (anhydrous)	1.15 g/Liter
$K_2HPO_4 \cdot H_2O$	0.20 g/Liter
$CaCl_2$	0.10 g/Liter
$MgCl_2 \cdot 6H_2O$	0.19 g/Liter

Sørensen Buffer:

A. NaH_2PO_4 27.8 g into 1 Liter

B. $Na_2HPO_4 \cdot 7H_2O$ 53.0 g into 1 Liter

Just prior to use mix 19 parts A with 81 parts B.

APPENDIX II

COMPONENT ANALYSIS OF MERCURY UPTAKE EQUILIBRIUM CURVE

Uptake rate of methyl mercury by red cells in plasma did not approach equilibrium as rapidly as the methyl mercury in washed cells (Figure 42), therefore, it was necessary to determine if the uptake rate had more than one component.

The present mercury uptake at equilibrium (Peq) was determined from Figure 44 at the time when the slope of uptake rate was zero (i.e., at 180 mins). The percent uptake at all times prior to equilibrium (P) was subtracted from the percent uptake at equilibrium and this value (Peq-P) plotted on the ordinate of semi-log paper against the corresponding time on the abscissa (Figure 44). The graph obtained in this manner showed multicomponent characteristics. In order to isolate the components, the linear portion of the curve (Component II) was extrapolated back to zero time. The extrapolated portion of the Component II was then subtracted from the curve (Peq-P) at their respective times to give Component I. As Component I is linear or nearly so, it appears that the

Figure 44.--Component analysis of methyl mercuric uptake by red blood cells. See text for details.

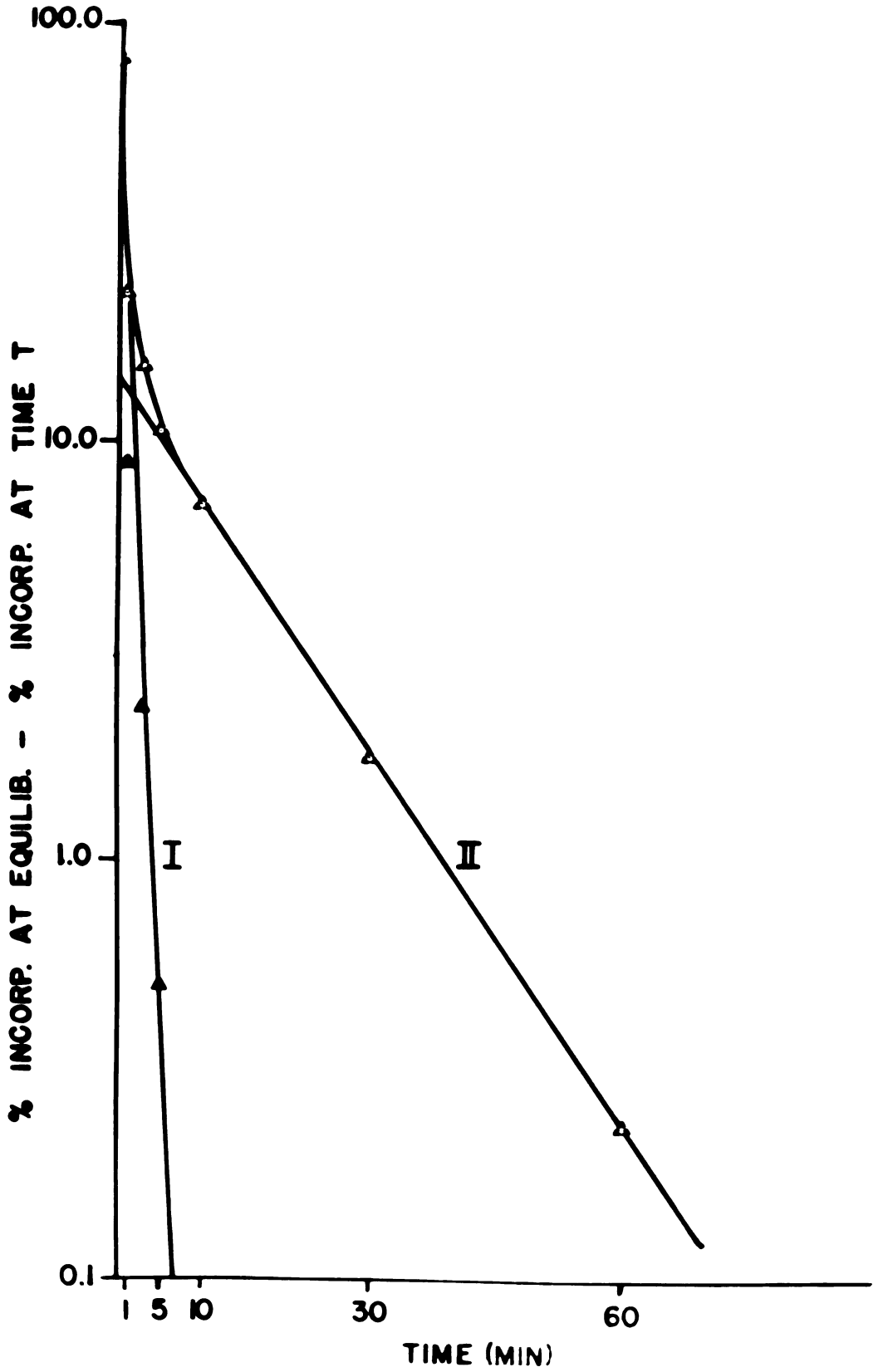
100.0
10.0
1.0
0.1
% INCORP. AT EQUILIB. - % INCORP. AT TIME T
I
II
1
5
10
30
60
TIME (MIN)

uptake of methyl mercury by whole blood is a two-component system. Mathematical description of the components can be written according to the general decay equation as follows:

Component I: $P_{tI} = P_{oI}e^{-}$

Where: $P_{tI} = P_{eq} - P_t$ at time t

$P_{oI} = P_{eq} - P_t$ at time o

e = base of natural logarithm

I = rate constant = $0.693/T_{1/2}$ = slope

t = time in minutes

$T_{1/2}$ = time required to change $P_{eq} - P_t$ by one-half

Component II: can be written in a similar manner substituting the $T_{1/2}$ for Component II.

$$P_{tII} = P_{oII}e^{-}\ II_t$$

The overall increase in percent incorporation of mercury into red blood cells with time can be written:

$$P_{total} = P_{eq} - (P_{oI}e^{-}\ It + P_{oII}e^{-}\ IIt)$$

Where: P_{total} = percent Hg in the RBC at time t

P_{eq} = percent Hg in RBC at equilibrium

P_{oI} = percent Hg in RBC due to Component I at time t

P_{oII} = percent Hg in RBC due to Component II at time t

e, I, II are described previously.

APPENDIX III

TRANSMISSION ELECTRON MICROSCOPY

TISSUE EMBEDDING PROCEDURE

1. Fix tissues 3-6 hrs in glutaraldehyde-Sørensen buffer at 4° C.

2. Rinse twice (30 min each) in Sørensen buffer.

3. Post fix in 1% OsO_4 2-3 hrs at room temperature.

4. Rinse in Sørensen buffer 30 mins. Tissues may be stored at 4° C for 2 weeks at this step only.

5. Dehydrate in graded concentrations (30-60 min per step) of ethanol or acetone as follows: % EtOH/HOH or Acetone/HOH 10, 25, 50, 75, 90, 95, 100, 100 (keep the last two steps in the desiccator when not changing solutions).

6. Infiltrate in 50% Spurrs (Polyscience Inc., Warrington, Pa.), 50% ethanol or acetone for 12 hrs (store Spurrs in freezer when not in use and be sure to allow Spurrs to reach room temperature before opening).

7. Infiltrate in 100% Spurrs for 12 hrs.

8. Place tissues in plastic embedding mould or other suitable receptacle and cover with fresh Spurrs. Cure at 70° C for 8 hrs.

9. Store blocks in desiccator until ready to cut.

APPENDIX IV

SCANNING ELECTRON MICROSCOPY

TISSUE PREPARATION

1. Excise tissues and fix in 50% glutaraldehyde 3-6 hrs.

2. Rinse 6 times, 30 mins each, with Sørensen buffer. Tissues may be stored up to 4 weeks at this step only.

Freeze drying:

3a. Quick freeze tissues in isopentane cooled with liquid nitrogen. The tissues may be pinned to small styrofoam blocks with insect pins and floated upside down on the isopentane.

4a. Once frozen, dry in freeze dryer at below -40° C, 5-10μ pressure for a minimum of 12 hrs.

Critical point drying:

3b. Dehydrate in ethanol using 60 min steps of the following: % EtOH/dist. HOH, 10, 25, 50, 75, 90, 95, 100, 100.

4b. Infiltrate with 50% amyl acetate (AA) (Mallinckrodt Chemical Works, St. Louis, Mo.) in EtOH for 1 hr and then in two changes of 100% AA for 1 hr each.

5b. Place in critical point dryer (DCP1 Critical Point Dryer, Denton Vacuum, Inc.) and flush with liquid CO_2 until the banana odor of amyl acetate is no longer present in effluent.

6b. Close outlet valve, wait 5 mins and close inlet valve when sample pressure is at 900 psig.

7b. Heat sample holder with water at 49-50° C. The CO_2 will pass through the critical point at 1050 psig. Allow pressure to reach 1600 psig.

8b. Hold pressure at 1600 psig for 10 min (do not exceed 1700 psig, bleed lines if necessary).

9b. Release pressure over 5 minute duration. Samples are now dry.

10b. If any amyl acetate odor is noted in effluent during step 9b, repeat steps 5b-9b.

APPENDIX V

PILLAR CELL STRUCTURE

Figure 45 shows the structure of the pillar cell body. The large nucleus (N) is surrounded by a nuclear membrane which is porous (P). White and black arrow points to the basal lamina which can clearly be seen to connect to the basal lamina on the opposite side of the pillar cell (bottom of the figure). Connecting elements of the basal lamina pass through the pillar cells in several locations (Hughes and Wright, 1970) and are believed to have contractile properties or supportive functions similar to those of mammalian reticular cells in lymph or splenic tissues (Hughes and Weibel, 1972).

Figure 45.--Transmission electron micrograph of the pillar cell body. Nucleus (N); nuclear pores (P); basal lamina (bl). 4% glutaraldehyde fix, 1% OsO_4 postfix, LC and UA stain. 43,000x.

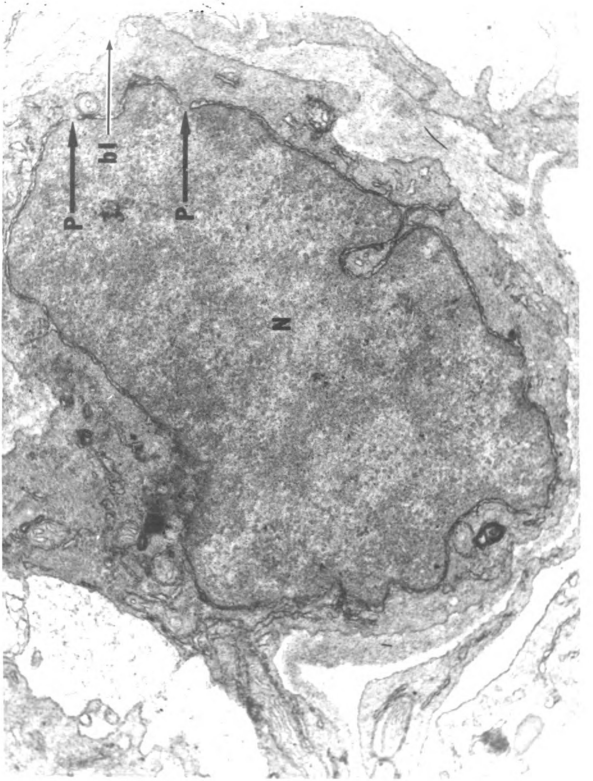
D
D
N

APPENDIX VI

SURFACE FEATURES OF LAMELLAE FROM THE BLACK BULLHEAD AND NORTHERN PIKE

Lamellar epithelia from various species of teleosts were examined with the SEM to ascertain whether the ridges found on rainbow trout epithelia were characteristic of all fish. Instead of a common ridge pattern, the lamellar surface from 10 species studied showed great variability, from no ridges at all in the common carp, or small "bumps" in the black bullhead (Figure 46A) to comparatively long ridges from northern pike (Figure 46B). Teleologically, the purpose of such wide variation of respiratory surfaces is unknown; more studies are needed of other species before sound conclusions can be drawn.

Figures 46A and 46B.--Scanning electron micrographs of the lamellar surface from two species of teleosts. Figure 46A: black bullhead (14,500x); Figure 46B: northern pike (7,300x). Arrow in Figure 46B points to a chloride cell on the lamellar surface. 50% glutaraldehyde fix (both Figure 46A and Figure 46B).

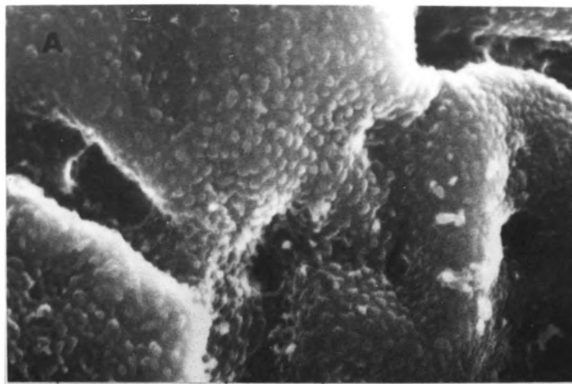
A

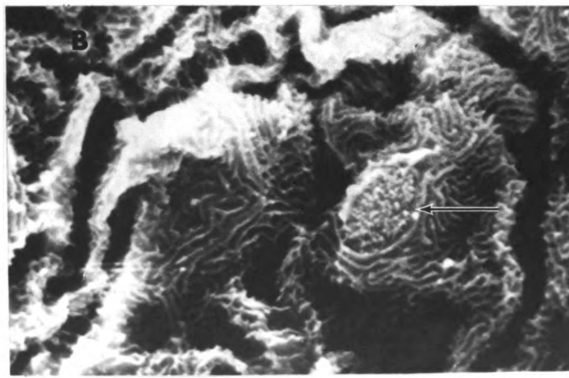
B